

NUCLEAR DATA AND MEASUREMENTS SERIES

ANL/NDM-67

Non-Evaluation Applications for Covariance Matrices

by

Donald L. Smith

May 1982

**ARGONNE NATIONAL LABORATORY,
ARGONNE, ILLINOIS 60439, U.S.A.**

NUCLEAR DATA AND MEASUREMENTS SERIES

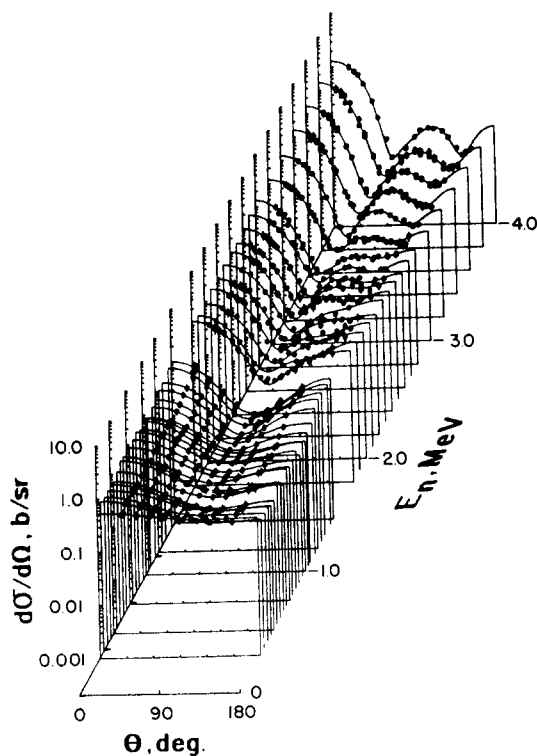
ANL/NDM-67

NON-EVALUATION APPLICATIONS
FOR COVARIANCE MATRICES*

by

Donald L. Smith

May 1982



U of C - AUA - USDOE

ARGONNE NATIONAL LABORATORY,
ARGONNE, ILLINOIS 60439, U.S.A.

The facilities of Argonne National Laboratory are owned by the United States Government. Under the terms of a contract (W-31-109-Eng-38) among the U. S. Department of Energy, Argonne Universities Association and The University of Chicago, the University employs the staff and operates the Laboratory in accordance with policies and programs formulated, approved and reviewed by the Association.

MEMBERS OF ARGONNE UNIVERSITIES ASSOCIATION

The University of Arizona	The University of Kansas	The Ohio State University
Carnegie-Mellon University	Kansas State University	Ohio University
Case Western Reserve University	Loyola University of Chicago	The Pennsylvania State University
The University of Chicago	Marquette University	Purdue University
University of Cincinnati	The University of Michigan	Saint Louis University
Illinois Institute of Technology	Michigan State University	Southern Illinois University
University of Illinois	University of Minnesota	The University of Texas at Austin
Indiana University	University of Missouri	Washington University
The University of Iowa	Northwestern University	Wayne State University
Iowa State University	University of Notre Dame	The University of Wisconsin-Madison

NOTICE

This report was prepared as an account of work sponsored by the United States Government. Neither the United States nor the United States Department of Energy, nor any of their employees, nor any of their contractors, subcontractors, or their employees, makes any warranty, express or implied, or assumes any legal liability or responsibility for the accuracy, completeness or usefulness of any information, apparatus, product or process disclosed, or represents that its use would not infringe privately-owned rights. Mention of commercial products, their manufacturers, or their suppliers in this publication does not imply or connote approval or disapproval of the product by Argonne National Laboratory or the U. S. Department of Energy.

ANL/NDM-67

NON-EVALUATION APPLICATIONS
FOR COVARIANCE MATRICES*

by

Donald L. Smith

May 1982

*This work supported by the U.S. Department of Energy.

Applied Physics Division
Argonne National Laboratory
9700 South Cass Avenue
Argonne, Illinois 60439
USA

NUCLEAR DATA AND MEASUREMENTS SERIES

The Nuclear Data and Measurements Series presents results of studies in the field of microscopic nuclear data. The primary objective is the dissemination of information in the comprehensive form required for nuclear technology applications. This Series is devoted to: a) measured microscopic nuclear parameters, b) experimental techniques and facilities employed in measurements, c) the analysis, correlation and interpretation of nuclear data, and d) the evaluation of nuclear data. Contributions to this Series are reviewed to assure technical competence and, unless otherwise stated, the contents can be formally referenced. This Series does not supplant formal journal publication but it does provide the more extensive information required for technological applications (e.g., tabulated numerical data) in a timely manner.

OTHER ISSUES IN THE ANL/NDM SERIES ARE:

- ANL/NDM-1 Cobalt Fast Neutron Cross Sections—Measurement and Evaluation by P. T. Guenther, P. A. Moldauer, A. B. Smith, D. L. Smith and J. F. Whalen, July 1973.
- ANL/NDM-2 Prompt Air-Scattering Corrections for a Fast-Neutron Fission Detector: $E_n \leq 5$ MeV by Donald L. Smith, September 1973.
- ANL/NDM-3 Neutron Scattering from Titanium; Compound and Direct Effects by E. Barnard, J. deVilliers, P. Moldauer, D. Reitmann, A. Smith and J. Whalen, October 1973.
- ANL/NDM-4 ^{90}Zr and ^{92}Zr ; Neutron Total and Scattering Cross Sections by P. Guenther, A. Smith and J. Whalen, July 1974.
- ANL/NDM-5 Delayed Neutron Data - Review and Evaluation by Samson A. Cox, April 1974.
- ANL/NDM-6 Evaluated Neutronic Cross Section File for Niobium by R. Howerton, Lawrence Livermore Laboratory and A. Smith, P. Guenther and J. Whalen, Argonne National Laboratory, May 1974.
- ANL/NDM-7 Neutron Total and Scattering Cross Sections of Some Even Isotopes of Molybdenum and the Optical Model by A. B. Smith, P. T. Guenther and J. F. Whalen, June 1974.
- ANL/NDM-8 Fast Neutron Capture and Activation Cross Sections of Niobium Isotopes by W. P. Poenitz, May 1974.
- ANL/NDM-9 Method of Neutron Activation Cross Section Measurement for $E_n = 5.5$ –10 MeV Using the $\text{D}(d,n)\text{He-3}$ Reaction as a Neutron Source by D. L. Smith and J. W. Meadows, August 1974.
- ANL/NDM-10 Cross Sections for (n,p) Reactions on ^{27}Al , $^{46,47,48}\text{Tl}$, $^{54,56}\text{Fe}$, ^{58}Ni , ^{59}Co and ^{64}Zn from Near Threshold to 10 MeV by Donald L. Smith and James W. Meadows, January 1975.
- ANL/NDM-11 Measured and Evaluated Fast Neutron Cross Sections of Elemental Nickel by P. Guenther, A. Smith, D. Smith and J. Whalen, Argonne National Laboratory and R. Howerton, Lawrence Livermore Laboratory, July 1975.
- ANL/NDM-12 A Spectrometer for the Investigation of Gamma Radiation Produced by Neutron-Induced Reactions by Donald L. Smith, April 1975.
- ANL/NDM-13 Response of Several Threshold Reactions in Reference Fission Neutron Fields by Donald L. Smith and James W. Meadows, June 1975.
- ANL/NDM-14 Cross Sections for the $^{66}\text{Zn}(n,p)^{66}\text{Cu}$, $^{113}\text{In}(n,n')^{113\text{m}}\text{In}$ and $^{115}\text{In}(n,n')^{115\text{m}}\text{In}$ Reactions from Near Threshold to 10 MeV by Donald L. Smith and James W. Meadows, July 1975.

- ANL/NDM-15 Radiative Capture of Fast Neutrons in ^{165}Ho and ^{181}Ta by W. P. Poenitz, June 1975.
- ANL/NDM-16 Fast Neutron Excitation of the Ground-State Rotational Band of ^{238}U by P. Guenther, D. Havel and A. Smith, September 1975.
- ANL/NDM-17 Sample-Size Effects in Fast-Neutron Gamma-Ray Production Measurements: Solid-Cylinder Samples by Donald L. Smith, September 1975.
- ANL/NDM-18 The Delayed Neutron Yield of ^{238}U and ^{241}Pu by J. W. Meadows January 1976.
- ANL/NDM-19 A Remark on the Prompt-Fission-Neutron Spectrum of ^{252}Cf by P. Guenther, D. Havel, R. Sjoblom and A. Smith, March 1976.
- ANL/NDM-20 Fast-Neutron-Gamma-Ray Production from Elemental Iron: $E_n \lesssim 2$ MeV by Donald L. Smith, May 1976.
- ANL/NDM-21 Note on the Experimental Determination of the Relative Fast-Neutron Sensitivity of a Hydrogenous Scintillator by A. Smith, P. Guenther and R. Sjoblom, June 1976.
- ANL/NDM-22 Note on Neutron Scattering and the Optical Model Near $A=208$ by P. Guenther, D. Havel and A. Smith, September 1976.
- ANL/NDM-23 Remarks Concerning the Accurate Measurement of Differential Cross Sections for Threshold Reactions Used in Fast-Neutron Dosimetry for Fission Reactors by Donald L. Smith, December 1976.
- ANL/NDM-24 Fast Neutron Cross Sections of Vanadium and an Evaluated Neutronic File by P. Guenther, D. Havel, R. Howerton, F. Mann, D. Smith, A. Smith and J. Whalen, May 1977.
- ANL/NDM-25 Determination of the Energy Scale for Neutron Cross Section Measurements Employing a Monoenergetic Accelerator by J. W. Meadows, January 1977.
- ANL/NDM-26 Evaluation of the $\text{In-115}(n,n')\text{In-115}$ Reaction for the ENDF/B-V Dosimetry File by Donald L. Smith, December 1976.
- ANL/NDM-27 Evaluated (n,p) Cross Sections of ^{46}Ti , ^{47}Ti and ^{48}Ti by C. Philis and O. Bersillon, Bruyeres-le-Chatel, France and D. Smith and A. Smith, Argonne National Laboratory, January 1977.
- ANL/NDM-28 Titanium-II: An Evaluated Nuclear Data File by C. Philis, Centre d'Etudes de Bruyères-le-Châtel, R. Howerton, Lawrence Livermore Laboratory and A. B. Smith, Argonne National Laboratory, June 1977.
- ANL/NDM-29 Note on the 250 keV Resonance in the Total Neutron Cross Section of ^6Li by A. B. Smith, P. Guenther, D. Havel and J. F. Whalen, June 1977.

- ANL/NDM-30 Analysis of the Sensitivity of Spectrum-Average Cross Sections to Individual Characteristics of Differential Excitation Functions by Donald L. Smith, March 1977.
- ANL/NDM-31 Titanium-I: Fast Neutron Cross Section Measurements by P. Guenther, D. Havel, A. Smith and J. Whalen, May 1977.
- ANL/NDM-32 Evaluated Fast Neutron Cross Section of Uranium-238 by W. Poenitz, E. Pennington, and A. B. Smith, Argonne National Laboratory and R. Howerton, Lawrence Livermore Laboratory, October 1977.
- ANL/NDM-33 Comments on the Energy-Averaged Total Neutron Cross Sections of Structural Materials by A. B. Smith and J. F. Whalen, June 1977.
- ANL/NDM-34 Graphical Representation of Neutron Differential Cross Section Data for Reactor Dosimetry Applications by Donald L. Smith, June 1977.
- ANL/NDM-35 Evaluated Nuclear Data File of Th-232 by J. Meadows, W. Poenitz, A. Smith, D. Smith and J. Whalen, Argonne National Laboratory and R. Howerton, Lawrence Livermore Laboratory, February 1978.
- ANL/NDM-36 Absolute Measurements of the $^{233}\text{U}(n,f)$ Cross Section Between 0.13 and 8.0 MeV by W. P. Poenitz, April 1978.
- ANL/NDM-37 Neutron Inelastic Scattering Studies for Lead-204 by D. L. Smith and J. W. Meadows, December 1977.
- ANL/NDM-38 The Alpha and Spontaneous Fission Half-Lives of ^{242}Pu by J. W. Meadows, December 1977.
- ANL/NDM-39 The Fission Cross Section of ^{239}Pu Relative to ^{235}U from 0.1 to 10 MeV by J. W. Meadows, March 1978.
- ANL/NDM-40 Statistical Theory of Neutron Nuclear Reactions by P. A. Moldauer, February 1978.
- ANL/NDM-41 Energy-Averaged Neutron Cross Sections of Fast-Reactor Structural Materials by A. Smith, R. McKnight and D. Smith, February 1978.
- ANL/NDM-42 Fast Neutron Radiative Capture Cross Section of ^{232}Th by W. P. Poenitz and D. L. Smith, March 1978.
- ANL/NDM-43 Neutron Scattering from ^{12}C in the Few-MeV Region by A. Smith, R. Holt and J. Whalen, September 1978.
- ANL/NDM-44 The Interaction of Fast Neutrons with ^{60}Ni by A. Smith, P. Guenther, D. Smith and J. Whalen, January 1979.
- ANL/NDM-45 Evaluation of $^{235}\text{U}(n,f)$ between 100 KeV and 20 MeV by W. P. Poenitz, July 1979.

- ANL/NDM-46 Fast-Neutron Total and Scattering Cross Sections of ^{107}Ag in the MeV Region by A. Smith, P. Guenther, G. Winkler and J. Whalen, January 1979.
- ANL/NDM-47 Scattering of MeV Neutrons from Elemental Iron by A. Smith and P. Guenther, March 1979.
- ANL/NDM-48 ^{235}U Fission Mass and Counting Comparison and Standardization by W. P. Poenitz, J. W. Meadows and R. J. Armani, May 1979.
- ANL/NDM-49 Some Comments on Resolution and the Analysis and Interpretation of Experimental Results from Differential Neutron Measurements by Donald L. Smith, November 1979.
- ANL/NDM-50 Prompt-Fission-Neutron Spectra of ^{233}U , ^{235}U , ^{239}Pu and ^{240}Pu Relative to that of ^{252}Cf by A. Smith, P. Guenther, G. Winkler and R. McKnight, September 1979.
- ANL/NDM-51 Measured and Evaluated Neutron Cross Sections of Elemental Bismuth by A. Smith, P. Guenther, D. Smith and J. Whalen, April 1980.
- ANL/NDM-52 Neutron Total and Scattering Cross Sections of ^6Li in the Few MeV Region by P. Guenther, A. Smith and J. Whalen, February 1980.
- ANL/NDM-53 Neutron Source Investigations in Support of the Cross Section Program at the Argonne Fast-Neutron Generator by James W. Meadows and Donald L. Smith, May 1980.
- ANL/NDM-54 The Nonelastic-Scattering Cross Sections of Elemental Nickel by A. B. Smith, P. T. Guenther and J. F. Whalen, June 1980.
- ANL/NDM-55 Thermal Neutron Calibration of a Tritium Extraction Facility using the $^6\text{Li}(n,t)^4\text{He}/^{197}\text{Au}(n,\gamma)^{198}\text{Au}$ Cross Section Ratio for Standardization by M. M. Bretscher and D. L. Smith, August 1980.
- ANL/NDM-56 Fast-Neutron Interactions with ^{182}W , ^{184}W and ^{186}W by P. T. Guenther, A. B. Smith and J. F. Whalen, December 1980.
- ANL/NDM-57 The Total, Elastic- and Inelastic-Scattering Fast-Neutron Cross Sections of Natural Chromium, Peter T. Guenther, Alan B. Smith and James F. Whalen, January 1981.
- ANL/NDM-58 Review of Measurement Techniques for the Neutron Capture Process by W. P. Poenitz, August 1981.
- ANL/NDM-59 Review of the Importance of the Neutron Capture Process in Fission Reactors, Wolfgang P. Poenitz, July 1981.
- ANL/NDM-60 Neutron Capture Activation Cross Sections of $^{94,96}\text{Zr}$, $^{98,100}\text{Mo}$, and $^{110,114,116}\text{Cd}$ at Thermal and 30 keV Energy, John M. Wyrick and Wolfgang P. Poenitz, (to be published).

- ANL/NDM-61 Fast-neutron Total and Scattering Cross Sections of ^{58}Ni by Carl Budtz-Jørgensen, Peter T. Guenther, Alan B. Smith and James F. Whalen, September 1981.
- ANL/NDM-62 Covariance Matrices and Applications to the Field of Nuclear Data, by Donald L. Smith, November 1981.
- ANL/NDM-63 On Neutron Inelastic-Scattering Cross Sections of ^{232}Th , ^{233}U , ^{235}U , ^{238}U , ^{239}U , and ^{239}Pu and ^{240}Pu by Alan B. Smith and Peter T. Guenther, January 1982.
- ANL/NDM-64 The Fission Fragment Angular Distributions and Total Kinetic Energies for $^{235}\text{U}(n,f)$ from .18 to 8.83 MeV by J. W. Meadows, and Carl Budtz-Jørgensen, (to be published).
- ANL/NDM-65 Note on the Elastic Scattering of Several MeV Neutrons from Elemental Calcium by A. B. Smith and P. T. Guenther, (to be published).
- ANL/NDM-66 Fast-neutron Scattering Cross Sections of Elemental Silver by A. B. Smith and P. T. Guenther (to be published).

TABLE OF CONTENTS

	<u>Page</u>
PREFACE.....	viii
ABSTRACT.....	ix
1. INTRODUCTION.....	1
2. SELECTED APPLICATIONS.....	2
2.1 Calibration of the Neutron Energy Scale for Monoenergetic Neutrons Produced by an Accelerator.....	2
2.2 Calibration of a Ge(Li) Detector Energy Scale.....	11
2.3 Derivation of a Half Life from Decay Data.....	19
2.4 Derivation of the Relative Efficiency Curve for a Ge(Li) Detector.....	23
2.5 Normalization of a Relative Efficiency Curve for a Ge(Li) Detector.....	30
2.6 Background Subtraction for a Spectrum.....	34
2.7 Simultaneous Fitting of Two Peaks in a Spectrum.....	40
2.8 Uncertainty Estimation for Integrals of Fitted Peak Shapes...	46
2.9 Cross Section Error Resulting from Uncertainty in Neutron Energy Scale.....	50
2.10 Covariance Matrix for a Measured Neutron Spectrum.....	57
2.11 Uncertainty Determination for a Calculated Integral Quantity	65
2.12 Legendre Polynomial Fit to an Angular Distribution Data Set..	72
2.13 Combination of Dominant Error Components for Neutron Cross Section Measurements.....	81
3. CONCLUSIONS.....	89
ACKNOWLEDGEMENTS.....	90
REFERENCES.....	91
APPENDIX: FORTRAN-IV Subroutines for Use in Linear and Non-linear Least- Squares Analyses.....	93

PREFACE

Many nuclear researchers are reluctant to get involved with covariance matrices because they perceive the topic as complex and relevant only to the specialized area of evaluation. This is a misconception which should be dispelled. Covariance methods are not intrinsically difficult, and the applications transcend the area of nuclear data evaluation. This report offers several examples which illustrate the potential. More workers in the field would learn these methods if they recognized some specific applications to their work. They will not be so motivated if they continue to identify covariance matrices solely with evaluations. The field of nuclear data would benefit from a wider understanding of covariance matrices. Covariance techniques represent an important addition to any data-analysis repertoire. Data producers should recognize that they acquire more influence over interpretation and utilization of their results if they report them in ways which encourage proper treatment of errors and correlations by evaluators. Users of evaluated results achieve greater objectivity in assessing the sensitivity of their derived results to the input if they understand the significance of the error and correlation information which many evaluations provide. There appears to be a need to make covariance methods more widely accessible, and to publicize the potential applications throughout the nuclear data community.

NON-EVALUATION APPLICATIONS FOR COVARIANCE MATRICES*

by

Donald L. Smith
Applied Physics Division
Argonne National Laboratory
9700 South Cass Avenue
Argonne, Illinois 60439
USA

ABSTRACT

The possibilities for application of covariance matrix techniques to a variety of common research problems other than formal data evaluation are demonstrated by means of several examples. These examples deal with such matters as fitting spectral data, deriving uncertainty estimates for results calculated from experimental data, obtaining the best values for plurally-measured quantities, and methods for analysis of cross section errors based on properties of the experiment. The examples deal with realistic situations encountered in the laboratory, and they are treated in sufficient detail to enable a careful reader to extrapolate the methods to related problems.

*This work supported by the U.S. Department of Energy.

I. INTRODUCTION

One objective of this report is to encourage the reader to learn about covariance matrices, and to start applying these techniques in dealing with some common analysis problems in research. The report is directed toward workers in the field of nuclear data. The content consists of a discussion of several common topics from this field which are herein addressed using covariance techniques. The reader should not expect to find a comprehensive survey of all possible applications. However, these examples should provide enough insight to facilitate extrapolation of the methods to many other specific applications.

This report was not prepared to be a self-contained working document. It actually supplements an earlier report [1] which treats the fundamental procedures of covariance analysis as applied to nuclear data research. The earlier report is referenced extensively in the present document, and the reader will find it necessary to consider these two works together. The reader will not find a comprehensive list of references to other work in this report. There is an extensive literature, and many fine contributions have been made available by other workers in the field. Those recent works most often examined by this author in the context of the present investigation were the works of Mannhart [2], Peele [3] and Schmittroth [4]. However, another objective of the present report is to remedy a deficiency of Ref. 1, namely a limitation in the number of realistic examples which are helpful in understanding the basic concepts. Since the objective is to teach, simplicity and clarity are emphasized at the expense of completeness in both content and reference documentation.

When the reader considers the examples in Section 2, it will be apparent that several of them involve data "evaluation". This is unavoidable since the fitting of data, or selection of "best" values from measured results, is certainly "evaluation". The title of this report is an unfortunate simplification which is not quite correct from a purist point of view. However, the term "evaluation" has come to represent the activity undertaken by specialists within the field who formally consider reported cross sections and other nuclear data with the objective of generating a body of recommended numerical values, and estimated uncertainties, which are intended to be employed uniformly in physical and engineering applications by other individuals designated as "users". The present report avoids consideration of this function and focuses on individual applications of covariance matrices in experimental data reduction and other related research activities.

2. SELECTED APPLICATIONS

This section discusses thirteen topics which are likely to be encountered in nuclear data research. These are not very complicated examples, but they are generally problems which have been considered in our laboratory. Much of the analysis was performed using the FORTRAN - IV subroutines described in the Appendix. The interested reader may wish to study the Appendix as well as the examples of this section, and incorporate these subroutines into his own working library of computer programs.

2.1 Calibration of the Neutron Energy Scale for Monoenergetic Neutrons Produced by an Accelerator

Nearly monoenergetic neutrons can be produced by bombardment of several light elements with charged particles. By selecting the incident charged-particle energy to be a specific value, and by observing the neutrons at a specific angle, one can determine the neutron energy quite well to within the experimental resolution, which is often defined mainly by the thickness of the target that is being bombarded by the charged particles. The charged-particle energy is generally defined by using magnetic analysis and beam-defining slits.

The situation is somewhat different for total cross section experiments performed in our laboratory. The apparatus for this experiment utilizes the charged-particle beam port at zero degrees. Therefore, it is not possible to relate charged-particle energy to the field strength of an analyzing magnet for a fixed geometry. However, the accelerator voltage can be read using a digital voltmeter (DVM). This has proved to be a reproducible quantity which effectively defines the charged-particle beam energy and thus the neutron energy, indirectly [5].

A procedure for direct calibration of the neutron energy E versus the DVM reading v is provided by the inherent nature of this experiment. One can perform measurements with various transmission samples, where the cross sections exhibit well-known resonances. The calibration curve can be generated from data on resonance energy E_i versus DVM reading v_i for n points along the curve.

The energy versus DVM is represented by the function F with

$$E_i \approx F(v_i, \vec{p}) = \sum_{j=1}^m p_j v_i^{j-1} \quad (i=1, n). \quad (2.1.1)$$

Thus

$$\vec{E} \approx \vec{A} \bullet \vec{p}, \quad (2.1.2)$$

where matrix \bar{A} is given by

$$A_{ij} = v_i^{j-1} \quad (i = 1, n; j = 1, m). \quad (2.1.3)$$

This corresponds to a simple polynomial relationship between E and v . The DVM, v , is read to the 0.1 scale range (e.g., 32.1). Thus there is uncertainty, E_v , which does not exceed 0.05, due to round off. For each of the calibration points E_i , there is a corresponding v_i . However, the relationship is uncertain due to two effects:

- (i) The energy E_i of the calibration resonance is uncertain by an error E_{Ri} , as reported in the literature.
- (ii) The reading of the DVM, v_i , corresponding to the resonance E_i , is uncertain by E_v .

The procedure of selecting \bar{p} to optimize the fit indicated in Eq. (2.1.2), as described in Ref. 1, assumes that E_i is uncertain but not v_i . This dilemma can be avoided for practical purposes by combining both uncertainties (i) and (ii) into a single uncertainty E_{Ei} in E_i , as embodied by the following equation:

$$E_{Ei}^2 \approx E_{Ri}^2 + \left(\frac{\partial E}{\partial v}\right)_i^2 E_v^2. \quad (2.1.4)$$

This is not the only approach to this problem, but it is one which avoids further computational difficulties and allows for adequate treatment of the present calibration problem.

Realistically, all these error components are essentially uncorrelated, e.g., the uncertainty E_v in reading DVM is of the same magnitude along the whole scale, but completely independent for each determination of v . Thus, the covariance matrix \bar{V}_E for \bar{E} is

$$V_{Eij} = \begin{cases} E_{Ei}^2 & i=j, \\ 0 & i \neq j. \end{cases} \quad (2.1.5)$$

The procedure for solving this problem is described in Section VII, Ref. 1. The key equations are Eqs. (129) and (130) from this reference. Expressed in terms of the present variables

$$\bar{V}_p = (\bar{A}^T \bullet \bar{V}_E^{-1} \bullet \bar{A})^{-1} \quad (2.1.6)$$

$$\vec{p} = \bar{V}_p \bullet \bar{A}^T \bullet \bar{V}_E^{-1} \bullet \vec{E}, \quad (2.1.7)$$

where "T" designates a transposed matrix and "-1" indicates the inverse of the given matrix. This solution minimizes the chi-square given by

$$\chi^2 = (\vec{E} - \bar{A} \bullet \vec{p})^T \bullet \bar{V}_E^{-1} \bullet (\vec{E} - \bar{A} \bullet \vec{p}). \quad (2.1.8)$$

The error vector \vec{E}_p and correlation matrix \bar{C}_p for the solution \vec{p} is derived from

$$E_{pi} = V_{pii}^{1/2} \quad (i = 1, m), \quad (2.1.9)$$

$$C_{pij} = V_{pij} / (E_{pi} E_{pj}) \quad (i, j = 1, m). \quad (2.1.10)$$

The result of this calibration procedure is the formula

$$E = F(v, \vec{p}) = \sum_{j=1}^m p_j v^{j-1}, \quad (2.1.11)$$

which is then used to calculate the neutron energy, E, corresponding to any DVM reading, v. For a DVM reading, v, what is the uncertainty in the derived energy, E? According to the formalism of Section III, Ref. 1.

$$\Delta E^2 = (\bar{S} \bullet \vec{E}_p)^T \bullet \bar{C}_p \bullet (\bar{S} \bullet \vec{E}_p), \quad (2.1.12)$$

where \bar{S} is the sensitivity matrix

$$\bar{S} = \begin{bmatrix} (\partial F/\partial p_1) & & 0 \\ & \ddots & \\ 0 & & (\partial F/\partial p_m) \end{bmatrix}. \quad (2.1.13)$$

Since

$$(\partial F/\partial p_j) = v^{j-1}, \quad (2.1.14)$$

Eq. (2.1.12) becomes

$$\Delta E^2 = \sum_{\ell=1}^m \sum_{j=1}^m v^{\ell+j-2} C_{p\ell j} E_{p\ell} E_{pj}. \quad (2.1.15)$$

However, this is the uncertainty in E when v is assumed to be precisely known. This is not the case, since we recognize that v is uncertain by E_v , and it is reasonable to add to the error expressed in Eq. (2.1.15). Then,

$$\Delta E^2 \approx \sum_{\ell=1}^m \sum_{j=1}^m v^{\ell+j-2} C_{p\ell j} E_{p\ell} E_{pj} + \left(\frac{\partial E}{\partial v}\right)^2 E_v^2, \quad (2.1.16)$$

where

$$\frac{\partial E}{\partial v} = \sum_{j=2}^m (j-1) p_j v^{j-2}. \quad (2.1.17)$$

The correlations introduced by fitting a polynomial calibration curve to the resonance data play an explicit role in Eq. (2.1.16). Clearly, the wrong error ΔE is calculated if the errors \tilde{E}_p are assumed uncorrelated (i.e., $C_{p\ell j} = \delta_{\ell j}$, the Kronecker delta function) as is often done in such analyses.

This formalism is powerful enough to permit us to examine an additional question: "What is the correlation in the errors ΔE_1 and ΔE_j for two energies E_1 and E_j derived from the calibration curve for two values of voltage v_1 and v_j , respectively?" To solve this problem, one refers to Section IV of Ref. 1.

Then,

$$E_i = E(\vec{p}, v_i, v_j), \quad (2.1.18)$$

$$E_j = E(\vec{p}, v_i, v_j). \quad (2.1.19)$$

Define augmented matrices \bar{S}_{xi} , \bar{S}_{xj} and \bar{C}_x , and the augmented vector \vec{E}_x as follows:

$$\bar{S}_{xk} = \begin{bmatrix} (\partial E / \partial p_1)_k & & & & 0 \\ & \dots & & & \\ & & (\partial E / \partial p_m)_k & & \\ & & & (\partial E / \partial v_i)_k & \\ 0 & & & & (\partial E / \partial v_j)_k \end{bmatrix}, \quad (2.1.20)$$

(k = i or j)

$$\bar{C}_x = \begin{bmatrix} \bar{C}_p & 0 \\ & 1 & \\ 0 & & 1 \end{bmatrix}, \quad (2.1.21)$$

$$\vec{E}_x = \begin{bmatrix} \vec{E}_p \\ E_{vi} \\ E_{vj} \end{bmatrix}. \quad (2.1.22)$$

Since E_i does not depend upon v_j and E_j does not depend upon v_i ,

$$(\partial E / \partial v_i)_j = (\partial E / \partial v_j)_i = 0. \quad (2.1.22a)$$

Use is made in Eq. (2.1.21) of the fact that the errors in v_i and v_j are uncorrelated. Now, define the matrix \bar{M} by

$$\bar{M} = \begin{bmatrix} M_{11} & M_{1j} \\ M_{ji} & M_{jj} \end{bmatrix}, \quad (2.1.23)$$

where

$$M_{k\ell} = (\bar{S}_{xk} \bullet \bar{E}_x)^T \bullet \bar{C}_x \bullet (\bar{S}_{x\ell} \bullet \bar{E}_x). \quad (2.1.24)$$

(k, \ell = i or j)

Following some algebra, one can conclude that

$$M_{kk} = (\Delta E_k)^2 \quad (k = i \text{ or } j), \quad (2.1.25)$$

where ΔE_k is the value derived from Eq. (2.1.16). Thus, the correlation in the errors ΔE_i and ΔE_j , q_{ij} , is

$$q_{ij} = M_{ij} / (\Delta E_i \Delta E_j). \quad (2.1.26)$$

Consider the data in Table (2.1.1) as a numerical example. Application of the formalism described in the present section indicates that the best chi-square is obtained with a five-parameter fit, and that problems with limited precision in the computer lead to instability for higher-order fits, as indicated in Table (2.1.2). The normalized chi-square is the actual chi-square divided by the number of degrees of freedom ($n - m$ for this example). A normalized chi-square of around unity indicates a fit consistent with the assigned errors.

The result for a five-parameter analysis is shown in Fig. (2.1.1). Strong correlations in the errors for the parameters \bar{p} are evident. Negative signs for elements in \bar{C}_p imply anti-correlations. Were it not for these anti-correlations the error ΔE for E derived from the curve for a given v would be much larger than the 4-6 keV uncertainty indicated. This is evident from the role of \bar{C}_p in Eq. (2.1.16). The reader can investigate the correlations between errors in energies derived for two different voltages by using the formalism outline in Eqs. (2.1.18) to (2.1.26).

Table 2.1.1
Resonance Calibration Data

DVM ^a	Resonance ^b Energy (MeV)	Origin
31.9	0.565	Silicon
35.9	0.813	Silicon
37.6	0.930	Silicon
39.6	1.047	Silicon
42.1	1.205	Silicon
54.4	1.925	Silicon
57.17 ^c	2.078	Carbon
74.25 ^c	3.008	Carbon
98.2	4.220	Silicon
117.4	5.125	Oxygen

^a v = DVM, uncertainty ± 0.05 .

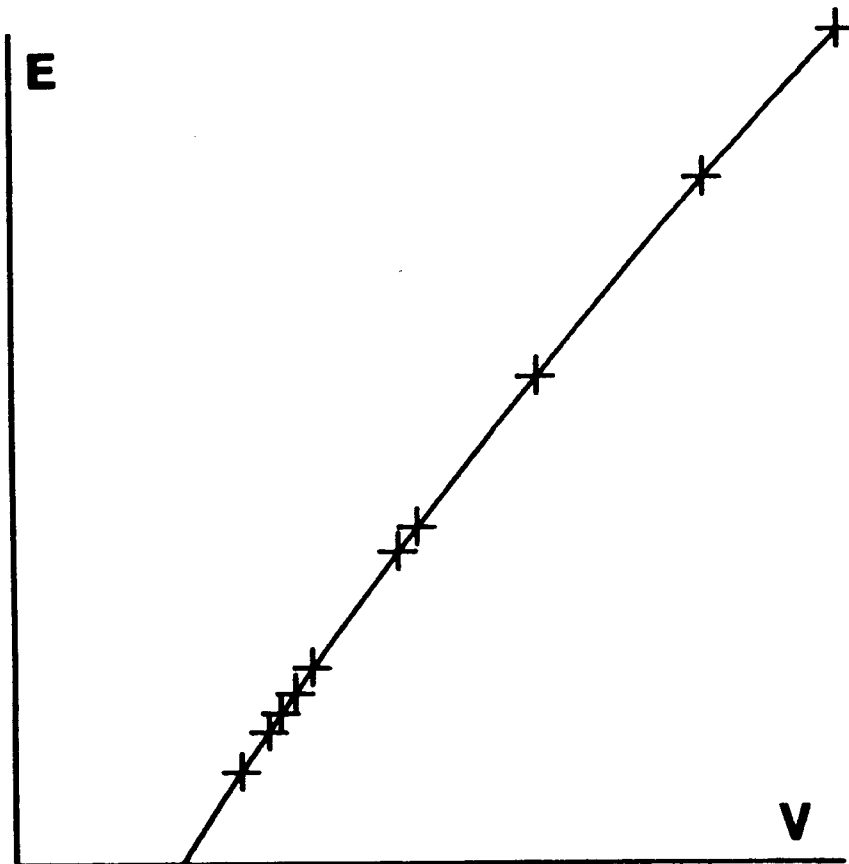
^b Assumed uncertainty ± 2 keV for all resonance energies.

^c Average of more than one determination accounts for extra digits beyond meter scale range.

Table 2.1.2
Normalized Chi-Square vs. Order of Fit

Number of Parameters Used in Fit	Normalized Chi-Square
2	316.4
3	4.601
4	1.221
5	1.019
6	309.9 (unstable) ^a

^a Apparent instability of result is attributed to precision limitations for the computer used in this analysis.



Values Derived from Fitted Curve

V, E, EE
.3000E 02 .4326E 00 .5814E-02
.4000E 02 .1074E 01 .3649E-02
.5000E 02 .1671E 01 .3702E-02
.6000E 02 .2238E 01 .3718E-02
.7000E 02 .2782E 01 .4160E-02
.8000E 02 .3306E 01 .4229E-02
.9000E 02 .3814E 01 .4198E-02
.1000E 03 .4307E 01 .4713E-02
.1100E 03 .4783E 01 .4489E-02

Fit Information

V, E, EE
.3190E 02 .5650E 00 .4000E-02
.3590E 02 .8130E 00 .4000E-02
.3760E 02 .9300E 00 .4000E-02
.3960E 02 .1047E 01 .4000E-02
.4210E 02 .1205E 01 .4000E-02
.5440E 02 .1925E 01 .4000E-02
.5717E 02 .2078E 01 .4000E-02
.7425E 02 .3008E 01 .4000E-02
.9820E 02 .4220E 01 .4000E-02
.1174E 03 .5125E 01 .4000E-02
P, EP
-.1789E 01 .9731E-01
.8492E-01 .6284E-02
-.4243E-03 .1424E-03
.2548E-05 .1349E-05
-.7008E-08 .4536E-08
CP
.1000E 01-.9964E 00 .9862E 00-.9713E 00 .9538E 00
-.9964E 00 .1000E 01-.9965E 00 .9873E 00-.9744E 00
.9862E 00-.9965E 00 .1000E 01-.9970E 00 .9893E 00
-.9713E 00 .9873E 00-.9970E 00 .1000E 01-.9976E 00
.9538E 00-.9744E 00 .9893E 00-.9976E 00 .1000E 01
CHI2, CHI2NM
.5097E 01 .1019E 01

Figure 2.1.1:

Calibration of neutron energy vs. accelerator voltage. V = accelerator voltage, E = neutron energy, EE = uncertainty in neutron energy. Input calibration point errors are uncorrelated, but errors in values read from derived curve are correlated from one voltage to another. P = parameters of fit, EP = errors in P, and CP are correlations for EP. CHI2 and CHI2NM are the chi-square and normalized chi-square, respectively.

2.2 Calibration of a Ge(Li) Detector Energy Scale

Ge(Li) detectors can be used to measure gamma-ray energies with high accuracy, but first they must be calibrated. The relationship between pulse height for a full-energy peak line and the gamma ray energy can be nearly linear over a moderate range of energies if high-quality electronic components are utilized in the pulse analysis chain (preamplifier, linear amplifier and analog-to-digital converter). However, nonlinearities must be taken into account to realize the full accuracy potential of these detector systems. Nonlinear effects are especially important for low gamma ray energies or for calibration of very wide energy ranges. See Ref. [6] for more details.

Energy scale calibration is most often achieved by utilizing calibration sources which emit one or more gamma rays whose energies are well known. Thus, one generates a calibration data base consisting of sets of multiplets (x_i , Δx_i , E_i , ΔE_{gi}), where x_i is the peak channel for a gamma ray of energy E_i in the recording device. The Δx_i are the uncertainties in the peak channels while the ΔE_{gi} are the given errors in the energies of the calibration lines. The object of the calibration procedure is to represent the energy E as a function of x , $E(x)$. A polynomial relation is adequate for applied purposes, so

$$E(\vec{p}, x) = \sum_{j=1}^m p_j x^{j-1}. \quad (2.2.1)$$

The fitting problem consists of finding the set of parameters \vec{p} which gives the best fit of the polynomial expansion to the given calibration data. However, before proceeding with the fitting analysis, it is necessary to examine the input data errors and their correlations.

According to Eq. (2.2.1), this problem treats x as the independent variable while E is the dependent variable. The error analysis formalism discussed in this report considers data where the errors in the dependent variable values (E_i) are included while those for the independent variable values (x_i) are neglected. In the present problem, both E_i and x_i are uncertain. This dilemma can be resolved for practical purposes by simply adding the error in x_i to the error in E_i according to the formula

$$E_{Ei}^2 \approx \Delta E_{gi}^2 + \left(\frac{\partial E}{\partial x}\right)_i^2 \Delta x_i^2. \quad (2.2.2)$$

The partial derivatives, $(\partial E/\partial x)_i$, can be estimated a priori from the trend of the calibration data. The errors Δx_i can be assumed to be uncorrelated, but it is likely that the errors ΔE_{gi} are at least partially correlated, if they correspond to a specific radioactive source. Thus, e.g., there will be some correlation between ΔE_{gi} and ΔE_{gj} if both of these lines are ^{152}Eu gamma-decay lines, but there will be no correlation if one line is from ^{152}Eu and the other

is from ^{133}Ba . The nature of the correlations would be expected to be different for each source since the calibration energies are most likely to have originated from different experiments. Information of this nature is very hard to come by. So, for this example a model assumption will be made. It will be assumed that the total errors E_{Ei} and E_{Ej} are correlated according to a matrix \bar{C}_E defined as follows:

$$C_{Eij} = \begin{cases} 0 & \text{if the lines "i" and "j" arise from} \\ & \text{two distinct radioactive sources,} \\ \delta E_k^2 \left[1 - \frac{|E_i - E_j|}{\Delta E_k} \right] / (E_{Ei} E_{Ej}), & \text{if the lines} \\ & \text{"i" and "j" arise from the radioactive} \\ & \text{source labelled "k".} \end{cases} \quad (2.2.3)$$

Here, δE_k designates an estimated correlated error component for the source "k" and ΔE_k is the magnitude of the maximum energy difference for any two calibration lines in source "k". Thus, the given error ΔE_{gi} is assumed to consist of a random component ΔE_{Ri} and the correlated component δE_k so that

$$\Delta E_{gi}^2 = \Delta E_{Ri}^2 + \delta E_k^2. \quad (2.2.4)$$

The degree of correlation between the errors diminishes according to the energy separation of the lines, for two lines originating from the same radioactive source.

Once the input $x_1(\vec{x})$, $E_1(\vec{E})$, errors $E_{E1}(\vec{E}_E)$ and correlation matrix \bar{C}_E are available, as indicated above, the fitting can proceed according to the procedures of Section VII, Ref. 1.

Define the matrix \bar{A} according to

$$A_{ij} = (\partial E / \partial p_j)_i = x_i^{j-1} \quad (i = 1, n; j = 1, m). \quad (2.2.5)$$

Then

$$\vec{E} \approx \bar{A} \bullet \vec{p}, \quad (2.2.6)$$

$$\bar{V}_p = (\bar{A}^T \bullet \bar{V}_E^{-1} \bullet \bar{A})^{-1}, \quad (2.2.7)$$

$$\vec{p} = \bar{V}_p \bullet \bar{A}^T \bullet \bar{V}_E^{-1} \bullet \vec{E}, \quad (2.2.8)$$

where \bar{V}_E is a covariance matrix defined by

$$V_{Eij} = C_{Eij} E_{Ei} E_{Ej} \quad (i, j = 1, n), \quad (2.2.9)$$

and \bar{V}_E^{-1} is its inverse. The best solution to the approximate expression Eq. (2.2.6), is \vec{p} as given by Eq. (2.2.8). The solution covariance matrix is \bar{V}_p , and the solution errors are \vec{E}_p given by

$$E_{Pj} = (V_{Pjj})^{1/2} \quad (j = 1, m). \quad (2.2.10)$$

The chi-square and normalized chi-square are:

$$X^2 = (\vec{E} - \bar{A} \bullet \vec{p})^T \bullet \bar{V}_E^{-1} \bullet (\vec{E} - \bar{A} \bullet \vec{p}), \quad (2.2.11)$$

$$(X^2)_{\text{norm}} = X^2 / (n - m). \quad (2.2.12)$$

The correlation matrix \bar{C}_p is:

$$C_{pij} = V_{pij} / (E_{pi} E_{pj}) \quad (i, j = 1, m). \quad (2.2.13)$$

The solution vector \vec{p} defines the calibration curve according to Eq. (2.2.1). Once this curve is established, it is very interesting to find out what the error would be in the determination of the energy E_u of an unknown line located at x_u . The formalism of Section III, Ref. 1 can deal with this problem. Clearly

$$E_u = E(\vec{p}, x_u) = \sum_{j=1}^m p_j x_u^{j-1}. \quad (2.2.14)$$

Error in E_u arises from uncertainty in x_u and \vec{p} . The error in x_u is uncorrelated to the \vec{p} errors.

Define

$$\vec{E}_y = \begin{bmatrix} \vec{E}_p \\ E_{xu} \end{bmatrix}, \quad (2.2.15)$$

$$\bar{C}_y = \begin{bmatrix} \bar{C}_p & 0 \\ 0 & 1 \end{bmatrix}, \quad (2.2.16)$$

$$\bar{S}_y = \begin{bmatrix} (\partial E / \partial p_1)_u & \dots & 0 \\ \dots & (\partial E / \partial p_m)_u & \dots \\ 0 & \dots & (\partial E / \partial x)_u \end{bmatrix}, \quad (2.2.17)$$

where

$$(\partial E / \partial x)_u = \sum_{j=2}^m (j-1) p_j x_u^{j-2}, \quad (2.2.18)$$

$$(\partial E / \partial p_j)_u = x_u^{j-1} \quad (j = 1, m). \quad (2.2.19)$$

Then the equation

$$E_{Eu}^2 = (\bar{S}_y \bullet \vec{E}_y)^T \bullet \bar{C}_y \bullet (\bar{S}_y \bullet \vec{E}_y) \quad (2.2.20)$$

gives the desired error in E_u .

The input for the specific example to be considered in this section appears in Table (2.2.1). The indicated gamma ray lines originate from four sources: Eu-154, Ba-133, Sb-125 and Se-75. These data provide the basis

for a calibration of the energy range 120-900 keV. The channel uncertainties, Δx , are the dominant source of error in the calibration procedure, based on Eq. (2.2.2) and the data from Table (2.2.1). The Δx uncertainties are assumed to be uncorrelated, therefore, the matrix C_E , as defined in Eq. (2.2.3), exhibits only weak correlations which never exceed a few percent. Nevertheless, these correlations are included in the present analysis since inclusion creates no difficulties.

Figure (2.2.1) provides the results of the fitting analysis for $m = 5$, where the best chi-square was achieved as indicated in Table (2.2.2). The errors E_p are strongly correlated, as is often the case in such fitting analyses. This figure also indicates values of E derived for various x by means of the formalism described in this section. The errors in the derived energies are ≈ 0.5 keV, and the dominant error source is the uncertainty of ± 0.5 channel in locating a peak centroid.

Table 2.2.1
Ge(Li) Detector Energy Calibration Data

Source	E (keV)	ΔE_g (keV)	x	Δx	δE_k (keV)	ΔE_k (keV)	Index
Eu-154 ↓	123.1	0.03	172.7	0.5	0.02	750.1	1
	247.9	0.03	301.7	0.5	↓	↓	↓
	591.7	0.07	691.0	0.5	↓	↓	↓
	723.3	0.04	842.7	0.5	↓	↓	↓
	756.7	0.05	881.6	0.5	↓	↓	↓
	873.2	0.05	1016.7	0.5	↓	↓	↓
Ba-133 ↓	276.3	0.2	332.5	0.5	0.1	107.4	2
	302.7	0.2	361.7	0.5	↓	↓	↓
	355.9	0.14	421.2	0.5	↓	↓	↓
	383.7	0.18	452.6	0.5	↓	↓	↓
Sb-125 ↓	176.3	0.03	224.9	0.5	0.02	495.1	3
	380.5	0.07	448.8	0.7	↓	↓	↓
	427.9	0.03	502.7	0.5	↓	↓	↓
	463.4	0.03	543.3	0.5	↓	↓	↓
	600.6	0.07	700.7	0.5	↓	↓	↓
	606.7	0.07	707.5	0.7	↓	↓	↓
	635.9	0.05	741.4	0.5	↓	↓	↓
	671.4	0.05	782.3	0.7	↓	↓	↓
Se-75 ↓	135.9	0.1	184.3	0.5	0.05	264.6	4
	198.4	0.1	248.5	1.0	↓	↓	↓
	264.3	0.1	319.7	0.5	↓	↓	↓
	279.2	0.1	335.8	0.5	↓	↓	↓
	303.6	0.1	363.3	1.0	↓	↓	↓
	400.5	0.1	471.7	0.7	↓	↓	↓

Table 2.2.2
Normalized Chi-Square vs. Order of Fit

Number of Parameters Used in Fit	Normalized Chi-Square
2	61.68
3	12.77
4	2.484
5	0.8165
6	127.3 ^a

^a Apparent instability of result is attributed to precision limitations for the computer used in this analysis.

Fit Information

X	E	EE
.1727E 03	.1231E 03	.4470E 00
.3017E 03	.2479E 03	.4470E 00
.6910E 03	.5917E 03	.4515E 00
.8427E 03	.7233E 03	.4478E 00
.8816E 03	.7567E 03	.4488E 00
.1017E 04	.8732E 03	.4488E 00
.3325E 03	.2763E 03	.4888E 00
.3617E 03	.3027E 03	.4888E 00
.4212E 03	.3559E 03	.4675E 00
.4526E 03	.3837E 03	.4810E 00
.2249E 03	.1763E 03	.4470E 00
.4488E 03	.3805E 03	.6283E 00
.5027E 03	.4279E 03	.4470E 00
.5433E 03	.4634E 03	.4470E 00
.7007E 03	.6006E 03	.4515E 00
.7075E 03	.6067E 03	.6283E 00
.7414E 03	.6359E 03	.4488E 00
.7823E 03	.6714E 03	.6264E 00
.1843E 03	.1359E 03	.4571E 00
.2485E 03	.1984E 03	.8976E 00
.3197E 03	.2643E 03	.4571E 00
.3358E 03	.2792E 03	.4571E 00
.3633E 03	.3036E 03	.8976E 00
.4717E 03	.4005E 03	.6524E 00

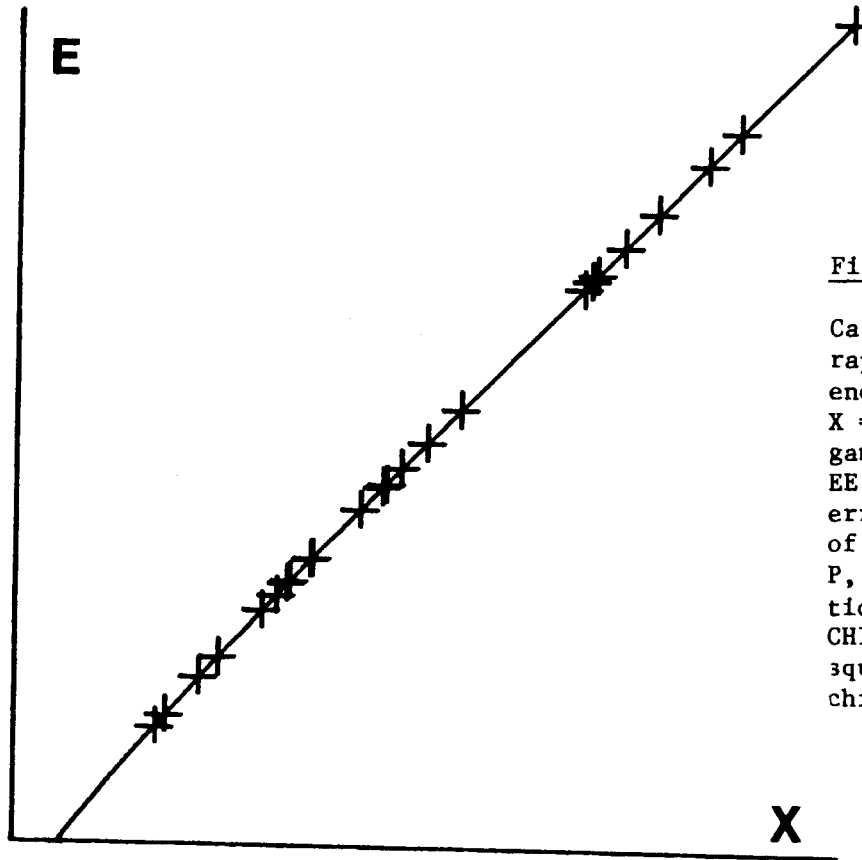


Figure 2.2.1:

Calibration of gamma-ray energy vs. full-energy peak channel. X = channel, E = gamma-ray energy, EE = gamma-ray energy error. P = parameters of fit, EP = errors in P, and CP are correlations for EP. CHI2 and CHI2NM are the chi square and normalized chi square, respectively.

P, EP

-.6252E 02	.2496E 01
.1175E 01	.2281E-01
-.6207E-03	.6981E-04
.0130E-06	.8587E-07
-.2166E-09	.3648E-10

CP				
.1000E 01	-.9859E 00	.9610E 00	-.9329E 00	.9054E 00
-.9568E 00	.1000E 01	-.9923E 00	.9759E 00	-.9562E 00
.9610E 00	-.9923E 00	.1000E 01	-.9951E 00	.9839E 00
-.9329E 00	.9759E 00	-.9951E 00	.1000E 01	-.9966E 00
.9054E 00	-.9562E 00	.9839E 00	-.9966E 00	.1000E 01
CHI2, CHI2N				
.4551E 02	.8186E 00			

Values Derived from Fitted Curve

X	E	EE
.2000E 03	.1511E 03	.5414E 00
.3000E 03	.2463E 03	.5000E 00
.4000E 03	.3372E 03	.4744E 00
.5000E 03	.4255E 03	.4779E 00
.6000E 03	.5127E 03	.4552E 00
.7000E 03	.5995E 03	.4734E 00
.8000E 03	.6863E 03	.4350E 00
.9000E 03	.7729E 03	.5134E 00

2.3 Derivation of a Half Life from Decay Data

Certain problems, by the nature of the parameters involved, can be transformed mathematically into an equivalent problem which can be analyzed using linear least-squares fitting techniques. Once the solution is obtained for the transformed problem, one can deduce the best solution for the original problem, and the errors, by performing an inverse transformation. This section presents such a situation as an example.

One of the experiments performed in this laboratory was a measurement of the half life for the decay of the isomeric level at 0.396-MeV excitation in ^{111}Cd [7]. A natural Cd sample was irradiated with fast neutrons. The yield of 245-keV gamma rays originating from $^{111\text{m}}\text{Cd}$ decays was measured with a Ge(Li) detector. The irradiated sample was counted over several half lives in intervals which were short compared to the half life. These data were corrected for deadtime and finite counting time effects. Errors in the derived activities were estimated from statistics and from a knowledge of other parameters of the measurement. Random errors were dominant, so the total errors are treated as essentially uncorrelated. The derived activity data set to be analyzed consists of a set of n multiplets of values (t_i, y_i, E_{y_i}) , with t_i the time, y_i the activity and E_{y_i} the error in y_i . the assumed functional relationship is

$$y = y_0 e^{-t/\tau}, \quad (2.3.1)$$

where τ is the mean life. Thus,

$$\ln y = \ln y_0 - \frac{t}{\tau}, \quad (2.3.2)$$

and so

$$z = p_1 + p_2 t, \quad (2.3.3)$$

if the following variable changes are made:

$$\begin{aligned} z &= \ln y, \\ p_1 &= \ln y_0, \\ p_2 &= -1/\tau. \end{aligned} \quad (2.3.4)$$

Now,

$$\partial z / \partial y = 1/y, \quad (2.3.5)$$

$$\text{so } E_z = E_y / y, \quad (2.3.6)$$

and thus we transform the data set (t_1, y_1, E_{y1}) to the equivalent set (t_1, z_1, E_{z1}) in order to proceed with the analysis. From Eq. (2.3.3), it is deduced that

$$z_i \approx p_1 + p_2 t_i \quad (i = 1, n), \quad (2.3.7)$$

or

$$\vec{z} \approx \bar{A} \bullet \vec{p} \quad (2.3.8)$$

in vector notation, where

$$A_{ij} = t_i^{j-1} \quad (i = 1, n; j = 1, 2). \quad (2.3.9)$$

Now, the standard equations and methods from Ref. 1 can be applied:

$$\bar{V}_p = (\bar{A}^T \bullet \bar{V}_z^{-1} \bullet \bar{A})^{-1}, \quad (2.3.10)$$

$$\vec{p} = \bar{V}_p \bullet \bar{A}^T \bullet \bar{V}_z^{-1} \bullet \vec{z}, \quad (2.3.11)$$

and the chi-square is

$$\chi^2 = (\vec{z} - \bar{A} \bullet \vec{p})^T \bullet \bar{V}_z^{-1} \bullet (\vec{z} - \bar{A} \bullet \vec{p}), \quad (2.3.12)$$

where \bar{V}_z is the covariance matrix derived from the data according to:

$$V_{zij} = \begin{cases} E_{zi}^2 \quad \text{or} \quad E_{yi}^2 / y_i^2 & (i = j), \\ 0 & (i \neq j). \end{cases} \quad (2.3.13)$$

Since the error E_T in the half life, T , is sought, further analysis is required:

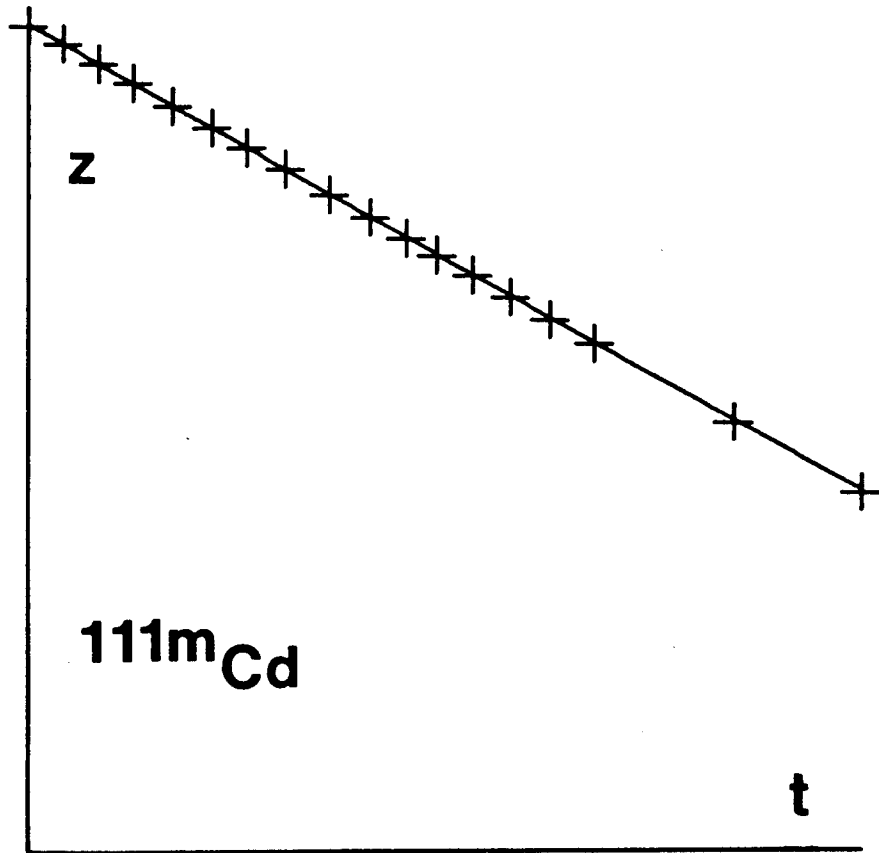
$$T = \tau \ln 2 = - \ln 2 / p_2, \quad (2.3.14)$$

$$\partial T / \partial p_2 = \ln 2 / p_2^2, \quad (2.3.15)$$

$$E_T = (\ln 2 / p_2^2) E_{p2}, \quad (2.3.16)$$

$$E_{p2} = (V_{p22})^{1/2}. \quad (2.3.17)$$

Numerical values for this example appear in Fig. (2.3.1). The plot presents the natural logarithm of the decay rate versus time. A linear fit is made to the transformed data, and the half life is related to the slope of the fitted line. for this example, the derived half life error is 0.12%; but, this is too small since the normalized chi-square, CHI^2_{NM} in Fig. (2.3.1), is 3.307. Thus, the error should be scaled by the square root of this value (equal to 1.82) to $\pm 0.22\%$, based on the actual scatter of the data (as discussed on pp. 33-34 of Ref. 1). Therefore, this experiment yields the value 48.99 ± 0.11 minutes for the half life of ^{111}mCd , when the data are analyzed as indicated in the present section.



T	Y	EY	Z	EZ
.0000E 00	.1153E 04	.2000E 01	.7050E 01	.1735E-02
.1200E 02	.9876E 03	.2000E 01	.6895E 01	.2025E-02
.2400E 02	.8298E 03	.2000E 01	.6721E 01	.2410E-02
.3600E 02	.7019E 03	.1500E 01	.6554E 01	.2137E-02
.4950E 02	.5777E 03	.1500E 01	.6359E 01	.2597E-02
.6300E 02	.4794E 03	.1500E 01	.6173E 01	.3129E-02
.7500E 02	.4031E 03	.1500E 01	.5999E 01	.3721E-02
.8800E 02	.3365E 03	.1200E 01	.5819E 01	.3566E-02
.1030E 03	.2714E 03	.1200E 01	.5604E 01	.4422E-02
.1170E 03	.2228E 03	.1200E 01	.5406E 01	.5386E-02
.1290E 03	.1858E 03	.1200E 01	.5225E 01	.6459E-02
.1395E 03	.1612E 03	.1000E 01	.5063E 01	.6203E-02
.1515E 03	.1358E 03	.1000E 01	.4911E 01	.7364E-02
.1645E 03	.1129E 03	.8000E 00	.4727E 01	.7086E-02
.1780E 03	.9248E 02	.8000E 00	.4527E 01	.8651E-02
.1930E 03	.7532E 02	.8000E 00	.4322E 01	.1062E-01
.2395E 03	.3857E 02	.5000E 00	.3652E 01	.1296E-01
.2820E 03	.2103E 02	.5000E 00	.3046E 01	.2378E-01

$$CZ(I,J) = \begin{cases} 1 & I=J \\ 0 & I \neq J \end{cases}$$

P,EP	.009E 01	.1107E-02
	-.1415E-01	.1747E-04
CP	.1000E 01	.6938E 00
	-.0938E 00	.1000E 01
CHI2	CHI2NM	
	.5292E 02	.3307E 01
HALF,EHALF		
	.469918E 02	.604841E-01

Figure 2.3.1: Derivation of the half life for ^{111m}Cd from decay data. T = time in minutes, Y = decay rate at time T, EY = error in Y. Z and EZ are transformed variables (see Section 2.3 of text). CZ = correlation matrix for EZ. P = parameters of fit, EP = errors for P, CP = correlation matrix for EP. CHI2 and CHI2NM are the chi-square and normalized chi-square for the fit, respectively.

2.4 Derivation of the Relative Efficiency Curve for a Ge(Li) Detector

Calibration of the relative efficiency of a photon detector as a function of gamma-ray energy is an important step in experiments such as those intended to measure $(n, n'\gamma)$ cross sections [6]. Most often, one measures the yield in the full-energy peak. It has been found that the relationship between efficiency ϵ and photon energy E can be approximated by the formula

$$\ln \epsilon = \sum_{j=1}^m p_j (\ln E)^{j-1} \quad (2.4.1)$$

In order to determine the coefficients p_j , the expression Eq. (2.4.1) is fitted to calibration data. Suppose one uses a series of K radioactive sources, each having several lines of known relative intensity. The aggregate of these K sources yields n lines. The normalizations of the various sets of relative efficiencies are different owing to different source strengths. Assume that one source is considered as a reference source, and all others are normalized relative to this one source, thereby eliminating all but one normalization constant. This procedure could be done, e.g., graphically. One thus obtains pairs of values

$[E_1(k_1), \epsilon_1(k_1)], \dots, [E_n(k_n), \epsilon_n(k_n)]$, where k_1 through k_n identify the

source $k = 1, \dots, K$. It is then assumed that each efficiency ϵ_i has a total error $E_{\epsilon i}$ which is composed of several components, i.e.,

$$E_{\epsilon i}^2 = E_{\epsilon Ri}^2 + E_{\epsilon Sk}^2 + E_{\epsilon Nk}^2, \quad (2.4.2)$$

where

$E_{\epsilon Ri}$ = random error,

$E_{\epsilon Sk}$ = a shape error characteristic of source k ,

$E_{\epsilon Nk}$ = A normalization error which comes from adjusting the "k" source shape to the reference source data.

For convenience, let $k = 1$ designate the reference source; therefore, $E_{\epsilon N1} = 0$. The energy error is assumed negligible in this analysis.

Ultimately, we define the correlation matrix \overline{C}_ϵ for the errors $E_{\epsilon i}$ as follows:

$$C_{\epsilon ij} = \begin{cases} 1 & \text{if } i = j, \\ \delta_{k_ik_j} (E_{\epsilon Nk}^2 + F_{ijk} E_{\epsilon Sk}^2) / (E_{\epsilon i} E_{\epsilon j}) & \\ \text{if } i \neq j, \text{ and } k \text{ is the common value,} & \\ \text{where } k_i = k_j, \text{ and } \delta_{k_ik_j} \text{ is the Kronecker delta.} & \end{cases} \quad (2.4.3)$$

Here, assume that

$$F_{ijk} = 1 - \frac{|E_i - E_j|}{\Delta E_k}, \quad (2.4.4)$$

when the two gamma ray lines with energies E_i and E_j originate from the same source "k". The interpretation of the correlation matrix \overline{C}_ϵ is relatively simple. First, there is a correlated error $E_{\epsilon Nk}$ for all lines "i" and "j" from the same source, "k", which originates due to normalization of this set to the reference source. If $k = 1$ (reference source itself), then the term vanishes. The second component is modified by the factor F_{ijk} . The purpose of this factor is to weaken the correlation between two lines from the same source as the energy separation increases. The shape correlation is assumed to vanish between the two lines in any set, "k", whose energy difference $|E_i - E_j|$ equals the maximum energy difference, ΔE_k , for the set. This, of course, is strictly an assumption which can be modified if more specific information on correlations is available.

The experimental calibration data given above cannot be used directly for a least-squares analysis. The values $(E_i, \epsilon_i, E_{\epsilon i})$ and \overline{C}_ϵ must be converted to an equivalent set (t_i, z_i, E_{zi}) and \overline{C}_z where

$$t_i = \ln E_i \quad (i = 1, n), \quad (2.4.5)$$

$$z_i = \ln \epsilon_i \quad (i = 1, n). \quad (2.4.6)$$

Then, Eq. (2.4.1) becomes

$$z = \sum_{j=1}^m p_j t^{j-1}. \quad (2.4.7)$$

Clearly,

$$E_{zi} = (\partial z_i / \partial \epsilon_i) E_{\epsilon i} = E_{\epsilon i} / \epsilon_i \quad (i = 1, n), \quad (2.4.8)$$

but conversion of \bar{C}_ϵ to \bar{C}_z is not so obvious.

Utilizing the formalism from Section IV, Ref. 1:

$$z_i = z(\epsilon_1, \dots, \epsilon_n) = \ln \epsilon_i \quad (i = 1, n),$$

$$S_i = \begin{bmatrix} 0 & & & 0 \\ & \ddots & & \\ & & (\partial z_i / \partial \epsilon_i) & \\ 0 & & & \ddots & 0 \end{bmatrix} \quad (i=1, n), \quad (2.4.9)$$

thus the covariance matrix \bar{V}_z is given by

$$V_{zij} = (\bar{S}_i \bullet \vec{E}_\epsilon)^T \bullet \bar{C}_\epsilon \bullet (\bar{S}_j \bullet \vec{E}_\epsilon) \quad (2.4.10)$$

(i, j = 1; n),

and the correlation matrix \bar{C}_z is

$$C_{zij} = V_{zij} / (E_{zi} E_{zj}) \quad (2.4.11)$$

(i, j = 1, n).

Eq. (2.4.10) reduces to the expression

$$V_{zij} = E_{\epsilon_i} E_{\epsilon_j} C_{\epsilon ij} / (\epsilon_i \epsilon_j) \quad (2.4.12)$$

(i, j = 1, n).

Based on Eqs. (2.4.8), (2.4.11) and (2.4.12), it is concluded that

$$C_{zij} = C_{\epsilon ij} \quad (i, j = 1, n). \quad (2.4.13)$$

Define \bar{A} according to

$$A_{ij} = t_i^{j-1} \quad (i = 1, n; j = 1, m). \quad (2.4.14)$$

Then, the standard equations from Section VII, Ref. 1, apply:

$$\vec{z} \approx \bar{A} \bullet \vec{p}, \quad (2.4.15)$$

$$\bar{V}_p = (\bar{A}^T \bullet \bar{V}_z^{-1} \bullet \bar{A})^{-1}, \quad (2.4.16)$$

$$\vec{p} = \bar{V}_p \bullet \bar{A}^T \bullet \bar{V}_z^{-1} \bullet \vec{z}, \quad (2.4.17)$$

with chi-square given by

$$\chi^2 = (\vec{z} - \bar{A} \bullet \vec{p})^T \bullet \bar{V}_z^{-1} \bullet (\vec{z} - \bar{A} \bullet \vec{p}). \quad (2.4.18)$$

Once the solution is available, it is necessary to perform an inverse transformation to find the error in ϵ for a given E , and the correlation in the efficiency errors at two different energies. According to Section III, Ref. 1, and neglecting errors in t ,

$$z = z(\vec{p}, t), \quad (2.4.19)$$

$$E_z^2 = (\bar{S} \bullet \bar{E}_p)^T \bullet \bar{C}_p \bullet (\bar{S} \bullet \bar{E}_p), \quad (2.4.20)$$

$$\bar{S} = \begin{bmatrix} (\partial z / \partial p_1) & & 0 \\ & \ddots & \\ 0 & & (\partial z / \partial p_m) \end{bmatrix}, \quad (2.4.21)$$

$$(\partial z / \partial p_j) = t^{j-1} \quad (j=1, m). \quad (2.4.22)$$

But, since

$$z = \ln \epsilon, \quad (2.4.23)$$

with

$$t = \ln E, \quad (2.4.24)$$

then

$$\epsilon = e^z, \quad (2.4.25)$$

and

$$E_\epsilon = (\partial\epsilon/\partial z) E_z = \epsilon^z E_z. \quad (2.4.26)$$

For the errors at two different energies E_i and E_j , we have

$$\epsilon_i = \epsilon(\vec{p}, E_i), \quad (2.4.27)$$

$$\epsilon_j = \epsilon(\vec{p}, E_j), \quad (2.4.28)$$

and

$$M_{ij} = (\bar{S}_i \bullet \vec{E}_p)^T \bullet \bar{C}_p \bullet (\bar{S}_j \bullet \vec{E}_p), \quad (2.4.29)$$

according to the formalism from Section VII, Ref. 1, with

$$\bar{S}_i = \begin{bmatrix} (\partial\epsilon/\partial p_1)_i & & 0 \\ & \ddots & \\ 0 & & (\partial\epsilon/\partial p_m)_i \end{bmatrix}, \quad (2.4.30)$$

$$(\partial\epsilon/\partial p_j)_i = \tau_i^{j-1} \epsilon_i. \quad (2.4.31)$$

Table (2.4.1) provides the numerical values for a specific example. Two sources, ^{152}Eu and ^{154}Eu , provide data which can be used to calibrate a Ge(Li) detector for relative efficiency over the energy range 250-1600 keV. ^{152}Eu is treated as the reference source, and the ^{154}Eu points were adjusted to ^{152}Eu graphically, with an assumed normalization error, $E_{N2} = 5.0$ relative units. A shape error parameter of ± 5.0 relative units is assumed for both ^{152}Eu and ^{154}Eu . The correlation matrix \bar{C} (and thus \bar{C}_p) is calculated from these data according to Eq. (2.4.3), but this 23×23 matrix is too large to exhibit here.

Application of the formalism in this Section leads to the results presented in Fig. (2.4.1), for $m = 2$. A three-parameter fit leads to a slightly poorer fit (larger normalized chi-square), and higher-order fits were unstable due to computer precision limitations. Since the normalized chi-square for $m = 2$ is near unity, the solution represented by Fig. (2.4.1) is satisfactory. The formalism also permits derivation of the efficiency at an arbitrary energy point along the curve, and it provides the corresponding uncertainty. The results for several selected energies also appear in Fig. (2.4.1). From this analysis, it appears that the relative efficiency can be determined with an uncertainty of the order of 1-2%, depending upon the energy.

Table 2.4.1. Ge(Li) Detector Relative Efficiency Data

Source	E (keV)	ϵ (Rel)	^a			ΔE_k (keV)	Index
			$E_{\epsilon G}$ (Rel)	E_{SK} (Rel)	E_{Nk} (Rel)		
Eu-152	244.7	1229.0	60.22	5.0	0	1163.3	1
	296.0	974.4	101.3				
	344.3	856.2	25.69				
	367.8	832.0	65.72				
	411.1	817.0	49.02				
	444.0	696.7	39.71				
	778.9	411.5	15.64				
	867.3	400.1	18.80				
	964.0	348.7	13.95				
	1088.0	304.8	14.33				
	1112.0	311.2	12.45				
Eu-154	1408.0	244.4	9.78			1349.0	2
	248.0	1185.0	42.64	5.0	5.0		
	444.4	743.6	55.77				
	591.7	513.0	27.71				
	692.4	497.7	21.90				
	723.3	443.3	12.41				
	756.9	433.6	15.60				
	873.2	384.7	13.85				
	1000.0	336.8	9.43				
	1274.0	263.4	5.27				
	1495.0	249.2	14.21				
1597.0	241.1	8.68					

^a $E_{\epsilon G}^2 = E_{\epsilon R}^2 + E_{\epsilon SK}^2$ as defined in text of Section 2.4.

Fitting Information

```

E,F,EF
,2447E 03 ,1222E 04 ,6022E 02 4.7%
,2960E 03 ,9744E 03 ,1013E 03
,3443E 03 ,8562E 03 ,2569E 02
,3678E 03 ,8320E 03 ,6572E 02
,4111E 03 ,8170E 03 ,4902E 02
,4440E 03 ,6967E 03 ,3971E 02
,7789E 03 ,4115E 03 ,1564E 02
,8673E 03 ,4001E 03 ,1880E 02 4.7%
,9640E 03 ,3487E 03 ,1395E 02 4.9%
,1088E 04 ,3048E 03 ,1433E 02
,1112E 04 ,3112E 03 ,1245E 02
,1408E 04 ,2444E 03 ,9780E 01
,2480E 03 ,1185E 04 ,4293E 02
,4444E 03 ,7436E 03 ,5599E 02
,5917E 03 ,5130E 03 ,2816E 02
,6924E 03 ,4977E 03 ,2246E 02
,7233E 03 ,4433E 03 ,1338E 02
,7569E 03 ,4336E 03 ,1638E 02
,8732E 03 ,3847E 03 ,1472E 02
,1000E 04 ,3368E 03 ,1067E 02
,1274E 04 ,2634E 03 ,7264E 01
,1495E 04 ,2492E 03 ,1500E 02
,1597E 04 ,2411E 03 ,1002E 02

P,EP
,1205E 02 ,1121E 00 6.32%
-,9020E 00 ,1739E-01 2.1%
CP
,1000E 01 ,.9944E 00
-,9944E 00 ,1000E 01
CHI2,CHI2NM
,2447E 02 ,1165E 01
    
```

Values Derived from Fitted Curve

```

E,F,EF
,2000E 03 ,1438E 04 ,3257E 02 2.2%
,4000E 03 ,7696E 03 ,1069E 02
,6000E 03 ,5339E 03 ,6328E 01
,8000E 03 ,4118E 03 ,5267E 01 1.3%
,1000E 04 ,3368E 03 ,1067E 01
,1200E 04 ,2857E 03 ,1790E 01
,1400E 04 ,2486E 03 ,1663E 01 1.4%
    
```

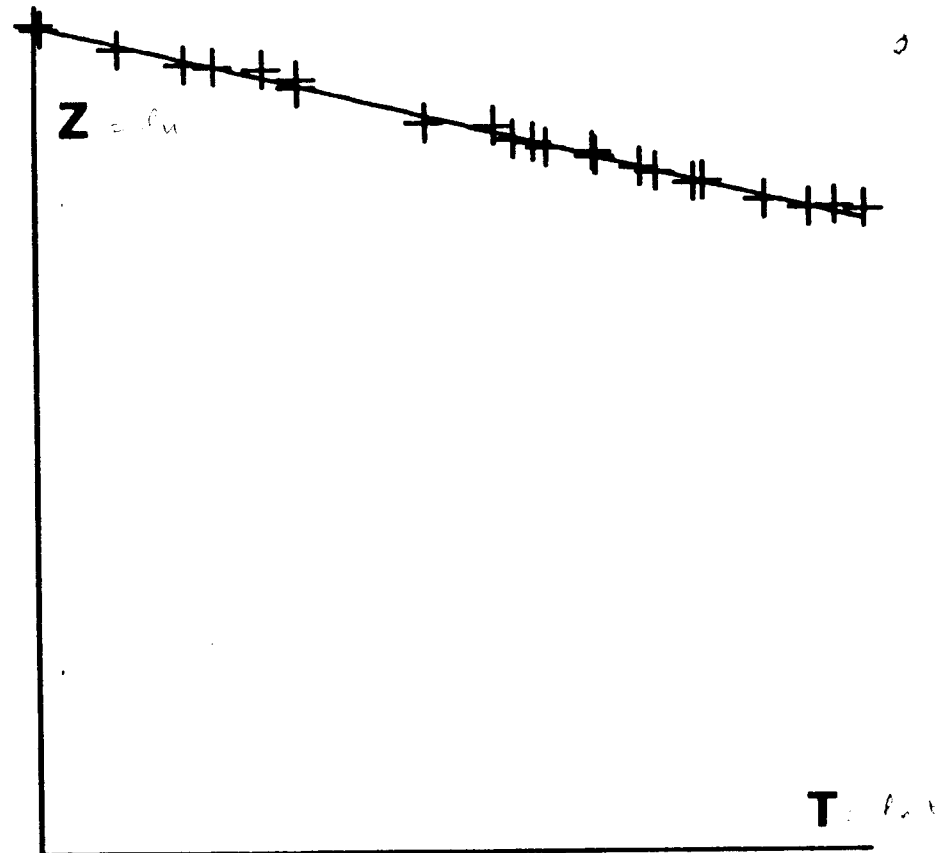


Figure 2.4.1: Results of relative efficiency calibration for a Ge(Li) detector. E = gamma-ray energy, F = relative full-energy efficiency, EF = error in F. The errors EF are partially correlated, but matrix is too large to exhibit. P = parameters of fit, EP = errors in P, CP = correlation matrix for EP. CHI2 is the chi-square and CHI2NM is the normalized chi-square, respectively. Z = natural logarithm of the relative efficiency, T = natural logarithm of the energy. Zero of T scale is suppressed in plot.

2.5 Normalization of a Relative Efficiency Curve for a Ge(Li) Detector

Section 2.4 deals with generation of a relative efficiency curve for a Ge(Li) detector. Often, however, one is required to know the absolute efficiency of the detector in a particular experimental configuration. One way to obtain such a calibration is to normalize the relative efficiency curve at a single energy by means of measurements performed using an absolutely-calibrated gamma-ray source [6].

Let ϵ_0 be the absolute efficiency at energy E_0 , with E_{ϵ_0} the uncertainty. Let ϵ_R be the relative efficiency, given by

$$\epsilon_R(\vec{p}, E) = \exp \left[\sum_{j=1}^m p_j (\ln E)^{j-1} \right]. \quad (2.5.1)$$

Then the absolute efficiency ϵ_A at energy E , based on normalization at energy E_0 , is

$$\epsilon_A(\vec{p}, \epsilon_0, E_0, E) = \epsilon_0 \epsilon_R(\vec{p}, E) / \epsilon_R(\vec{p}, E_0). \quad (2.5.2)$$

Generation of the covariance matrix for a set of derived efficiencies at n energies E_q ($q = 1, n$), is a problem in error propagation which follows the formalism of Section IV, Ref. 1. Define \vec{E}_x as

$$\vec{E}_x = \begin{bmatrix} \vec{E}_p \\ E_{\epsilon_0} \end{bmatrix}, \quad (2.5.3)$$

and \bar{C}_x , considering the errors in \vec{p} and ϵ_0 to be uncorrelated, as

$$\bar{C}_x = \begin{bmatrix} \bar{C}_p & 0 \\ 0 & 1 \end{bmatrix}. \quad (2.5.4)$$

Also, define a sensitivity matrix \bar{S}_x by

$$\bar{S}_x = \begin{bmatrix} (\partial \epsilon_A / \partial p_1) & & & 0 \\ & \ddots & & \\ & & (\partial \epsilon_A / \partial p_m) & \\ 0 & & & (\partial \epsilon_A / \partial \epsilon_0) \end{bmatrix}. \quad (2.5.5)$$

\bar{S}_x depends upon the energy, E. Based on Eqs. (2.5.1) and (2.5.2), the partial derivatives indicated in Eq. (2.5.5) are:

$$(\partial \epsilon_A / \partial p_k) = \epsilon_A [(\ln E)^{k-1} - (\ln E_0)^{k-1}] \quad (k = 1, m), \quad (2.5.6)$$

$$(\partial \epsilon_A / \partial \epsilon_0) = \epsilon_A / \epsilon_0. \quad (2.5.7)$$

Given a specific set of energies $E_1, \dots, E_q, \dots, E_n$, one can derive absolute efficiencies $\epsilon_{A1}, \dots, \epsilon_{Aq}, \dots, \epsilon_{An}$. The covariance matrix $\bar{V}_{\epsilon A}$ for these derived results can then be calculated from the formula

$$V_{\epsilon Aqr} = (\bar{S}_{xq} \bullet \vec{E}_x)^T \bullet \bar{C}_x \bullet (\bar{S}_{xr} \bullet \vec{E}_x) \quad (q, r = 1, n), \quad (2.5.8)$$

where \bar{S}_{xq} and \bar{S}_{xr} correspond to \bar{S}_x from Eq. (2.5.5), evaluated at energies E_q and E_r , respectively. From $\bar{V}_{\epsilon A}$, one can calculate the error $E_{\epsilon A}$ in the derived efficiencies and the correlation matrix $\bar{C}_{\epsilon A}$ according to the formulas:

$$E_{\epsilon Aq} = (V_{\epsilon Aqq})^{1/2} \quad (q = 1, n), \quad (2.5.9)$$

$$C_{\epsilon Aqr} = V_{\epsilon Aqr} / (E_{\epsilon Aq} E_{\epsilon Ar}) \quad (q, r = 1, n). \quad (2.5.10)$$

The relative efficiency curve ϵ_R derived in Section 2.4 will serve for use in a numerical example. The absolute efficiency for a true co-axial Ge(Li) detector was measured in a geometry which placed it at a distance ~ 142 cm from the origin of radiation. A calibrated U.S. National Bureau of Standards point source of ^{22}Na was used. The calibration energy was $E_0 = 1275$ keV, and the value $\epsilon_0 = 8.200 \times 10^{-5}$ ($\pm 1.9\%$) was obtained for this configuration. This is a full-energy-peak efficiency, inclusive of solid angle. The error of 1.9% consists of a 1.5% error in source strength calibration, and an error of 1.2% in the calibration measurement, combined in quadrature.

Figure (2.5.1) summarizes the results of an error propagation calculation based upon the methods described in this section. Absolute efficiencies were calculated at eight gamma-ray energies in the range 200-1600 keV. The errors in these derived quantities range from 1.9 - 3.8%. The absolute errors are smallest near the normalization energy $E_0 = 1275$ keV and largest at the 200 - keV point, which is the most remote in energy. The correlation pattern reflected in the 8×8 matrix CF is consistent with expectations. Correlations are strong (> 97%) for adjacent energy points, but they diminish to ~30% for the two points having the largest energy separation.

The errors in these derived efficiencies need not be adjusted since it was observed in Section 2.4 that the solution parameter set \hat{p} for the relative efficiency curve yielded a normalized chi-square of nearly unity.

P, EP							
.1205E 02	.1121E 00						
-.9020E 00	.1739E-01						
CP							
.1000E 01	-.9944E 00						
-.9944E 00	.1000E 01						
EO, FO, EFO							
.1274E 04	.0200E-05	.1256E-06					
E, F, EF							
.2000E 03	.4357E-04	.1629E-05					
.4000E 03	.2331E-04	.8456E-06					
.6000E 03	.1617E-04	.3732E-06					
.8000E 03	.1248E-04	.2577E-06					
.1000E 04	.1020E-04	.1985E-06					
.1200E 04	.8655E-05	.1647E-06					
.1400E 04	.7531E-05	.1436E-06					
.1600E 04	.6677E-05	.1296E-06					
CF							
.1000E 01	.9752E 00	.9072E 00	.8050E 00	.6825E 00	.5545E 00	.4322E 00	.3217E 00
.9752E 00	.1000E 01	.9778E 00	.9163E 00	.8273E 00	.7249E 00	.6210E 00	.5232E 00
.9072E 00	.9778E 00	.1000E 01	.9799E 00	.9267E 00	.8532E 00	.7715E 00	.6902E 00
.8050E 00	.9163E 00	.9799E 00	.1000E 01	.9830E 00	.9401E 00	.8829E 00	.8207E 00
.6825E 00	.8273E 00	.9267E 00	.9830E 00	.1000E 01	.9867E 00	.9541E 00	.9116E 00
.5545E 00	.7249E 00	.8532E 00	.9401E 00	.9867E 00	.1000E 01	.9901E 00	.9663E 00
.4322E 00	.6210E 00	.7715E 00	.8829E 00	.9541E 00	.9901E 00	.1000E 01	.9929E 00
.3217E 00	.5232E 00	.6902E 00	.8207E 00	.9116E 00	.9663E 00	.9929E 00	.1000E 01

Figure 2.5.1: Absolute efficiencies and corresponding covariance matrix for a Ge(Li) detector. P and EP are the relative efficiency curve parameters and errors, respectively, while CP is the correlation matrix for these parameters (see Section 2.4). EO, FO and EFO are the normalization point energy, absolute efficiency and error in the absolute efficiency, respectively. E, F and EF are the energy, derived efficiency and error in the derived efficiency, respectively, calculated at several energies. CF is the corresponding correlation matrix for these derived results.

2.6. Background Subtraction for a Spectrum

An isolated gamma-ray line in a Ge(Li) detector spectrum will often appear as shown in Fig. (2.6.1). Characteristically, there will be a rather distinct peak, which can be identified as the full-energy, single-escape or double-escape peak, superimposed upon a slowly varying distribution resulting from Compton events and general background. The peak yield minus background is sought. One possible procedure is to fit a smooth curve (usually a polynomial) to the distribution on each side of the peak, e.g., regions (i_1, i_2) and (i_3, i_4) indicated in Fig. (2.6.1). The underlying distribution in the region of the peak, i.e., (i_2, i_3) indicated in Fig. (2.6.1), is estimated by interpolation via the fitted polynomial.

Let

i = specific channel in the spectrum,

N_i = channel count,

and define a polynomial function F to represent the background distribution according to

$$F(x) = \sum_{j=1}^m p_j x^{j-1}, \quad (2.6.1)$$

where

x = floating point number representing channel number treated as a continuous variable,

\vec{p} = vector of polynomial expansion coefficients p_1, \dots, p_m .

If x_i is a floating point number equivalent to integer channel i , then we can define two sets of quantities \vec{z} (z_1, \dots, z_n) and \vec{y} (y_1, \dots, y_n) as follows:

$$\begin{aligned} z_1 &= x_{i_1} & , & & y_1 &= N_{i_1} & , \\ & \vdots & & & \vdots & & \\ & \vdots & & & \vdots & & \\ & \vdots & & & \vdots & & \\ z_{i_2-i_1+1} &= x_{i_2} & , & & y_{i_2-i_1+1} &= N_{i_2} & , \\ & \vdots & & & \vdots & & \\ z_{i_2-i_1+2} &= x_{i_3} & , & & y_{i_2-i_1+2} &= N_{i_3} & , \\ & \vdots & & & \vdots & & \\ z_n &= x_{i_4} & , & & y_n &= N_{i_4} & , \end{aligned} \quad (2.6.2)$$

$$n = i_2 + i_4 - i_1 - i_3 + 2 .$$

We seek a parameter set \vec{p} such that

$$y_k \approx F(z_k) = \sum_{j=1}^m p_j z_k^{j-1}. \quad (2.6.3)$$

Define matrix \bar{A} such that the elements are

$$A_{kj} = z_k^{j-1} \quad (k = 1, n \text{ and } j = 1, m). \quad (2.6.4)$$

Then, Eq. (2.6.3) assumes the form

$$\vec{y} \approx \bar{A} \bullet \vec{p} \quad (2.6.5)$$

which is equivalent to Eq. (113) in Ref. 1.

The procedures in Section VII of Ref. 1 can be applied to find the best-fit array \vec{p} , provided that we introduce a covariance matrix for \vec{y} . It is reasonable to assume that the uncertainty in the channel counts of a spectrum is largely statistical and that the channel-to-channel correlations can be neglected. Thus, an error vector $E_y (E_{y1}, \dots, E_{yn})$ is generated from the formula

$$E_{yk} = y_k^{1/2} \quad (k = 1, \dots, n), \quad (2.6.6)$$

and the correlation matrix \bar{C}_y is given by

$$C_{yij} = \delta_{ij} \quad (\text{Kronecker delta}) \quad (2.6.7)$$

(i, j = 1, n).

The covariance matrix \bar{V}_y is given by

$$V_{yij} = C_{yij} E_{yi} E_{yj} \quad (2.6.8)$$

(i, j = 1, n),

according to Eq. (34) of Ref. 1.

The solution to the problem follows readily from the procedures described in Section VII of Ref. 1:

$$\bar{V}_p = (\bar{A}^T \bullet \bar{V}_y^{-1} \bullet \bar{A})^{-1}, \quad (2.6.9)$$

$$\vec{p} = \bar{V}_p \bullet \bar{A}^T \bullet \bar{V}_y^{-1} \bullet \vec{y} , \quad (2.6.10)$$

with the chi-square given by

$$\chi^2 = (\vec{y} - \bar{A} \bullet \vec{p})^T \bullet \bar{V}_y^{-1} \bullet (\vec{y} - \bar{A} \bullet \vec{p}) . \quad (2.6.11)$$

This procedure yields the parameters \vec{p} and their covariance matrix. What is really sought is the net peak yield, minus background, and its uncertainty. The peak yield S is given by

$$\begin{aligned} S &= \sum_{i=i_\ell}^{i_h} [N_i - F(x_i)] \\ &= \sum_{i=i_\ell}^{i_h} [N_i - \sum_{j=1}^m p_j x_i^{j-1}] \\ &= N - \sum_{j=1}^m b_j p_j , \end{aligned} \quad (2.6.12)$$

where

$$N = \sum_{i=i_\ell}^{i_h} N_i , \quad (2.6.13)$$

$$b_j = \sum_{i=i_\ell}^{i_h} x_i^{j-1} \quad (j = 1, m) . \quad (2.6.14)$$

The error in N is

$$E_N = N^{1/2} , \quad (2.6.15)$$

and it is not correlated with the parameter errors \vec{E}_p . The procedures in Section III of Ref. 1 can be used to show that the error in S can be derived from the formula

$$E_S^2 = E_N^2 + \sum_{i=1}^m \sum_{j=1}^m C_{pij} b_i b_j E_{pi} E_{pj}. \quad (2.6.16)$$

\bar{C}_p is the error correlation matrix for \vec{p} and \vec{E}_p is the error vector for \vec{p} . These can be derived from the solution covariance matrix \bar{V}_p according to

$$E_{pi} = (V_{pii})^{1/2} \quad (i=1,m), \quad (2.6.17)$$

$$C_{pij} = V_{pij} / (E_{pi} E_{pj}) \quad (i,j=1,m). \quad (2.6.18)$$

The coefficients b_i are diagonal elements of a sensitivity matrix which has all zero off-diagonal elements.

The spectrum shown in Fig. (2.6.1) was analyzed using this formalism. Numerical results appear in Fig. (2.6.2). The background was fitted with a straight line ($m = 2$). The polynomial coefficient errors are quite large: $p_1 (\pm 13.2\%)$, $p_2 (\pm 73.2\%)$. These errors are anti-correlated to a high degree (83.4%). The normalized chi-square,

$$(\chi^2)_{\text{norm}} = \chi^2 / (n-m), \quad (2.6.19)$$

is 2.97 which implies that the scatter of points in the spectrum exceeds statistical expectations and therefore there is >90% chance of encountering p_1 or p_2 outside errors. The net peak yield minus background is 614.9 counts with error $\pm 4.9\%$. The statistical error in the total counts N for the region is the dominant factor. If correlations in the errors for the solution vector \vec{p} are ignored (as is usually the practice), the calculated error E_{Su} is $\pm 6.1\%$ which is noticeably larger than the result based on consideration of covariances.

Since the normalized chi-square for this problem is considerably larger than unity, one might consider scaling the solution covariance \bar{V}_p by this factor, as discussed in Ref. 1, pp. 33-34. Eq. (2.6.16) would then be modified accordingly to read

$$(E_S^2)_{\text{Adjusted}} = E_N^2 + \frac{\chi^2}{(n-m)} \sum_{i=1}^m \sum_{j=1}^m C_{pij} b_i b_j E_{pi} E_{pj} \quad (2.6.20)$$

The result for the present problem would be an increase in the error for S from $\pm 4.9\%$ to $\pm 5.6\%$.

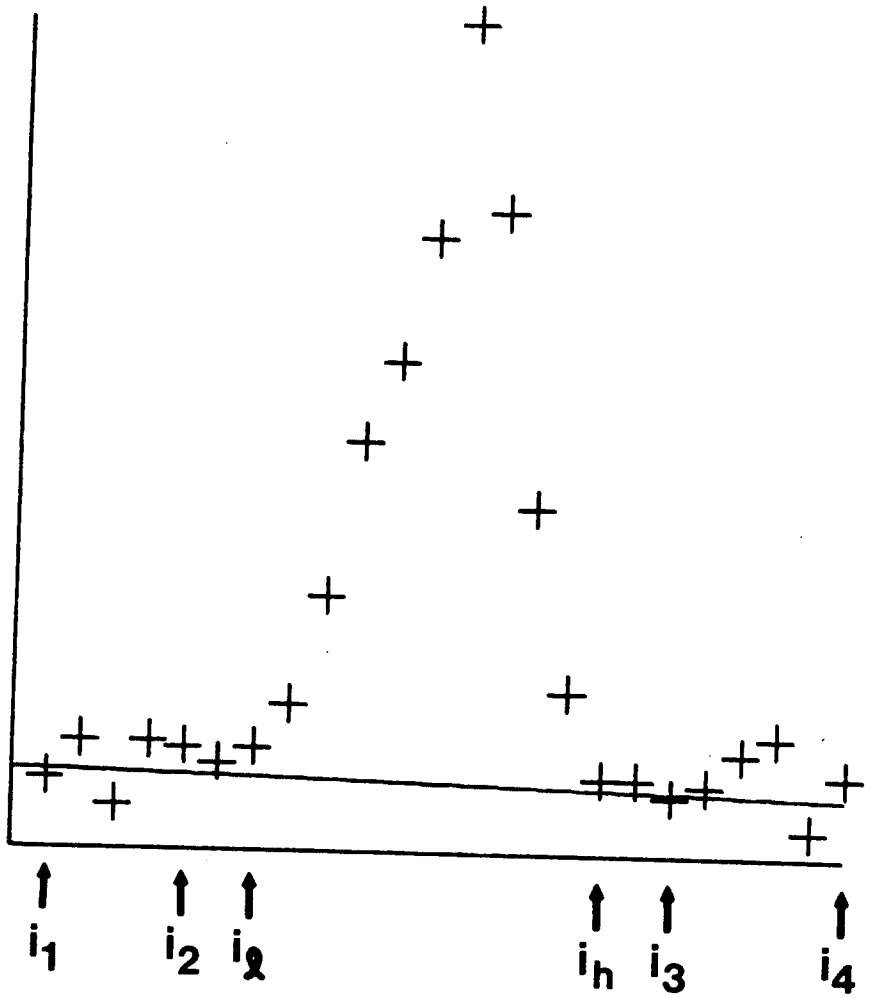


Figure 2.6.1: Plot of spectrum from the problem presented in Section 2.6. Solid curve is the fitted background. Peak yield consists of the total counts between the channels indexed by "l" and "h" minus the interpolated background represented by the curve drawn through this region.

```

NDATA
 24
I,ND
 1 13
 2 20
 3 8
 4 20
 5 19
 6 16
 7 19
 8 27
 9 47
10 76
11 91
12 114
13 154
14 119
15 64
16 30
17 14
18 14
19 11
20 13
21 19
22 22
23 5
24 15
I1,I2,I3,I4
 1 5 19 24
IL,IH
 7 17
K,z,Y,EY
 1 ,1000E 01 ,1300E 02 ,3606E 01
 2 ,2000E 01 ,2000E 02 ,4472E 01
 3 ,3000E 01 ,8000E 01 ,2828E 01
 4 ,4000E 01 ,2000E 02 ,4472E 01
 5 ,5000E 01 ,1900E 02 ,4359E 01
 6 ,1900E 02 ,1100E 02 ,3317E 01
 7 ,2000E 02 ,1300E 02 ,3606E 01
 8 ,2100E 02 ,1900E 02 ,4359E 01
 9 ,2200E 02 ,2200E 02 ,4690E 01
10 ,2300E 02 ,5000E 01 ,2236E 01
11 ,2400E 02 ,1500E 02 ,3873E 01

```

```

A
,1000E 01 ,1000E 01
,1000E 01 ,2000E 01
,1000E 01 ,3000E 01
,1000E 01 ,4000E 01
,1000E 01 ,5000E 01
,1000E 01 ,1900E 02
,1000E 01 ,2000E 02
,1000E 01 ,2100E 02
,1000E 01 ,2200E 02
,1000E 01 ,2300E 02
,1000E 01 ,2400E 02
P,EP,B
,1459E 02 ,1926E 01 ,1100E 02
-,1547E 00 ,1133E 00 ,1320E 03
CP
,1000E 01-,8343E 00
-,8343E 00 ,1000E 01
CHI2,CHI2NM
,2674E 02 ,2971E 01
S,ES,ESU,EN
,6149E 03 ,2998E 02 ,3778E 02 ,2748E 02

```

Figure 2.6.2: Part of computer printout generated by the program used to analyze background subtraction problem from Section 2.6. $ND = N_1$, $CHI2 = \chi^2$, and $CHI2NM = (\chi^2)/(n-m)$ for $n = 11$ and $m = 2$. All other parameters can be easily identified by referring to the text in Section 2.6.

2.7 Simultaneous Fitting of Two Peaks in a Spectrum

Consider the problem where two peaks in a spectrum are partially resolved, e.g., examine the 996- and 1005- keV full-energy peaks in a Ge(Li) detector spectrum of ^{154}Eu decay gamma rays. Although more complex peak shapes are often used for such fittings, simple Gaussian shapes will be used in the present analysis.

The input data consist of n points y_i , corresponding to background corrected channel counts. Assume a constant background B with error E_B . Then

$$y_i = N_i - B \quad (i = 1, n), \quad (2.7.1)$$

$$E_{y_i}^2 = N_i + E_B^2 \quad (i = 1, n),$$

where N_i is the raw channel count, subject only to uncorrelated statistical errors, and E_{y_i} is the total error in y_i . The background error E_B is 100% correlated through all the data points, so the covariance matrix V_y is given by

$$V_{y_{ij}} = \begin{cases} E_{y_i}^2 & (i = j) \\ E_B^2 & (i \neq j) \end{cases} \quad (i, j=1, n), \quad (2.7.2)$$

according to the discussion in Section III, Ref. 1.

A function F of variables x and \vec{p} is used to fit the data, so

$$y_i \approx F(x_i, \vec{p}) \quad (i = 1, n), \quad (2.7.3)$$

where x_i is the channel corresponding to y_i and \vec{p} is the parameter vector to be optimized by the fitting procedure. In the present example,

$$F(x, \vec{p}) = p_1 e^{-p_2^2(x - p_3)^2} + p_4 e^{-p_5^2(x - p_6)^2} \quad (2.7.4)$$

is assumed, so \vec{p} is a vector of dimension $m = 6$. Clearly F is nonlinear in most of its parameters, so linear least-squares analysis is not directly applicable. One approach is to select an initial-guess vector \vec{p}_0 , linearize the problem by performing a Taylor's series expansion, solve this linear problem by linear least squares, then iterate the procedure as often as is needed to converge toward a final solution \vec{p} which is acceptable. The procedure is described in Section IX of Ref. 1 and also in the present Appendix. The fundamentals will be outlined in this section as well, for the convenience of the reader. While there is no guarantee that this procedure always converges toward a reasonable solution, it is rather likely that it will in many cases, provided that the initial guess vector \vec{p}_0 is physically reasonable and not too violently different from the expected final solution \vec{p} , and that F is a physically valid approximation.

If \vec{s} , \vec{z} and \bar{A} are defined by

$$\vec{s} = \vec{p} - \vec{p}_0, \quad (2.7.5)$$

$$z_{oi} = y_i - F(x_i, \vec{p}_0) \quad (i = 1, n), \quad (2.7.6)$$

$$A_{ij} = \frac{\partial F}{\partial p_j}(x_i, \vec{p}_0) \quad (i = 1, n; j = 1, m), \quad (2.7.6a)$$

then the important formulas involved in deriving the solution are, the initial chi-square,

$$X_o^2 = \vec{z}_o^T \bullet \bar{V}_y^{-1} \bullet \vec{z}_o, \quad (2.7.7)$$

with

$$\bar{V}_p = (\bar{A}^T \bullet \bar{V}_y^{-1} \bullet \bar{A})^{-1}, \quad (2.7.8)$$

$$\vec{s} = \bar{V}_p \bullet \bar{A}^T \bullet \bar{V}_y^{-1} \bullet \vec{z}, \quad (2.7.9)$$

$$\vec{p} = \vec{p}_0 + \vec{s}, \quad (2.7.10)$$

$$z_i = y_i - F(x_i, \vec{p}), \quad (2.7.11)$$

and the solution chi-square,

$$X^2 = \vec{z}^T \bullet \bar{V}_y^{-1} \bullet \vec{z}. \quad (2.7.12)$$

The quantities \vec{p} , \bar{V}_p , \vec{z} and X^2 correspond to the first-pass solution. Iteration proceeds until convergence is achieved. One possible convergence criterion is to look for X^2 convergence, e.g., the solution is assumed to be reached when the fractional change in X^2 falls below some small number δ for the previous iteration. This is the approach discussed in the Appendix.

In this problem, the partial derivatives of F are

$$\frac{\partial F}{\partial p_1}(x, \vec{p}) = e^{-p_2^2(x - p_3)^2}, \quad (2.7.13)$$

$$\frac{\partial F(x, \vec{p})}{\partial p_2} = -2p_1 p_2 (x - p_3)^2 e^{-p_2^2 (x - p_3)^2}, \quad (2.7.14)$$

$$\frac{\partial F(x, \vec{p})}{\partial p_3} = 2p_1 p_2^2 (x - p_3) e^{-p_2^2 (x - p_3)^2}, \quad (2.7.15)$$

$$\frac{\partial F(x, \vec{p})}{\partial p_4} = e^{-p_5^2 (x - p_6)^2}, \quad (2.7.16)$$

$$\frac{\partial F(x, \vec{p})}{\partial p_5} = -2p_4 p_5 (x - p_6)^2 e^{-p_5^2 (x - p_6)^2}, \quad (2.7.17)$$

$$\frac{\partial F(x, \vec{p})}{\partial p_6} = 2p_4 p_5^2 (x - p_6) e^{-p_5^2 (x - p_6)^2}. \quad (2.7.18)$$

For this example, a background B of 85 counts with an error of ± 3 counts was estimated from the spectral data. Fig. (2.7.1) presents the important parameters of the problem. The first-guess parameters, \vec{p}_0 , correspond to a chi-square of 6995.0, a very large value. The first iteration reduced chi-square to 885.5, still quite large. The second iteration reduced chi-square even further to 177.1. This corresponds to a normalized chi-square of 8.855, since the number of degrees of freedom is 20 for this problem (26 points, 6 parameters). When a third iteration was attempted, there was a serious divergence of the analysis into a region of parameter space \vec{p} which is non-physical for this problem, and the resultant chi-square was enormous. Therefore, iteration was terminated at the second step, which produced the values given in Fig. (2.7.1) and yields the plot in Fig. (2.7.2).

From Fig. (2.7.2), it is clear that the two peaks are nearly resolved, and therefore the methods of Section 2.6 would probably be more applicable to the problem of determining the peak yield. Furthermore, the final normalized chi-square of 8.855 indicates, most likely, that the double-Gaussian spectrum shape assumed for the analysis was not very satisfactory. However, this example does offer some insight into role of covariances in such problems. Since the normalized chi-square is considerably larger than the value of about unity which one would expect from a good fit, one could scale the solution covariance matrix according to the rule

$$(\bar{V}_p)_{\text{adjusted}} = (\bar{V}_p) X^2 / (n-m), \quad (2.7.19)$$

as discussed on pp. 33-34 of Ref. 1. For this example, this would imply multiplying all parameter errors by about 3. The correlation matrix C_p in Fig. (2.7.1) indicates that the errors for the width and height parameters of each individual Gaussian component are strongly correlated. The errors due to the peak centroids are small and are uncorrelated. Furthermore, since the two peaks are nearly resolved in this example, the errors in the parameter triplets for the two different Gaussian components are very weakly correlated.

The problem of divergence during the iteration procedure requires further comment. First, when the function F is not an entirely satisfactory approximation to the data, one cannot expect small chi-square values to result from the fitting exercise, and one must be on the lookout for possible divergence. Then, the occurrence of divergencies may depend strongly upon the precision of the computer used in the analysis. Sudden, inexplicable divergence such as encountered in the present example can often be traced to limited computer precision.

```

X,Y,EY
.1000E 01 .1000E 01 .9747E 01
.2000E 01 .1700E 02 .1054E 02
.3000E 01 .1100E 02 .1025E 02
.4000E 01 .4000E 01 .9899E 01
.5000E 01 .2400E 02 .1086E 02
.6000E 01 .7000E 01 .1005E 02
.7000E 01 .5300E 02 .1212E 02
.8000E 01 .5900E 02 .1237E 02
.9000E 01 .1390E 03 .1526E 02
.1000E 02 .3270E 03 .2052E 02
.1100E 02 .7040E 03 .2825E 02
.1200E 02 .8670E 03 .3100E 02
.1300E 02 .6400E 03 .2709E 02
.1400E 02 .2420E 03 .1833E 02
.1500E 02 .8000E 02 .1319E 02
.1600E 02 .5200E 02 .1208E 02
.1700E 02 .4700E 02 .1187E 02
.1800E 02 .6100E 02 .1323E 02
.1900E 02 .2350E 03 .1814E 02
.2000E 02 .6230E 03 .2678E 02
.2100E 02 .1229E 04 .3637E 02
.2200E 02 .1480E 04 .3967E 02
.2300E 02 .9540E 03 .3237E 02
.2400E 02 .2950E 03 .1972E 02
.2500E 02 .3300E 02 .1127E 02
.2600E 02 .1100E 02 .9110E 01

```

```

ITERATION 0
CHI2 = .6995E 04 LTEST = .0000E 00
P
.9000E 03 .5000E 00 .1100E 02 .1100E 04 .3000E 00 .2260E 02

ITERATION 1
CHI2 = .8855E 03 LTEST = .8734E 00
P
.0756E 03 .3984E 00 .1175E 02 .9457E 03 .3714E 00 .2157E 02
IC
1

ITERATION 2
CHI2 = .1771E 03 LTEST = .8000E 00
P
.7682E 03 .4561E 00 .1187E 02 .1288E 04 .4975E 00 .2157E 02
IC
1

```

$$CY = \begin{cases} 1 & I=J \\ <0.1 & I \neq J \end{cases}$$

B = 85.0 EB = 3.0

```

CHI20,CHI2,CHI200
.6995E 04 .1771E 03 .8855E 01
P0,P,EP
.9000E 03 .7682E 03 .1834E 02
.5000E 00 .4561E 00 .8085E-02
.1100E 02 .1187E 02 .3230E-01
.1100E 04 .1288E 04 .2131E 02
.3000E 00 .4975E 00 .5234E-02
.2260E 02 .2157E 02 .2930E-01

```

Figure 2.7.1:

Parameters associated with double-Gaussian fitting problem. X,Y and EY designate the channel, background-subtracted channel counts and errors for the spectrum, respectively. CY is the 26X26 correlation matrix for the errors EY (not given). All off-diagonal elements of CY are smaller than 0.1. B and EB are the constant background subtracted from the spectrum and its error, respectively. Initial parameters and chi-square as well as outcome from the iterations are shown. P0 designates initial parameters; P and EP designate the solution parameters and errors, respectively. CP is the correlation matrix for EP.

CP	P1	P2	P3	P4	P5	P6
P1	1		Peak 1			
P2	0.61	1				
P3	0.03	0.01	1			
P4	-0.02	-0.06	0.03	1		Peak 2
P5	-0.06	0	0.05	0.65	1	
P6	-0.03	-0.06	0.03	0.08	0.13	1

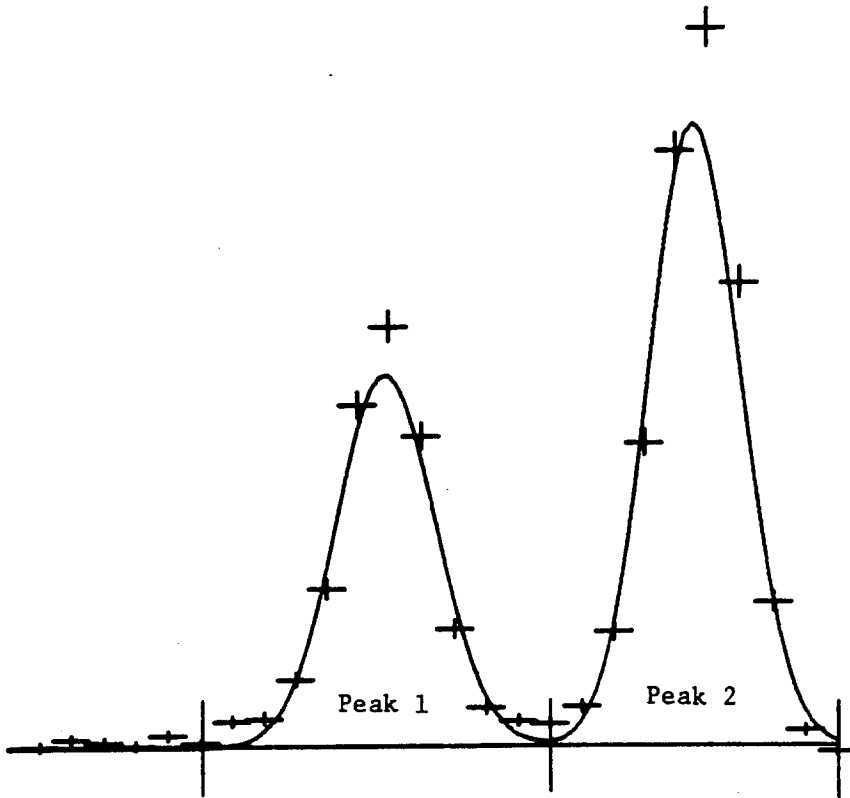


Figure 2.7.2: Plot of spectrum and double-Gaussian fit resulting from the analysis described in Section 2.7. The quality of the fit is not too satisfactory as is indicated by the final normalized chi-square value of 8.9 indicated in Figure 2.7.1. Probably, the peak shapes are not true Gaussians. Since the peak overlap is small in this instance, a better estimation of the peak yields would most likely be obtained if the background subtracted counts were simply summed over the indicated limits.

2.8 Uncertainty Estimation for Integrals of Fitted Peak Shapes

Section 2.7 dealt with the problem of fitting two close spectral peaks simultaneously with Gaussian functions. That analysis yielded a best-fit set of parameters \vec{p} and a covariance matrix \bar{V}_p , or alternatively, an error vector \vec{E}_p and correlation matrix \bar{C}_p for these errors.

The usefulness of information provided by fitting with a covariance formalism will be seen in the present example. Here, the errors in the two peak areas will be examined and the effect of correlations on these errors and on the error in the ratio of the peak areas will be considered. The methodology is from Sections III and IV of Ref. 1, and involves error propagation with the covariance formalism.

It follows from Section 2.7 that the areas a_1 and a_2 for the two Gaussian peaks are given by the expressions,

$$a_1(\vec{p}) = p_1 \int_{-\infty}^{\infty} e^{-p_2^2 (x - p_3)^2} dx = \pi^{1/2} p_1/p_2, \quad (2.8.1)$$

$$a_2(\vec{p}) = p_4 \int_{-\infty}^{\infty} e^{-p_5^2 (x - p_6)^2} dx = \pi^{1/2} p_4/p_5, \quad (2.8.2)$$

as derived from tables of definite integrals. The ratio R in the areas is given by

$$R(\vec{p}) = a_2(\vec{p})/a_1(\vec{p}) = p_4 p_2/(p_1 p_5). \quad (2.8.3)$$

The error E_R for R can be derived easily using Eq. (32) from Ref. 1, expressed in terms of the present variables as

$$E_R^2 = (\bar{S} \bullet \vec{E}_p)^T \bullet \bar{C}_p \bullet (\bar{S} \bullet \vec{E}_p). \quad (2.8.4)$$

\bar{S} is a sensitivity matrix given explicitly as

$$\bar{S} = \begin{bmatrix} (\partial R/\partial p_1) & 0 \\ & \ddots \\ 0 & (\partial R/\partial p_6) \end{bmatrix}. \quad (2.8.5)$$

The partial derivatives are evident from Eq. (2.8.3):

$$\begin{aligned} (\partial R/\partial p_1) &= -R/p_1, & (\partial R/\partial p_4) &= R/p_4, \\ (\partial R/\partial p_2) &= R/p_2, & (\partial R/\partial p_5) &= -R/p_5, \\ (\partial R/\partial p_3) &= 0, & (\partial R/\partial p_6) &= 0. \end{aligned} \quad (2.8.6)$$

The areas a_1 and a_2 form a vector \vec{a} . The covariance \bar{V}_a for \vec{a} can be derived using the vector error formalism from Section IV, Ref. 1. Thus,

$$V_{aij} = (\bar{S}_i \bullet \vec{E}_p)^T \bullet \bar{C}_p \bullet (\bar{S}_j \bullet \vec{E}_p) \quad (i, j = 1, 2), \quad (2.8.7)$$

$$E_{ai} = (V_{a11})^{1/2} \quad (i = 1, 2), \quad (2.8.7a)$$

$$\bar{S}_i = \begin{bmatrix} (\partial a_i/\partial p_1) & 0 \\ & \ddots \\ 0 & (\partial a_i/\partial p_6) \end{bmatrix} \quad (i = 1, 2). \quad (2.8.8)$$

The errors E_{a1} and E_{a2} in the peak areas are correlated according to the coefficient

$$C_{a12} = V_{a12}/(E_{a1} E_{a2}). \quad (2.8.9)$$

The fit of two Gaussian peaks to the spectral data in the example of Section 2.7 was of marginal quality. This was indicated by a normalized chi-square of 8.855 (Fig. 2.7.1). Thus, the error vector \vec{E}_a and R , as derived in the present section, should probably be scaled by a factor of about 3 to reflect the increased uncertainty represented by a normalized chi-square which exceeds unity.

Based on the data from Fig. (2.7.1), one obtains the results shown in Table (2.8.1) from an application of the present formalism. Inclusion of correlations for the parameter errors \hat{E}_p (Section 2.7) reduces the errors in both a_1 and a_2 . Since the two peaks are nearly resolved, the off-diagonal correlation coefficient, $C_{a_1 a_2}$, for the areas is only 0.09. Therefore, the error in the area ratio, R , is essentially that error which would be obtained by combining the errors in a_1 and a_2 in quadrature (uncorrelated).

If one sums the background-subtracted channel counts between limits shown in Fig. (2.7.2), one obtains the values 3193.0 ($\pm 2.3\%$) and 4942 ($\pm 1.7\%$) for yields of peaks 1 and 2, respectively. This error analysis assumes statistical uncertainty and an uncorrelated background error. These yields differ from the corresponding values, a_1 and a_2 in Table (2.8.1), by 7.0% and 7.7%, respectively. Since these differences exceed even the rescaled errors in Table (2.8.1), the contention stated in Fig. (2.7.2), that the best way to derive the peak yields for this example is simply to sum the background-subtracted counts, seems to be substantiated by the analysis presented in the present section. Peak fitting to obtain area estimates is a valid approach when the fitting functions represent the data well, or when the peaks cannot be resolved by any other method.

Table 2.8.1

Peak Areas, Ratios and Corresponding Errors for Fitted Gaussians

Correlations included:^a

a_1	=	2985.0	(± 1.9%)	[± 5.7%]
a_2	=	4589.0	(± 1.3%)	[± 3.9%]
R	=	1.537	(± 2.2%)	[± 6.6%]

Correlations ignored:^a

a_1	=	2985.0	(± 3%)	[± 9%]
a_2	=	4589.0	(± 2%)	[± 6%]
R	=	1.537	(± 2.3%)	[± 6.9]

^a(...) Errors derived from formalism

[...] Errors rescaled by normalized chi-square

2.9 Cross Section Error Resulting from Uncertainty in Neutron Energy Scale

Very few meetings of neutron data specialists seem to pass by without some discussion of the matter of energy scale uncertainty and the implications for the measurement of cross sections and other nuclear parameters. The controversy seems especially acute between experimenters who perform measurements at white-source facilities and those who perform measurements at monoenergetic-neutron facilities. Indeed, over the years there have evolved a number of puzzling discrepancies which have not been resolved. It seems like the resolution of these problems is perennially beyond the grasp of those involved [8]. There are probably three basic reasons why this is so:

- i. The complexities of nature: Cross sections fluctuate violently with energy over portions of the energy scale and periodic table - seemingly beyond current ability to deal with the effects.
- ii. Experimenters do not completely understand their experiments: A detailed understanding of all aspects of a complex modern experiment and maintenance of control over all the relevant parameters may exceed practical limitations - mostly those dictated by available time.
- iii. Data is rarely analyzed according to procedures which properly handle uncertainty propagation: Although the tools exist to perform these operations, they are rarely used. There are, of course, practical limitations to this just as there are for monitoring the experimental parameters during the data-taking phase of an experiment.

In this section, the propagation of uncertainties in certain parameters which affect neutron-energy scale for a monoenergetic experiment will be examined using covariance formalism. The impact upon derived cross sections will also be discussed.

Consider the ${}^7\text{Li}(p,n){}^7\text{Be}$ reaction as a monoenergetic neutron source (reaction Q-value is - 1.6444 MeV) [9]. the relationship between proton energy E and momentum p is

$$p^2 = E^2 + 2M_1 E, \quad (2.9.1)$$

where M_1 is the rest-mass energy of the proton,

$$M_1 = 931.478 A_1 \text{ MeV}, \quad (2.9.2)$$

with $A_1 = 1.0078$ amu. Even for the few-MeV energy range, relativistic effects are important and their neglect can lead to errors of several keV.

Measurement of primary proton momentum is achieved by deflecting these protons in a uniform static magnetic field. Thus

$$p = k R H, \quad (2.9.3)$$

where k is constant, R is the radius of curvature and H is the reading from a magnetic field probe (e.g., Nuclear Magnetic Resonance or Hall-Effect device). One source of error, and a random one at that, is uncertainty in R related to finite beam-slit apertures. Thus,

$$\Delta p = k H \Delta R, \quad (2.9.4)$$

$$(\Delta p/p) = (\Delta R/R) = \eta, \quad (2.9.5)$$

$$\Delta p = \eta p. \quad (2.9.6)$$

The error in the momentum introduced by wandering of the beam across the beam-slit gap is proportional to the momentum.

Ideally, one should perform the calibration implied by Eq. (2.9.3)-to determine the constant (kR)-using narrow slits. Assume that this is the case so that the effects of uncertainty in the radius of curvature are suppressed during the calibration procedure. Then, assume

$$p = b_1 + b_2 H. \quad (2.9.7)$$

Here b_2 is interpreted as (kR) while b_1 is a zero-point correction to account for instrumental effects and residual magnetism in the analyzing magnet. The object of calibration is to derive the best values for b_1 and b_2 .

Three calibration points are readily accessible to experimenters. These are the threshold points for neutron production from the ${}^7\text{Li}(p,n)$, ${}^{11}\text{B}(p,n)$ and ${}^27\text{Al}(p,n)$ reactions [9,10]. The calibration data consists of three proton energies E_i ($i=1,3$) and three corresponding probe readings H_i ($i=1,3$). There are errors δE_i ($i=1,3$) and δH_i ($i=1,3$). The errors δE_i are likely to be nearly random since threshold data from the literature comes from several origins. The errors δH_i are related to reproducibility and are thus random. The formalism from Ref. 1 assumes that all error is consolidated in the dependent variable, the energy E in this problem, thus

$$\Delta E_i^2 \approx \delta E_i^2 + (\partial E/\partial H)_i^2 \delta H_i^2. \quad (2.9.8)$$

The partial derivatives $(\partial E/\partial H)_i$ can be estimated readily from the trend of the calibration data. The formalism requires transformation to the momentum variable p via Eq. (2.9.1) and

$$\Delta p_i = (E_i + M_1) \Delta E_i / p_i \quad (i = 1,3). \quad (2.9.9)$$

The p_i form a vector \vec{p} , and the covariance matrix \bar{V}_p is given by

$$V_{pij} = \begin{cases} 0 & (j \neq i) \\ \Delta p_i^2 & (j = i) \end{cases} \quad (i, j=1,3), \quad (2.9.10)$$

since the errors are assumed independent as discussed above. The standard formulas from Ref. 1 become

$$\bar{V}_b = (\bar{A}^T \bullet \bar{V}_p^{-1} \bullet \bar{A})^{-1}, \quad (2.9.11)$$

$$\bar{b} = \bar{V}_b \bullet \bar{A}^T \bullet \bar{V}_p^{-1} \bullet \bar{p}, \quad (2.9.12)$$

$$X^2 = (\bar{p} - \bar{A} \bullet \bar{b})^T \bullet \bar{V}_p^{-1} \bullet (\bar{p} - \bar{A} \bullet \bar{b}), \quad (2.9.13)$$

$$\left. \begin{aligned} A_{i1} &= 1, \\ A_{i2} &= H_i, \end{aligned} \right\} \quad (i = 1,3), \quad (2.9.14)$$

where \bar{b} represents the best fit parameters b_1 and b_2 from Eq. (2.9.7), \bar{V}_b is the covariance matrix and X^2 tests the goodness of fit.

Now, select Q points with the correspondence:

<u>Probe</u>	<u>Proton Energy</u>	<u>Neutron Energy</u>	<u>Cross Section</u>				
H_q	$+$	E_q	$+$	E_{nq}	$+$	σ_q	$(q = 1, Q).$

At this point of the analysis, it is necessary to describe further the problem under consideration. Neutrons are produced by bombarding a thin film of lithium, and only the zero-degree neutrons will be considered. At a proton energy $E = 1.881$ MeV corresponding to the ${}^7\text{Li}(p,n)$ threshold, the loss of proton energy in the target is T_0 maximum. An error E_{T_0} arises because of uncertainty in the thickness of the target. This error is uncorrelated to other errors considered in this example. At an arbitrary proton energy E , the effective target thickness T is described reasonably well by the expression.

$$T \approx T_0 \exp(0.507 - 0.798 \ln(E_{\max})), \quad (2.9.15)$$

where E_{\max} is the incident proton energy before the beam enters the lithium target. So, given H_q , one derives the median proton energy E_q according to the formulas

$$(p_{\max})_q = b_1 + b_2 H_q, \quad (2.9.16)$$

$$(E_{\max})_q^2 = (p_{\max})_q^2 - 2M_1(E_{\max})_q, \quad (2.9.17)$$

$$T_q = T_0 \exp \left\{ 0.507 - 0.798 \ln [(E_{\max})_q] \right\}, \quad (2.9.18)$$

$$E_q \approx (E_{\max})_q - 1/2 T_q. \quad (2.9.19)$$

The median proton energy E_q leads to a distinct median zero-degree neutron energy E_{nq} . This neutron energy can be derived readily using standard kinematic formulas for two-body collisions, which the reader can obtain elsewhere. It is assumed that the cross section excitation function $\sigma(E_n)$ is known. Therefore, given E_{nq} , one can derive the cross section value $\sigma_q = \sigma(E_{nq})$.

At this point, all the information required to propagate errors from input parameters through to the energy scale and cross section is available. First, consider X^2 . If $X^2 \approx 1$, then the errors in b_j , E_{bj} , are

$$E_{bj} = (v_{bjj})^{1/2} \quad (j=1,2), \quad (2.9.20)$$

and the correlation matrix is \bar{C}_b , given by

$$C_{bij} = v_{bij}/(E_{bi}E_{bj}) \quad (i,j = 1,2). \quad (2.9.21)$$

However, if $X^2 \gg 1$, then the covariance matrix should be scaled by multiplying by X^2 , thereby increasing the errors \hat{E}_b . Now, define:

$$\bar{C}_x = \begin{bmatrix} \bar{C}_b & 0 \\ 0 & 1 \end{bmatrix}, \quad (2.9.22)$$

$$\vec{E}_x = \begin{bmatrix} \hat{E}_b \\ E_{To} \end{bmatrix}. \quad (2.9.23)$$

The covariance matrix \bar{V}_E for the derived neutron energies E_{nq} is given in terms of its elements by

$$V_{Eqr} = \begin{cases} (\bar{S}_{xq} \bullet \hat{E}_x)^T \bullet \bar{C}_x \bullet (\bar{S}_{xr} \bullet \hat{E}_x) & (r \neq q) \\ (\bar{S}_{xq} \bullet \hat{E}_x)^T \bullet \bar{C}_x \bullet (\bar{S}_{xq} \bullet \hat{E}_x) \\ + (\partial E_n / \partial p)_q^2 \eta^2 p_q^2 & (r = q), \end{cases} \quad (2.9.24)$$

(r,q=1,Q).

The matrices \bar{S}_{xq} and \bar{S}_{xr} ($q, r = 1, Q$) are the sensitivity matrices (sometimes called design matrices) for this problem. The form is

$$\bar{S}_{xq} = \begin{bmatrix} (\partial E_n / \partial b_1)_q & & 0 \\ & (\partial E_n / \partial b_2)_q & \\ & & (\partial E_n / \partial T_o)_q \end{bmatrix} \quad (2.9.25)$$

The momentum term appears only in the diagonal elements because the energy scale error introduced by the wandering of the proton beam across the beam slit gap is random in nature. The errors in the derived neutron energies and the error correlation matrix are given by:

$$E_{Eq} = (V_{Eqq})^{1/2} \quad (q = 1, Q), \quad (2.9.26)$$

$$C_{Eqr} = V_{Eqr} / (E_{Eq} E_{Er}) \quad (r, q = 1, Q). \quad (2.9.27)$$

The major task in this analysis is calculation of the partial derivatives $(\partial E_n / \partial b_j)_q$, $(\partial E_n / \partial T_o)_q$ and $(\partial E_n / \partial p)_q$. This can be done numerically using Eqs. (2.9.15) - (2.9.19) and the procedure described in the paragraph containing these equations.

Likewise, the cross section covariance matrix \bar{V}_σ can be obtained from

$$V_{\sigma qr} = \begin{cases} (\bar{S}_{yq} \bullet \vec{E}_x)^T \bullet \bar{C}_x \bullet (\bar{S}_{yr} \bullet \vec{E}_x) & (r \neq q), \\ (\bar{S}_{yq} \bullet \vec{E}_x)^T \bullet \bar{C}_x \bullet (\bar{S}_{yq} \bullet \vec{E}_x) \\ \quad + \left(\frac{\partial \sigma}{\partial p}\right)_q^2 \eta^2 p_q^2 & (r = q), \\ & (r, q = 1, Q), \end{cases} \quad (2.9.28)$$

with

$$\bar{S}_{yq} = \begin{bmatrix} (\partial \sigma / \partial b_1)_q & & 0 \\ & (\partial \sigma / \partial b_2)_q & \\ 0 & & (\partial \sigma / \partial T_o)_q \end{bmatrix} \quad (2.9.29)$$

$(q = 1, Q).$

The cross section errors and correlation matrix are:

$$E_{\sigma q} = (V_{\sigma qq})^{1/2} \quad (q = 1, Q), \quad (2.9.30)$$

$$C_{\sigma qr} = V_{\sigma qr} / (E_{\sigma q} E_{\sigma r}) \quad (q, r = 1, Q). \quad (2.9.31)$$

Next, consider a numerical example which illustrates the previous formalism. The $^{58}\text{Ni}(n, p)^{58}\text{Co}$ reaction exhibits a sharp threshold at $E_n \approx 0.5$ MeV although the reaction Q-value is positive. The reason is the effect of the Coulomb barrier penetration by the incident proton. Suppose $T_0 \approx 0.05$ MeV and $E_{T_0} = 0.005$ MeV. Assume the beam slit width is such that a random error of ± 0.002 MeV is observed for $E_n \approx 1$ MeV. The available threshold calibration data are given in Fig. (2.9.1). The normalized χ^2 is 0.2897 which indicates a very good fit of Eq. (2.9.7) to the data. This information is used to calculate the energy scale and $^{58}\text{Ni}(n, p)^{58}\text{Co}$ cross section errors at $E_n \approx 1, 2, 3, 4$ and 5 MeV. The energy scale errors due to slit wandering vary from ± 0.002 MeV at 1 MeV to ± 0.005 MeV at 5 MeV, and these errors are uncorrelated. The energy scale error due to uncertainty in the lithium target thickness varies from ± 0.002 MeV at 1 MeV to ± 0.001 MeV at 5 MeV (decreases with advancing neutron energy). This error component is 100% correlated for all energies. The energy scale errors due to probe calibration uncertainty vary from ± 0.0007 MeV at 1 MeV to ± 0.0045 MeV at 5 MeV. These errors are partially correlated (87-100%). Fig. (2.9.1) indicates the combined effects of all these error components. The result is an energy scale uncertainty ranging from ± 0.0029 MeV at 1 MeV to ± 0.0066 MeV at 5 MeV with correlations in the range 24-45%. The corresponding cross section errors and correlations are also indicated in Fig. (2.9.1). The cross section errors range from $\sim 1.8\%$ at 1 MeV where the $^{58}\text{Ni}(n, p)^{58}\text{Co}$ cross section changes rapidly with energy to $\sim 0.2\%$ at 5 MeV where the energy dependence is gradual. These are not large errors, and the input parameter uncertainties are realistic. So, it is hard to explain discrepancies ~ 0.02 - 0.05 MeV between monoenergetic and white source energy scales for this energy region, a not uncommon occurrence, on the basis of monoenergetic energy scale errors alone.

E, EH, EEDH, EC, EE						
.13806E 01	.27301E 04	.30000E 00	.12600E-02	.40000E-04	.38011E-03	
.36164E 01	.37752E 04	.40000E 00	.15900E-02	.15000E-02	.18293E-02	
.37969E 01	.52301E 04	.30000E 00	.22000E-02	.35000E-02	.41878E-02	
B, EB						
.28459E-01	.45544E-01					
.19940E-01	.14606E-04					
CB						
.10000E 01	-.99213E 00					
-.99213E 00	.10000E 01					
CHI2, CHI2NM						
.2597E 00	.2597E 00					

^a Calibration points listed are in the following order: Li-7(p,n), B-11(p,n) and Al-27(p,n).

Derived Energy and Cross Section Errors

TO, ETO, FEP						
.3000E-01	.5000E-02	.3500E-03				
H, EP, EN, EE, ESIG, ESIG						
.3279E 04	.2692E 01	.9874E 00	.2905E-02	.5405E-03	.1513E-04	
.4171E 04	.3655E 01	.1984E 01	.3426E-02	.3748E-01	.2255E-03	
.4701E 04	.4659E 01	.2988E 01	.4353E-02	.1713E 00	.1314E-02	
.5181E 04	.5630E 01	.3995E 01	.5453E-02	.3594E 00	.1273E-02	
.5617E 04	.6632E 01	.4990E 01	.6629E-02	.4454E 00	.8062E-03	
CE						
.1000E 01	.3982E 00	.3177E 00	.2701E 00	.2417E 00		
.3982E 00	.1000E 01	.3717E 00	.3617E 00	.3559E 00		
.3179E 00	.3717E 00	.1000E 01	.4106E 00	.4191E 00		
.2701E 00	.3617E 00	.4106E 00	.1000E 01	.4549E 00		
.2417E 00	.3559E 00	.4191E 00	.4549E 00	.1000E 01		
CSIG						
.1000E 01	.5911E 00	.5519E 00	.5321E 00	.5036E 00		
.5911E 00	.1000E 01	.9167E 00	.9253E 00	.8661E 00		
.5519E 00	.9167E 00	.1000E 01	.9860E 00	.8323E 00		
.5321E 00	.9253E 00	.9860E 00	.1000E 01	.8429E 00		
.5036E 00	.8661E 00	.8323E 00	.8429E 00	.1000E 01		

Figure 2.9.1: Input and results for proton energy calibration. E = calibration proton energy, H = NMR probe reading, EH = error in NMR reading, EC = error in proton calibration energy only, EE = composite proton energy error due to calibration and measurement effects, B = calibration constant, EB = error in calibration constant, CB = correlations in calibration constant errors, CHI2 and CHI2NM are chi-square and normalized chi-square for the fit, respectively, TO = lithium target thickness, ETO = error in lithium target thickness, FEP = constant which establishes proton energy error due to finite slit effects, EP = input proton energy for error propagation calculation, EN = neutron energy, EEN = error in neutron energy, SIG = cross section, ESIG = cross section error, CEN and CSIG are energy and cross section error correlations.

2.10 Covariance Matrix for a Measured Neutron Spectrum

Various approaches have been pursued in the quest to achieve a satisfactory nuclear data base for reactor applications. The differential approach involves measurement or calculation of microscopic nuclear quantities, such as cross sections, with attention to the dependence of said quantities on energy, angle, and even nuclear quantum numbers such as spin and parity. Progress has been made as a result of many experimental and theoretical studies, but there are shortcomings.

Differential data are not directly useful for analyzing actual reactor performance. Reactors are complicated instruments, so the link between microscopic differential data and reactors is only achieved at the expense of considerable computational effort, with attendant complications and uncertainties. Certain microscopic integral quantities such as reaction rates and spectrum-average cross sections can be related more closely to the performance of specific reactors, and therefore considerable attention has been paid to investigating these quantities. Ideally, microscopic differential and integral data, and macroscopic reactor performance characteristics should be consistent. A measure of the immaturity of this technology is the fact that often they are not. C/E discrepancies, as they are called, develop when measured integral results (E) fail to agree with computational results (C) involving the folding of differential nuclear data, using a model which one hopes will be adequate to describe a given reactor.

Meaningful discussion of C/E discrepancies is not possible without a reasonable formalism for consideration of errors. Progress has been made in assessing differential data errors and correlations. Errors and correlations for measured integral quantities have also been discussed. The weak link in the error assessment chain appears to be the specification of errors and correlations for the reactor parameters which must be folded by means of reactor model calculations with differential data in order to provide calculated results for comparison with integral experiments. The problem is not a new one, but progress has been slow.

Benchmark fields have been conceived in order to expedite the task of subjecting basic nuclear data or data evaluations to integral tests. Benchmark fields are basically low-power neutron sources whose spectra bear some resemblance to those which may be encountered in commercial machines, but otherwise are much simpler and, hopefully, much easier to characterize.

The benchmark field concept has provided some successes but there are serious limitations. Even the simplest reactor-source fields are rather strongly dependent upon nuclear data, especially neutron fission, capture and scattering data for the actinides and neutron capture and scattering data for the structural and coolant materials used in these reactors. Revisions in these data lead to revisions in neutron spectral forms for most of these fields. Only the ^{252}Cf spontaneous fission neutron spectrum and some accelerator-produced neutron fields appear to offer the possibility of serving as test spectra whose characterizations are relatively independent of the data base one hopes to test. Radioactive neutron sources such as Pu-Be have been used but have too many disadvantages to be seriously considered as benchmark fields.

In contrast to the considerable effort devoted to development of covariance information for differential and integral nuclear data, the investment of effort on development of covariance specifications for benchmark neutron spectra has been very modest. At present, there is no published covariance information available for the ^{252}Cf fission neutron spectrum, which is probably the best known neutron field available today for nuclear data testing. This is a surprising state of affairs considering the fact that there are several active research programs which involve measurement of integral nuclear data for the Californium field. The author is aware of one paper dealing with a covariance matrix for the Am-Li neutron spectrum [11].

In this section, the matter of development of covariance information for simple spectra based on ^{252}Cf spontaneous fission or accelerator neutron production will be addressed. It appears that the most important aspects of error characterization depend upon rather elementary quantities such as length, time, detector efficiency and counting statistics. It will be shown how these various uncertainty sources can be combined in order to provide covariances for the measured broad-energy neutron spectrum.

Californium and accelerator-source neutron spectra normally originate from near-point sources, and owe much of their simplicity to this fact. Characterization of the neutron spectrum at an arbitrary field point generally involves measurement of the intensity, energy distribution and distribution of incident-neutron directions. For a point source, all that are needed are the intensity and energy distribution. A detector capable of measuring pulse heights and interaction times for events produced by incident neutrons is required for the task. If time zero can be established, neutron time-of-flight (TOF) techniques can be used to define the neutron energy.

Assume that the spectrum is deduced from the measured yield in a series of consecutive energy bins with well-defined energy widths. y_i represents the measured total events, corrected for background if necessary, in the i th bin. ϵ_i represents the corresponding detector efficiency. E_i represents the median energy of the bin. Finally, ϕ_i represents the neutron spectrum. Actually, as defined here, ϕ_i is the product of the energy-bin width and the average value of the spectral density function over the bin interval. Thus,

$$\phi_i = y_i / \epsilon_i \quad (i = 1, n) \quad (2.10.1)$$

The spectrum depends implicitly on neutron energy as well, so we can write

$$\vec{\phi} = \vec{\phi}(\vec{y}, \vec{\epsilon}, \vec{E}) = \vec{\phi}(\vec{x}), \quad (2.10.2)$$

where

$$\vec{\phi} = \begin{bmatrix} \phi_1 \\ \vdots \\ \phi_n \end{bmatrix}. \quad (2.10.3)$$

It is very unlikely that ϕ , so defined, will be normalized, i.e., that

$$\sum_{i=1}^n \phi_i = 1. \quad (2.10.3a)$$

Other vectors from Eq. (2.10.2) are:

$$\vec{y} = \begin{bmatrix} y_1 \\ \vdots \\ y_n \end{bmatrix}, \quad (2.10.4)$$

$$\vec{\epsilon} = \begin{bmatrix} \epsilon_1 \\ \vdots \\ \epsilon_n \end{bmatrix}, \quad (2.10.5)$$

$$\vec{E} = \begin{bmatrix} E_1 \\ \vdots \\ E_n \end{bmatrix}, \quad (2.10.6)$$

$$\vec{x} = \begin{bmatrix} \vec{y} \\ \vec{\epsilon} \\ \vec{E} \end{bmatrix}. \quad (2.10.7)$$

Furthermore, corresponding errors \vec{E}_ϕ , \vec{E}_y , \vec{E}_ϵ , \vec{E}_E and \vec{E}_x can be defined with correlation matrices \bar{C}_ϕ , \bar{C}_y , \bar{C}_ϵ , \bar{C}_E and \bar{C}_x . Owing to the nature of the variables, the errors in \vec{y} , $\vec{\epsilon}$, and \vec{E} are uncorrelated between the different sets, so

$$\bar{C}_x = \begin{bmatrix} \bar{C}_y & & 0 \\ & \bar{C}_\epsilon & \\ 0 & & \bar{C}_E \end{bmatrix} \quad (2.10.8)$$

The error propagation formalism of Section IV, Ref. 1, can be applied to deduce the covariance matrix \bar{V}_ϕ for the derived spectrum $\vec{\phi}$. The applicable formula is

$$V_{\phi ij} = (\bar{S}_{xi} \bullet \vec{E}_x)^T \bullet \bar{C}_x \bullet (\bar{S}_{xj} \bullet \vec{E}_x) \quad (i, j = 1, n). \quad (2.10.9)$$

Thus, the errors \vec{E}_ϕ and correlation matrix \bar{C}_ϕ are obtained from

$$E_{\phi i} = (V_{\phi ii})^{1/2} \quad (i = 1, n), \quad (2.10.10)$$

$$C_{\phi ij} = V_{\phi ij} / (E_{\phi i} E_{\phi j}) \quad (i, j = 1, n). \quad (2.10.11)$$

\bar{S}_{xi} is a sensitivity (or design) matrix having the form governed by the following formulas:

$$\bar{S}_{xi} = \begin{bmatrix} \bar{S}_{yi} & 0 \\ 0 & \bar{S}_{\epsilon i} \\ 0 & \bar{S}_{Ei} \end{bmatrix} \quad (i = 1, n), \quad (2.10.12)$$

$$\bar{S}_{yi} = \begin{bmatrix} 0 & & & 0 \\ & \ddots & & \\ & & (\partial\phi_i/\partial y_i) & \\ & & & \ddots \\ 0 & & & & 0 \end{bmatrix} \quad (i = 1, n), \quad (2.10.13)$$

$$\bar{S}_{\epsilon i} = \begin{bmatrix} 0 & & & 0 \\ & \ddots & & \\ & & (\partial\phi_i/\partial \epsilon_i) & \\ & & & \ddots \\ 0 & & & & 0 \end{bmatrix} \quad (i = 1, n), \quad (2.10.14)$$

$$\bar{S}_{Ei} = \begin{bmatrix} 0 & & & 0 \\ & \ddots & & \\ & & (\partial\phi/\partial E)_i & \\ & & & \ddots \\ 0 & & & & 0 \end{bmatrix} \quad (i = 1, n), \quad (2.10.15)$$

$$(\partial\phi_i/\partial y_i) = \epsilon_i^{-1} = \phi_i/y_i \quad (i = 1, n), \quad (2.10.16)$$

$$(\partial\phi_i/\partial \epsilon_i) = -y_i/\epsilon_i^2 = -\phi_i/\epsilon_i \quad (i = 1, n). \quad (2.10.17)$$

The quantities $(\partial\phi/\partial E)_i$ can be estimated from the general trend of the spectrum shape.

Following some algebra, it can be shown from Eq. (2.10.9) that

$$\begin{aligned}
 v_{\phi ij} &= (\bar{S}_{yi} \bullet \vec{E}_y)^T \bullet \bar{C}_y \bullet (\bar{S}_{yj} \bullet \vec{E}_y) \\
 &+ (\bar{S}_{\epsilon i} \bullet \vec{E}_\epsilon)^T \bullet \bar{C}_\epsilon \bullet (\bar{S}_{\epsilon j} \bullet \vec{E}_\epsilon) \\
 &+ (\bar{S}_{Ei} \bullet \vec{E}_E)^T \bullet \bar{C}_E \bullet (\bar{S}_{Ej} \bullet \vec{E}_E) .
 \end{aligned}
 \tag{2.10.18}$$

The errors in \vec{y} are largely random in nature, thus

$$\begin{aligned}
 C_{yij} &\approx \delta_{ij} \quad (i, j = 1, n) . \\
 &\quad \text{(Kronecker delta)}
 \end{aligned}
 \tag{2.10.19}$$

Thus, it can be shown that

$$\begin{aligned}
 v_{\phi ij} &\approx \delta_{ij} \phi_i \phi_j (E_{yi}/y_i)(E_{yj}/y_j) \\
 &+ C_{\epsilon ij} \phi_i \phi_j (E_{\epsilon i}/\epsilon_i)(E_{\epsilon j}/\epsilon_j) \\
 &+ C_{Eij} (\partial\phi/\partial E)_i (\partial\phi/\partial E)_j E_{Ei} E_{Ej} .
 \end{aligned}
 \tag{2.10.20}$$

The determination of the covariance matrix \bar{V}_ϕ for the measured spectrum $\vec{\phi}$ reduces to the matter of obtaining the detector efficiency errors and correlations and the neutron energy scale errors and correlations. These are separable problems as seen from the preceding formalism. The errors in the detector counts are

$$E_{yi} \approx y_i^{1/2} \quad (i = 1, n),
 \tag{2.10.21}$$

so these need no further discussion.

Determination of $\vec{\epsilon}$, \vec{E}_ϵ and \bar{C}_ϵ depends upon the nature of the detector used and the procedure by which it was calibrated. Although the problem of developing a covariance matrix for the efficiency of an organic scintillator has been examined by the author, the details will not be discussed here since they apply to a specific detector. Consideration of this topic would detract from the objective of this section.

Consideration of the errors and correlations for the neutron energy scale is a more general topic which is worthy of inclusion in this section. The time-of-flight method can be applied in the case of Californium neutron-spectrum measurements since detection of the fission fragments yields a zero-time mark. For accelerator-source spectra, such as the thick-target ${}^9\text{Be}(d,n)$ reaction, pulsed beam techniques can be used to provide needed timing information. The gamma-ray flash from the accelerator target readily yields time zero.

The assumption of non-relativistic mechanics leads to noticeable simplification in the formulas, without an excessive sacrifice in accuracy, for error assessment in the MeV-energy range. However, the method can be applied in principle for relativistic analyses with few complications. The non-relativistic treatment is presented here.

Define the following variables:

- t_i = median neutron arrival time for i th bin,
- t_0 = zero time for the measurement (established from fission fragment or gamma-ray pulses).
- b = constant which calibrates TOF spectrum recording device (e.g., a pulse-height analyzer) in nanoseconds per channel,
- x_0 = channel which locates centroid for time zero in the spectrum,
- x_i = channel corresponding to the i th TOF spectrum bin,
- L = flight path,
- c = speed of light,
- h = constant equal to 72.3 ns/m which is the inverse velocity for a 1 MeV neutron.

The relationship between flight time and neutron energy is

$$t = (hL)/E^{1/2}. \quad (2.10.22)$$

Since

$$x_0 - x = -(t_0 - t)/b, \quad (2.10.23)$$

we have

$$E_i = h^2 L^2 / t_i^2 = h^2 L^2 / [qL + b(x_0 - x_i)]^2, \quad (2.10.24)$$

with q defined as c^{-1} . Thus, we can write

$$\vec{E} = \vec{E}(b, L, x_0, \vec{x}). \quad (2.10.25)$$

The energy errors can be related to the errors in b , L and x_0 . Therefore, the neutron energy scale covariance matrix \vec{V}_E can be derived from the formula

$$V_{E_{ij}} = (\bar{S}_{zi} \bullet \vec{E}_z)^T \bullet \bar{C}_z \bullet (\bar{S}_{zj} \bullet \vec{E}_z), \quad (i, j = 1, n) \quad (2.10.26)$$

where

$$\vec{z} = \begin{bmatrix} b \\ L \\ x_0 \end{bmatrix}, \quad (2.10.27)$$

and the corresponding errors E_b , E_L and E_{x_0} for b , L and x_0 form the vector

$$\vec{E}_z = \begin{bmatrix} E_b \\ E_L \\ E_{x_0} \end{bmatrix}. \quad (2.10.28)$$

The correlation matrix \bar{C}_z is just the unit matrix,

$$\bar{C}_z = \begin{bmatrix} 1 & 0 & 0 \\ 0 & 1 & 0 \\ 0 & 0 & 1 \end{bmatrix}, \quad (2.10.29)$$

since the parameters b , L and x_0 are independently determined. The sensitivity matrices have the form

$$\bar{S}_{zi} = \begin{bmatrix} (\partial E_i / \partial b) & 0 & 0 \\ 0 & (\partial E_i / \partial L) & 0 \\ 0 & 0 & (\partial E_i / \partial x_0) \end{bmatrix} \quad (i = 1, n), \quad (2.10.30)$$

with

$$(\partial E_i / \partial b) = E_i [-2(t_i - t_0) / (bt_i)] \quad (i = 1, n), \quad (2.10.31)$$

$$(\partial E_i / \partial L) = E_i [2(t_i - t_0) / (Lt_i)] \quad (i = 1, n), \quad (2.10.32)$$

$$(\partial E_i / \partial x_0) = E_i (-2b / t_i) \quad (i = 1, n). \quad (2.10.33)$$

Following some algebra, one arrives at the expression

$$\begin{aligned} V_{E_{ij}} &= E_i E_j [4(t_i - t_0)(t_j - t_0) / (t_i t_j)] (E_b / b)^2 \\ &+ E_i E_j [4(t_i - t_0)(t_j - t_0) / (t_i t_j)] (E_L / L)^2 \\ &+ E_i E_j [4b^2 / t_i t_j] E_{x_0}^2 \quad (i, j = 1, n). \end{aligned} \quad (2.10.34)$$

From this, one can deduce that the fractional energy errors are

$$\begin{aligned} (E_{Ei}/E_i)^2 &= [4(t_i - t_o)^2/t_i^2] (E_b/b)^2 \\ &+ [4(t_i - t_o)^2/t_i^2] (E_L/L)^2 \\ &+ [4 b^2/t_i^2] E_{xo}^2 \quad (i = 1, n). \end{aligned} \quad (2.10.35)$$

The correlation matrix \bar{C}_E is derived in the usual way from the formula

$$C_{Eij} = v_{Eij}/(E_{Ei} E_{Ej}) \quad (i, j = 1, n). \quad (2.10.36)$$

The spectrum $\bar{\psi}$, defined as $(\bar{\phi}/\xi)$ with ξ equal to $\sum_{i=1}^n \phi_i$, remains normalized, i.e., $\sum_{i=1}^n \psi_i = 1$ regardless of changes in $\bar{\phi}$. The covariance matrix \bar{V}_ψ can be derived using the standard error propagation rules; it has the form

$$v_{\psi ij} = \sum_{k=1}^n \sum_{\ell=1}^n (\xi \delta_{ik} - \phi_i) (\xi \delta_{j\ell} - \phi_j) C_{\phi k\ell} E_{\phi k} E_{\phi \ell} \quad (i, j=1, n). \quad (2.10.37)$$

It can be quite easily shown that this matrix has the interesting property that

$$\sum_{i=1}^n v_{\psi ij} = \sum_{j=1}^n v_{\psi ij} = 0 \quad (i, j=1, n). \quad (2.10.38)$$

This is equivalent to a statement of flux conservation for the spectrum.

A complete evaluation for the Californium neutron spectrum, inclusive of covariance information, should be performed. As indicated above, each experiment could be examined according to the relatively simple procedures indicated above. In practice, this might be a rather frustrating task since previously reported Californium spectrum results probably will not provide an evaluator with sufficient information about the details of the experiments to permit the generation of covariance matrices. In fact, it is very likely that the experimenters themselves no longer have this information available. The same considerations apply to accelerator-source benchmark fields. The conclusion is that future benchmark spectrum determinations should be undertaken with full consideration of covariance information, and the results should be reported in such a way that the required error information is available for evaluators. This is not likely to impose much extra work on experimenters, since the needed information is usually available at the time that the experiment is performed. What is needed is for the experimenter to provide somewhat more detailed documentation of error information than is traditional when reporting the results.

Development of covariance information for reactor-source benchmark fields could likely be a much more complex task. It is possible that this is an impractical goal for the near term. Since specification of these fields depends strongly upon changing nuclear data basis, the fields themselves become parts of the data base (or at least products of the data base). One might well ask whether such fields should not be evaluated simultaneously with the nuclear data base. If so, then the usefulness of these fields for independent testing of nuclear data should be seriously questioned.

2.11 Uncertainty Determination for a Calculated Integral Quantity

Integral-differential comparisons provide useful tests of nuclear data for reactor applications. However, it is important that such tests be performed properly. For example, it is not possible to say that a discrepancy exists between measured and calculated integral results if the differences are within the combined errors. But, how are the errors to be determined? Very often in the past, these errors have not been properly assessed so that controversies over "discrepancies" have continued without a rational basis for debate.

This section will indicate how integral and differential results may be properly compared using covariance error formalism. This will be accomplished by considering a symbolic example in which a calculated and measured spectrum-average cross section are compared. The reader should realize at the outset that this example is somewhat simplified in order to clarify the concepts. There are usually strong correlations between integral data for various reactions because of the way these measurements are performed. Foils of several materials are exposed to the same neutron spectrum and reaction rate ratios are measured. One or more reactions from the set serve as standards for spectrum-average cross section determination. Correlations between differential results for various reactions may also exist owing to common measurement techniques, common apparatus and, especially, the use of common standards. Simultaneous evaluations and/or integral-differential comparisons for several reactions should be carried out when the data are thus correlated [12].

For the present considerations, consider one reaction type with a differential cross section $\sigma(E)$ as a function of neutron energy, and a measured spectrum-average cross section σ_m for spectrum $\phi(E)$. Thus, the calculated integral result is

$$\sigma_c \approx \int_0^{\infty} \sigma(E) \phi(E) dE / \int_0^{\infty} \phi(E) dE. \quad (2.11.1)$$

For practical considerations assume σ_c can be calculated with adequate accuracy using group values and the formula

$$\sigma_c \approx \left(\sum_{j=1}^n \sigma_j \phi_j \right) / \left(\sum_{j=1}^n \phi_j \right), \quad (2.11.2)$$

with

$$\sigma_j = \sigma(E_j) \quad (j=1, n), \quad (2.11.3)$$

$$\phi_j = \phi(E_j) \quad (j=1, n) \quad . \quad (2.11.4)$$

Define $\vec{\sigma}$ as the collection of σ_j ($j=1, n$) and $\vec{\phi}$ as the collection of ϕ_j ($j=1, n$). Assume that matrices \bar{V}_ϕ and \bar{V}_σ are available. The importance of errors and correlations for the spectrum ϕ has generally been overlooked in the consideration of integral-differential discrepancies. Error vectors and correlation matrices, $(\bar{E}_\sigma, \bar{C}_\sigma)$ and $(\bar{E}_\phi, \bar{C}_\phi)$, can be considered since they provide information fully equivalent to the covariance matrices according to the equations

$$E_{\sigma j} = (V_{\sigma j j})^{1/2} \quad (j=1, n), \quad (2.11.5)$$

$$C_{\sigma i j} = V_{\sigma i j} / (E_{\sigma i} E_{\sigma j}) \quad (i, j=1, n), \quad (2.11.6)$$

$$E_{\phi j} = (V_{\phi j j})^{1/2} \quad (j=1, n), \quad (2.11.7)$$

$$C_{\phi i j} = V_{\phi i j} / (E_{\phi i} E_{\phi j}) \quad (i, j=1, n). \quad (2.11.8)$$

The measured spectrum-average cross section has an error E_{σ_m} . Furthermore, there may be a correlation between the measured integral result and the differential results. The most likely source of correlation between the measured integral cross section σ_m and the differential results σ is a normalization constant corresponding to 100% correlated items such as sample material composition, gamma-decay branching, etc. So, assume

$$\vec{\sigma} = g \vec{\sigma}^*, \quad (2.11.9)$$

$$\sigma_m = g \sigma_m^*, \quad (2.11.10)$$

where g is the common factor. Then the errors can be expressed as

$$E_{\sigma j}^2 = \sigma_j^2 [(E_g^2/g^2) + (E_{\sigma j}^{*2}/\sigma_j^{*2})] \quad (j=1, n), \quad (2.11.11)$$

$$E_{\sigma_m}^2 = \sigma_m^2 [(E_g^2/g^2) + (E_{\sigma_m}^{*2}/\sigma_m^{*2})]. \quad (2.11.12)$$

The first term in each of Eqs. (2.11.11) and (2.11.12) represents a fully correlated error shared by the integral and differential results because of the common normalization factor.

It is useful to define an augmented cross section vector \vec{s} given as

$$\vec{s} = \begin{bmatrix} \vec{\sigma} \\ \sigma_m \end{bmatrix} . \quad (2.11.13)$$

The corresponding augmented covariance matrix,

$$\bar{V}_s = \begin{bmatrix} \bar{V}_\sigma & \sigma_m (E_g^2/g^2) \vec{\sigma} \\ \sigma_m (E_g^2/g^2) \vec{\sigma}^T & E_{\sigma m}^2 \end{bmatrix} , \quad (2.11.14)$$

includes the terms common to the integral and differential results, with $\vec{\sigma}^T$ the transpose of $\vec{\sigma}$. The corresponding error vector \vec{E}_s and correlation matrix \bar{C}_s are given by

$$\vec{E}_s = \begin{bmatrix} \vec{E}_\sigma \\ E_{\sigma m} \end{bmatrix} , \quad (2.11.15)$$

$$C_{sij} = V_{sij} / (E_{si} E_{sj}) \quad (i, j=1, n+1). \quad (2.11.16)$$

It is instructive to write \bar{C}_s in the form

$$\bar{C}_s = \begin{bmatrix} \bar{C}_\sigma & \vec{\psi} \\ \vec{\psi}^T & 1 \end{bmatrix} \quad (2.11.17)$$

where

$$\psi_i = \frac{(E_g^2/g^2)}{(E_{\sigma i}/\sigma_i)(E_{\sigma m}/\sigma_m)} \quad (i = 1, n). \quad (2.11.18)$$

$\vec{\psi}$ represents the correlation parameters linking the measured integral and differential results.

With the above considerations in mind, it is possible to provide a unified assessment of the errors and correlations for the measured and calculated spectrum-average cross sections. The variables of the analysis are ϕ , $\bar{\sigma}$ and σ_m . Define

$$\vec{x} = \begin{bmatrix} \phi \\ \bar{\sigma} \\ \sigma_m \end{bmatrix} = \begin{bmatrix} \phi \\ s \end{bmatrix}, \quad (2.11.19)$$

$$\vec{E}_x = \begin{bmatrix} E_\phi \\ E_{\bar{\sigma}} \\ \sigma_m \end{bmatrix} = \begin{bmatrix} E_\phi \\ E_s \end{bmatrix}, \quad (2.11.20)$$

$$\bar{C}_x = \begin{bmatrix} \bar{C}_\phi & 0 & 0 \\ 0 & \bar{C}_{\bar{\sigma}} & \vec{\psi} \\ 0 & \vec{\psi}^T & 1 \end{bmatrix} = \begin{bmatrix} \bar{C}_\phi & 0 \\ 0 & \bar{C}_s \end{bmatrix}. \quad (2.11.21)$$

There are no assumed correlations between the spectrum errors \vec{E}_ϕ and the other parameters errors.

Define \vec{f} by

$$\vec{f} = \begin{bmatrix} f_1 \\ f_2 \end{bmatrix} = \begin{bmatrix} \sigma_c \\ \sigma_m \end{bmatrix}, \quad (2.11.22)$$

with

$$f_1 = f_1(\vec{x}), \quad (2.11.23)$$

$$f_2 = f_2(\vec{x}). \quad (2.11.24)$$

The covariance matrix \bar{V}_f provides all the desired information about the errors and correlations for the calculated and measured spectrum-average cross sections. Thus,

$$V_{fkl} = (\bar{S}_k \bullet \vec{E}_x)^T \bullet \bar{C}_x \bullet (\bar{S}_l \bullet \vec{E}_x) \quad (k, l=1,2). \quad (2.11.25)$$

The sensitivity matrices \bar{S}_1 and \bar{S}_2 must now be examined, we have

$$\bar{S}_k = \begin{bmatrix} \bar{S}_{\phi k} & 0 \\ 0 & \bar{S}_{\sigma k} \\ & S_{\sigma mk} \end{bmatrix} = \begin{bmatrix} \bar{S}_{\phi k} & 0 \\ 0 & \bar{S}_{\sigma k} \end{bmatrix} \quad (k = 1,2), \quad (2.11.26)$$

with

$$S_{\sigma m1} = (\partial f_1 / \partial \sigma_m) = 0, \quad (2.11.27)$$

$$S_{\sigma m2} = (\partial f_2 / \partial \sigma_m) = 1, \quad (2.11.28)$$

$$\bar{S}_{\phi k} = \begin{bmatrix} (\partial f_k / \partial \phi_1) & 0 \\ & \ddots \\ 0 & (\partial f_k / \partial \phi_n) \end{bmatrix} \quad (k = 1,2), \quad (2.11.29)$$

$$\bar{S}_{\sigma k} = \begin{bmatrix} (\partial f_k / \partial \sigma_1) & 0 \\ & \ddots \\ 0 & (\partial f_k / \partial \sigma_n) \end{bmatrix} \quad (k = 1,2). \quad (2.11.30)$$

It can be seen that

$$\bar{S}_{\phi 2} = \bar{0} \quad (2.11.31)$$

since f_2 does not depend upon $\vec{\phi}$, and

$$\bar{S}_{\sigma 2} = \bar{0} \quad (2.11.32)$$

since f_2 does not depend upon $\vec{\sigma}$ either.

Clearly, from Eqs. (2.11.21) and (2.11.25),

$$\begin{aligned}
 V_{fkl} &= (\bar{S}_{\phi k} \bullet \ddagger \dot{E}_{\phi})^T \bullet \bar{C}_{\phi} \bullet (\bar{S}_{\phi l} \bullet \ddagger \dot{E}_{\phi}) \\
 &+ (\bar{S}_{s k} \bullet \ddagger \dot{E}_s)^T \bullet \bar{C}_s \bullet (\bar{S}_{s l} \bullet \ddagger \dot{E}_s).
 \end{aligned}
 \tag{2.11.33}$$

Following considerable matrix algebra, one obtains

$$\begin{aligned}
 V_{f11} &= (\bar{S}_{\phi 1} \bullet \ddagger \dot{E}_{\phi})^T \bullet \bar{C}_{\phi} \bullet (\bar{S}_{\phi 1} \bullet \ddagger \dot{E}_{\phi}) \\
 &+ (\bar{S}_{\sigma 1} \bullet \ddagger \dot{E}_{\sigma})^T \bullet \bar{C}_{\sigma} \bullet (\bar{S}_{\sigma 1} \bullet \ddagger \dot{E}_{\sigma}),
 \end{aligned}
 \tag{2.11.34}$$

$$V_{f12} = V_{f21} = E_{\sigma m} (\bar{S}_{\sigma 1} \bullet \ddagger \dot{E}_{\sigma})^T \bullet \ddagger \dot{\psi},
 \tag{2.11.35}$$

$$V_{f22} = E_{\sigma m}^2.
 \tag{2.11.36}$$

The errors are

$$E_{f1} = (V_{f11})^{1/2},
 \tag{2.11.37}$$

$$E_{f2} = (V_{f22})^{1/2},
 \tag{2.11.38}$$

with correlation coefficient

$$C_{f12} = C_{f21} = V_{f12} / (E_{f1} E_{f2}).
 \tag{2.11.39}$$

The partial derivatives needed for these calculations are

$$\left(\frac{\partial f_1}{\partial \phi_1} \right) = \frac{\sigma_1}{\left(\sum_{j=1}^n \phi_j \right)} - \frac{\ddagger \dot{\sigma}^T \bullet \ddagger \dot{\phi}}{\left(\sum_{j=1}^n \phi_j \right)^2} \quad (i = 1, n),
 \tag{2.11.40}$$

$$\left(\frac{\partial f_1}{\partial \sigma_1} \right) = \phi_1 / \left(\sum_{j=1}^n \phi_j \right) \quad (i = 1, n).
 \tag{2.11.41}$$

Some recent evaluations provide information on \bar{V}_σ , but no programmatic effort has been made to examine the correlations existing between the differential and integral values, namely the parameters ψ . Furthermore, information on covariance matrices \bar{V}_ϕ for standard broad-energy spectra used for differential data testing is sparse. So, the outstanding current obstacle to application of the method described in this section is lack of the requisite input information on errors and correlations, especially for standard benchmark spectra. This is an area of investigation which must be pursued by researchers if progress is to be made in the area of integral-differential data testing.

2.12 Legendre Polynomial Fit to an Angular Distribution Data Set

We will consider an angular distribution data set corresponding to the elastic scattering of 2.89 MeV neutrons from a sample of Fe-54 metal. The elastically scattered neutrons are measured by time of flight, using several organic scintillators whose efficiency shapes as a function of neutron energy have been measured by observing their response to the known spontaneous-fission-neutron spectrum of Cf-252 [13]. Normalization of the scattered-neutron detector array is accomplished by performing measurements of the well-known differential scattering cross section for carbon. Various significant errors and their correlations for this experiment will be discussed briefly here, and the covariance formalism from Ref. 1 will be applied to the process of fitting a measured angular distribution with a Legendre polynomial expansion. A description of the apparatus appears in Ref. 14.

Random Error (R):

The dominant source of random error for the measured differential cross section points is the determination of the peak counts for the elastic peak in the time-of-flight spectrum. The errors originate from statistical and background subtraction uncertainty (e.g., Section 2.6). The differential cross sections and random errors for the present example appear in Table (2.12.1).

Normalization Error (S₁)

Four sources of error in the measured differential cross section have been identified, each of which involves a scale factor affecting the cross section at all angles. The composite error is thus fully correlated for the data in Table (2.12.1). It is assumed that there is $\approx 1\%$ error which results from uncertainty in the yield of a monitor detector which measures the relative neutron fluences for Fe-54 and carbon scattering runs. Another $\approx 0.5\%$ fully-correlated error comes from uncertainty in the number of Fe-54 atoms for the sample. Uncertainty in the absorption of neutrons by the Fe-54 sample produces an error of $\approx 1\%$ in the effective neutron fluence which can be assumed to be nearly fully correlated. Finally, a fully correlated error of $\approx 2\%$ is assumed for the integrated carbon scattering cross section. The combined fully-correlated error is $\approx 2.5\%$.

Angle Error (S₂)

The relative angles for the measurements are rather well known, but there is uncertainty in determining the zero angle and thus the absolute angular scale. It is assumed that an uncertainty of ± 0.3 deg exists. The resultant uncertainty in the differential cross section depends upon the sensitivity of a particular differential cross section to angle. Estimated uncertainties appear in Table (2.12.1). These are fully-correlated errors.

Intercalibration of the Several Detectors in the Multi-Angle System (S₃)

The origins of uncertainty are many and complex. Based upon experience, the error appears to total $\approx 3\%$ from this category. Correlations are difficult to judge, so it is assumed that the errors are $\approx 50\%$ correlated as a compromise between the assumptions of full correlation or no correlation.

Multiple-Scattering Correction (S₄)

Again, the uncertainty and associated correlations are difficult to estimate. An estimated uncertainty of ≈2% is reasonable, and it is clear that the errors for adjacent angles are more strongly correlated than for widely-separated angles. As an approximation, it is assumed that the correlation behaves according to

$$C(\theta_1, \theta_j) = 1 - \frac{|\theta_1 - \theta_j|}{180}, \quad (2.12.1)$$

where θ_1 and θ_j are the laboratory angles in degrees for two differential cross section data points.

The least-squares analysis is a straight forward application of the procedures in Section VII of Ref. 1. A vector \vec{y} of dimension n is defined by

$$y_i = (d\sigma/d\Omega)_i \quad (2.12.2)$$

where $(d\sigma/d\Omega)_i$ is the experimental differential cross section for angle θ_i . The angular distribution is to be approximated by the function f which is the Legendre-polynomial expansion

$$f(\theta) = \sum_{j=1}^m P_j P_{j-1}(\cos \theta_i). \quad (2.12.3)$$

We seek \vec{p} (p_1, \dots, p_m) so that

$$y_i \approx f(\theta_i) \quad (i = 1, n), \quad (2.12.4)$$

or

$$\vec{y} \approx \vec{A} \bullet \vec{p}, \quad (2.12.4a)$$

where

$$A_{ij} = P_{j-1}(\cos \theta_i) \quad (i = 1, n; j = 1, m). \quad (2.12.5)$$

Based on the discussion above, the covariance matrix \bar{V}_y can be derived from the equations

$$V_{y_{1i}} = E_{R_i}^2 + E_{S_{1i}}^2 + E_{S_{2i}}^2 + E_{S_{3i}}^2 + E_{S_{4i}}^2 \quad (i = 1, n), \quad (2.12.6)$$

$$V_{y_{ij}} = E_{S_{1i}} E_{S_{1j}} + E_{S_{2i}} E_{S_{2j}} + 0.5 E_{S_{3i}} E_{S_{3j}} + C(\theta_i, \theta_j) E_{S_{4i}} E_{S_{4j}} \quad (i \neq j), \quad (2.12.7)$$

with $C(\theta_i, \theta_j)$ from Eq. (2.12.1). The correlation matrix \bar{C}_y is calculated using Eq. (34) of Ref. 1:

$$C_{y_{ij}} = V_{y_{ij}} / (E_{y_i} E_{y_j}) \quad (i, j = 1, n), \quad (2.12.8)$$

where

$$E_{y_i} = (V_{y_{1i}})^{1/2} \quad (i = 1, n). \quad (2.12.9)$$

The correlation matrix for the data in Table (2.12.1) is given in Table (2.12.2).

The solution minimizes the chi-square expression

$$\chi^2 = (\vec{y} - \bar{A} \bullet \vec{p})^T \bullet \bar{V}_y^{-1} \bullet (\vec{y} - \bar{A} \bullet \vec{p}). \quad (2.12.10)$$

We assume $m=9$, and derive the solution from the formulas

$$\bar{V}_p = (\bar{A}^T \bullet \bar{V}_y^{-1} \bullet \bar{A})^{-1}, \quad (2.12.11)$$

$$\vec{p} = \bar{V}_p \bullet \bar{A}^T \bullet \bar{V}_y^{-1} \bullet \vec{y}. \quad (2.12.12)$$

Three possibilities are considered for this problem:

- (1) Include all errors from Table (2.12.1) and the covariance matrix as derived from Eqs. (2.12.6) and (2.12.7).

- (ii) Include all errors from Table (2.12.1), but assume them to be uncorrelated.
- (iii) Consider only random errors from Table (2.12.1).

These three different assumptions lead to three different solutions for \vec{p} and the error vector \vec{E}_p , as given in Table (2.12.3). The computed values of chi-square were <1 for each of the fits performed, which implied that the Legendre expansion was capable of fitting the data to well within the assumed errors—even if only the random errors are considered. The differences in the derived coefficient vectors \vec{p} are small for these three fitting approaches, and each yields an integrated cross section of 2.389 b to the fourth significant figure. Therefore the only practical difference lies in the errors and correlations. Method (i) yields an error of 3.9% for the integrated cross section, method (ii) yields 1.9%, and method (iii) yields 0.4%. The correlation matrix \bar{C}_p differs considerably for each of these solutions. The explicit matrices for methods (i) and (iii) are given in Table (2.12.4) for general interest. The widely different correlation matrices would have an impact on some uncertainties, e.g. the uncertainty for the relative scattered neutron yield at two different angles.

Figure (2.12.1) shows the fit to the data points yielded by method (i) analysis. Very little difference was seen for the other two fitted curves.

Table 2.12.1
Differential Cross Sections and Errors
for Neutron Elastic Scattering from Fe-54 at 2.89 MeV

Laboratory Angle (deg)	Differential Cross Section (b/sr)	Error Components (b/sr) ^a					Total Error (b/sr)
		Random (R)	Normalization (S ₁)	Angle Uncertainty (S ₂)	Detector Calibration ^b (S ₃)	Scattering Correction (S ₄)	
17.3	1.0662	0.0053	0.02666	-0.0072	0.03199	0.02132	0.04763
27.2	0.8040	0.0044	0.0201	-0.0123	0.02412	0.01608	0.03762
44.1	0.3571	0.0031	0.008928	-0.0063	0.01071	0.007142	0.01717
63.0	0.0846	0.0015	0.002115	-0.00159	0.002538	0.001692	0.004308
81.0	0.0471	0.0010	0.001178	0.00057	0.001413	0.000942	0.002366
99.0	0.0884	0.0015	0.00221	0.00039	0.002652	0.001768	0.004177
116.0	0.1071	0.0016	0.002678	0	0.003213	0.002142	0.004964
131.0	0.1046	0.0015	0.002615	-0.00015	0.003138	0.002092	0.004831
146.0	0.0931	0.0014	0.002328	-0.00015	0.002793	0.001862	0.004321
155.9	0.0885	0.0014	0.002213	-0.00039	0.002655	0.00177	0.004146

^aSee Section 2.12 in text for discussion.

^bNegative sign implies that an increase in angle leads to a decrease in the differential cross section. The sign should be included in Eq. (2.12.7).

Table 2.12.2
Correlation Matrix \bar{C}_y Derived from Data in Table 2.12.1

I \ J	1	2	3	4	5	6	7	8	9	10
1	1									
2	.74	1								
3	.71	.76	1							
4	.66	.71	.72	1						
5	.56	.50	.49	.47	1					
6	.60	.56	.56	.55	.63	1				
7	.61	.59	.59	.58	.60	.66	1			
8	.60	.59	.59	.57	.58	.64	.67	1		
9	.58	.57	.57	.56	.56	.62	.65	.67	1	
10	.57	.57	.58	.57	.53	.60	.64	.66	.67	1

Table 2.12.3
 Solution Parameters and Errors for the
 Three Different Fitting Procedures Discussed in the Text

	(i)	(ii)	(iii)
P ₁	.1901 ± .0075	.1902 ± .0036	.1902 ± .0007
P ₂	.2602 ± .0119	.2604 ± .0088	.2605 ± .0013
P ₃	.3486 ± .0152	.3488 ± .0119	.3486 ± .0019
P ₄	.3050 ± .0136	.3050 ± .0135	.3052 ± .0021
P ₅	.1413 ± .0105	.1413 ± .0170	.1405 ± .0028
P ₆	.0332 ± .0091	.0331 ± .0172	.0326 ± .0030
P ₇	.0102 ± .0094	.0102 ± .0179	.0088 ± .0035
P ₈	.0048 ± .0068	.0048 ± .0127	.0036 ± .0031
P ₉	.0055 ± .0092	.0057 ± .0165	.0039 ± .0043

Table 2.12.4
Correlation Matrix \bar{C}_p for Solutions (i) and (iii)

(i)

I \ J	1	2	3	4	5	6	7	8	9
1	1								
2	.93	1							
3	.95	.96	1						
4	.88	.89	.91	1					
5	.51	.50	.65	.71	1				
6	.08	.13	.21	.44	.72	1			
7	.03	-.03	.16	.19	.73	.67	1		
8	0	0	.06	.19	.52	.68	.65	1	
9	.06	-.04	.13	-.03	.44	.21	.66	.53	1

(iii)

I \ J	1	2	3	4	5	6	7	8	9
1	1								
2	.37	1							
3	.45	.31	1						
4	.03	.30	.04	1					
5	.15	-.13	.48	.16	1				
6	-.25	.08	-.05	.49	.29	1			
7	.21	-.25	.40	-.08	.68	.27	1		
8	.05	.15	-.07	.27	.26	.48	.33	1	
9	.35	-.14	.50	-.28	.54	-.04	.60	.36	1

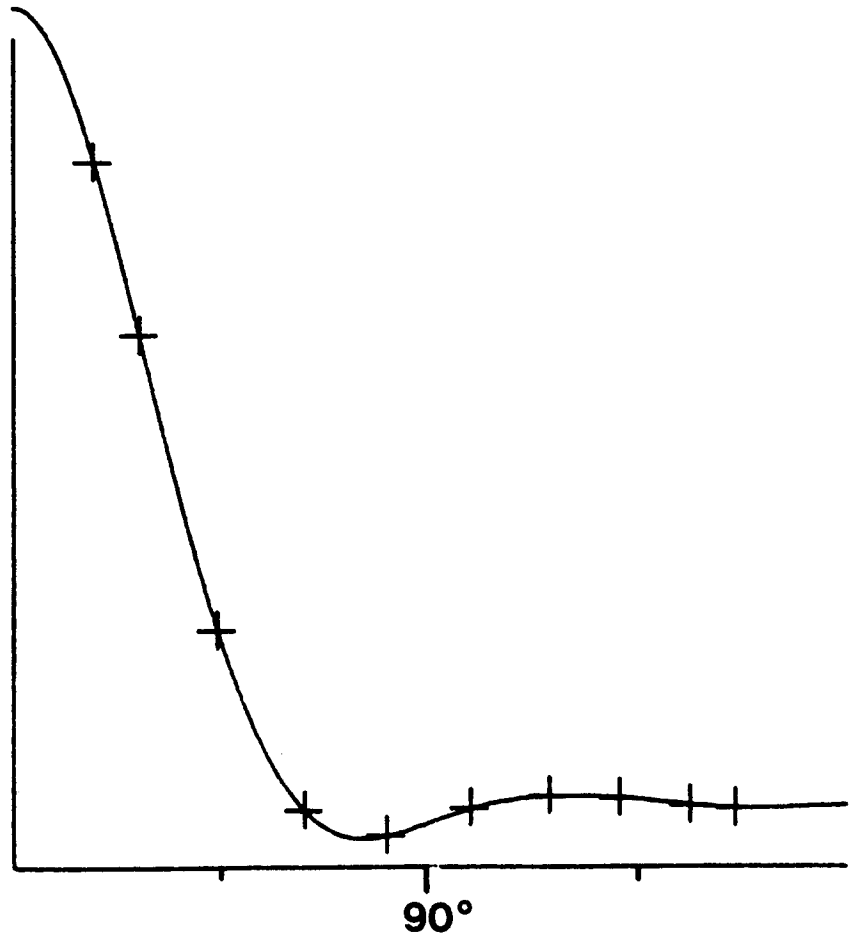


Figure 2.12.1: Linear plot of neutron elastic scattering distribution for Fe-54 at 2.89 MeV. Solid curve is a 9-parameter Legendre expansion which has been fitted to the experimental differential cross section points using covariance methods.

2.13 Combination of Dominant Error Components for Neutron Cross Section Measurements

The interested reader will no doubt wish to know how the various techniques discussed in this report might be put to practical use to analyze the errors for a cross section measurement. This is a difficult topic to address; there are so many special situations that it is not reasonable to expect a general procedure for performing error analyses. Also, the subject would not be appropriately served by giving a specific example since the basic concepts might be masked by excessive detail. Therefore, the subject will be treated by considering a symbolic cross section ratio experiment. The reader who understands this material can readily extrapolate to specific applications.

Derivation of cross sections from raw data involves application of various corrections. The approaches to this task are as varied as the styles of the experimenters. One can choose to combine the raw detector counts, then apply a number of multiplicative factors to account for the corrections. These individual correction factors can be examined separately using several methods. When applied to determination of a cross section ratio, the form of the analysis is:

$$R = \sigma_2/\sigma_1 = (Y_2 N_1/Y_1 N_2) \prod_{k=1}^m F_k, \quad (2.13.1)$$

where

Y_1, Y_2 = measured detector counts,

N_1, N_2 = sample atom numbers,

F_k = correction factors.

Other data analysis procedures may involve more detailed simulation of the experiment using a digital computer [15]. In this way, the corrections become rather intertwined, but the end result is the same.

From the point of view of error analysis, the approach indicated by Eq. (2.13.1) is the most useful. In principle, one could perform a detailed error analysis for a computer model calculation by simply assessing the uncertainty and correlations for all input parameters, calculating appropriate sensitivity coefficients, etc. This is not usually a practical approach. The experimenter who wishes to do a reasonably accurate yet still practical assessment of the experimental errors must carefully analyze the experiment and identify the key components for the purpose of error assessment. Certain parameters are very well known and introduce very little error. One can avoid

considering these to minimize labor. Other parameters introduce errors which are so strongly correlated, if not completely so, for all the measured points that it is sensible to assume 100% correlation, thereby avoiding the task of determining exact correlations.

In other situations, the correlations, while not vanishingly small, are small enough so that the results will not be seriously affected by neglecting these correlations. The neglect of these small correlations can also lead to considerable simplification. Correlations intermediate in magnitude can be problematic. The experimenter must make practical decisions. If the error component is substantial, and the impact upon the results warrants the requisite labor, then the investigator can proceed to do whatever may be needed in order to make an accurate assessment of the correlation pattern. Correlations are introduced by common dependency upon implicit variables which may be difficult to identify. On the other hand, if the impact of an error component is small, then approximation methods are justified.

It should be evident from this discussion that the data analysis process may well require the development of two distinct analytical models. The model used to derive cross sections or cross section ratios from new data might be quite detailed, including a number of small corrections which involve very little error. A second, simplified model should be envisioned for the purpose of error assessment. This model includes the main features of the cross section calculations, including those factors which account for most of the error. It should not be forgotten that error derivation involves considerable estimation, therefore the experimenter can be forgiven if the model used to combine these estimated errors falls short of an exact description of the complete data analysis process.

Eq. (2.13.1) provides a useful analytical model for discussing error analysis for a typical cross section ratio experiment. The correction factors F_k should address aspects of the experiment which are very weakly cross correlated, and can thus be treated as uncorrelated for modeling purposes. The F_k are not primary variables, but represent relatively distinct features of the experiment such as geometry, multiple scattering, radiation absorption, efficiency, etc., which are most strongly dependent upon distinct sets of primary variables. Proper selection of the factors F_k allows for examination of error components one by one, with eventual combination of the essentially decoupled components in a relatively uncomplicated fashion.

Suppose n ratios R_i are measured at energies E_i ($i=1,n$), then

$$R_i = R_i(Y_{1i}, Y_{2i}, N_{1i}, N_{2i}, F_{1i}, \dots, F_{mi}, E_i) \quad (i=1,n), \quad (2.13.2)$$

according to Eq. (2.13.1). Let \vec{R} , \vec{Y}_1 , \vec{Y}_2 , \vec{N}_1 , \vec{N}_2 , $\vec{F}_1, \dots, \vec{F}_m$ and \vec{E} represent all the experimental quantities indicated in Eq. (2.13.2). Then, in vector notation, Eq. (2.13.2) becomes

$$\vec{R} = \vec{R}(\vec{Y}_1, \vec{Y}_2, \vec{N}_1, \vec{N}_2, \vec{F}_1, \dots, \vec{F}_m, \vec{E}). \quad (2.13.3)$$

The dependence upon \vec{E} is implicit since this variable does not appear in Eq. (2.13.1). However, energy scale errors may be important if the measured quantities fluctuate considerably with energy, so this source of uncertainty should be examined by the experimenter (e.g., see Section 2.9).

Given the errors and correlations $(\vec{E}_{Y1}, \vec{C}_{Y1}), \dots, (\vec{E}_E, \vec{C}_E)$, one seeks to derive for R the errors E_R and correlations \vec{C}_R . The error propagation formalism applicable to this problem is described in Section IV of Ref. 1. Define

$$\vec{E}_x = \begin{bmatrix} \vec{E}_{Y1} \\ \vec{E}_{Y2} \\ \vec{E}_{N1} \\ \vec{E}_{N2} \\ \vec{E}_{F1} \\ \vdots \\ \vec{E}_{Fm} \\ \vec{E}_E \end{bmatrix}, \tag{2.13.4}$$

and

$$\vec{C}_x \approx \begin{bmatrix} \vec{C}_{Y1} & & & & & & & & & 0 \\ & \vec{C}_{Y2} & & & & & & & & \\ & & \vec{C}_{N1} & & & & & & & \\ & & & \vec{C}_{N2} & & & & & & \\ & & & & \vec{C}_{F1} & & & & & \\ & & & & & \dots & & & & \\ & & & & & & \vec{C}_{Fm} & & & \\ 0 & & & & & & & & \vec{C}_E & \end{bmatrix}. \tag{2.13.5}$$

Eq. (2.13.5) is an explicit statement of the assumption that correlations between the various categories of errors are negligible. Also define

The intrinsic simplicity of the \bar{S} matrices leads to further reductions for Eq. (2.13.9)

$$\begin{aligned}
 V_{Rij} = & R_i R_j \left[\left(\frac{E_{Y1i}}{Y_{1i}} \right) \left(\frac{E_{Y1j}}{Y_{1j}} \right) C_{Y1ij} + \left(\frac{E_{Y2i}}{Y_{2i}} \right) \left(\frac{E_{Y2j}}{Y_{2j}} \right) C_{Y2ij} \right. \\
 & + \left(\frac{E_{N1i}}{N_{1i}} \right) \left(\frac{E_{N1j}}{N_{1j}} \right) C_{N1ij} + \left(\frac{E_{N2i}}{N_{2i}} \right) \left(\frac{E_{N2j}}{N_{2j}} \right) C_{N2ij} \\
 & + \left(\frac{E_{F1i}}{F_{1i}} \right) \left(\frac{E_{F1j}}{F_{1j}} \right) C_{F1ij} + \dots + \left(\frac{E_{Fmi}}{F_{mi}} \right) \left(\frac{E_{Fmj}}{F_{mj}} \right) C_{Fmij} \left. \right] \\
 & + (\partial R / \partial E)_i (\partial R / \partial E)_j E_{Ei} E_{Ej} C_{Eij} \quad (i, j = 1, n)
 \end{aligned} \tag{2.13.10}$$

The partial derivative $(\partial R / \partial E)_i$ at energy E_i can be estimated by plotting the measured ratios R versus energy E . A smooth curve drawn as an eyeguide through these results becomes the basis for estimating the partial derivatives.

Eq. (2.13.10) may simplify more depending upon the nature of the various correlation matrices. The detector counts Y_1 and Y_2 are probably subject primarily to random errors (uncorrelated from one point to the next), so

$$\begin{aligned}
 C_{Y1ij} \approx C_{Y2ij} \approx \delta_{ij} \quad (\text{Kronecker delta}) \\
 (i, j = 1, n).
 \end{aligned} \tag{2.13.11}$$

The correlation pattern for the sample atom numbers \bar{N}_1 and \bar{N}_2 depend upon the nature of the experiment. Two extreme possibilities are as follows.

At one extreme, a pair of samples is used for all the measurements. An example would be a fission ratios experiment where the two deposits are placed in a back-to-back fission chamber and this apparatus is exposed to a neutron source for the measurement of cross section ratios. In this case

$$\begin{aligned}
 N_{1i} &= N_1, \\
 E_{N1i} &= E_{N1}, \\
 N_{2i} &= N_2, \\
 E_{N2i} &= E_{N2},
 \end{aligned} \quad (i = 1, n) \tag{2.13.12}$$

and

$$C_{N1ij} = C_{N2ij} = 1 \quad (i, j = 1, n). \quad (2.13.13)$$

The sample atom errors are 100% correlated for the entire data set.

The other extreme is also possible. Suppose each measurement involves a distinct pair of samples. The sample materials may be uniform and contribute negligibly to the ratio errors, but random errors in the sample masses must be considered. Then

$$C_{N1ij} \approx C_{N2ij} \approx \delta_{ij} \quad (i, j = 1, n) \quad (2.13.14)$$

Partial correlations arise if both sample composition (correlated) and sample mass (random) errors must be included.

Similarly, geometric correction errors may be uncorrelated, partially correlated or 100% correlated depending upon how the experiment is conducted. If the geometry is fixed and undisturbed through the entire experiment, then the errors are correlated 100% for all the data points. However if random positioning errors for the detectors are dominant and the experimental setup is adjusted prior to each measurement, then the correlations vanish. The important point to be made is that the experimenter must provide enough information about the way an experiment was actually conducted to enable the correlations to be identified. This is rarely done in the literature, so development of covariance matrix information for evaluations generally involves much guess work. Improvements in practices for reporting results are needed.

Provision of error and error correlation information for certain factors from Eq. (2.13.1) can be quite a speculative enterprise even for the experimenter. A good example is the application of multiple scattering corrections. Scattering correction calculations are generally complex, involving scattering cross sections, neutron source properties and geometrical parameters as input. The correction factor can be written in the form.

$$F_{ki} = M_i = 1 + \alpha_i \quad (i = 1, n), \quad (2.13.15)$$

with α generally much smaller than unity. It is simply not worth the effort in most experiments to try to make a rigorous assessment of the error in F_k . Instead, one might choose to assume that α is uncertain by a fractional amount P_M for each data point:

$$\Delta\alpha_i/\alpha_i \equiv P_M \quad (i = 1, n) \quad (2.13.16)$$

The error E_{M_i} in M_i is thus

$$E_{M_i} \approx \alpha_i P_M. \quad (2.13.17)$$

Furthermore, it might be assumed that the correlation is given by

$$C_{M_{ij}} = 1 - \frac{|E_i - E_j|}{\Delta E_{\max}}, \quad (2.13.18)$$

where ΔE_{\max} is the energy range covered by the experiment, i.e.,

$$|E_i - E_j| \leq \Delta E_{\max} \quad (i, j = 1, n). \quad (2.13.19)$$

Eq. (2.13.18) states an assumption that the scattering correction errors are strongly correlated for data points nearby in energy, but not so for widely separated energy points. The approach indicated here for a scattering correction is not fundamental, but merely demonstrates the sort of steps an experimenter may take to provide plausible error and error correlation information in situations where a precise treatment of the problem is obviously impractical.

The partial error components lead to an error vector \vec{E}_R calculated from the equation

$$E_{Ri} = (V_{Ri1})^{1/2} \quad (i = 1, n). \quad (2.13.20)$$

The correlation matrix \bar{C}_R is given by

$$C_{Rij} = V_{Rij} / (E_{Ri} E_{Rj}) \quad (i, j = 1, n). \quad (2.13.21)$$

One of the major challenges to be met in the field of nuclear data is the management of large quantities of numerical data. Suppose n cross section ratios are measured, then n errors might be generated and $n(n-1)/2$ distinct correlation coefficient as well, for a total of $(n^2 + 3n)/2$. If $n = 100$, this implies 5150 pieces of data. Clearly, this becomes an unmanageable problem very quickly, and illustrates a fundamental problem associated with reporting errors and covariances: It would seem to require many more numbers to specify the errors and correlations than to present the fundamental measured results.

Actually, there is rarely as much unique information available about the experiment as is implied by the size of the covariance matrix. In fact, it is generally agreed by evaluators that experimentors normally should not provide covariance matrices along with their results. Tables providing dominant error components, and sufficient information to enable generation of correlation matrices is suggested. This available information can then be manipulated according to the needs of the situation. Even though experimenters should not be expected to generate covariance matrices for their measured results, it is important that they understand the process. Only then will they understand how errors are derived and propagated, and therefore be prepared to examine which of the errors in their experiments are significant and which are not.

The discussion in this section has been structured around consideration of measured cross section ratios since most neutron data experiments involve the measurement of ratios. If an experimenter measures ratios, his responsibility is limited to reporting only the ratios and corresponding error and correlation information. However, most users are interested in the cross sections derived from the ratios. Thus,

$$\sigma_{2i} = R_i \sigma_{1i} \quad (i = 1, n), \quad (2.13.22)$$

where σ_2 are the unknown cross sections and σ_1 the standard cross sections. Rules for combining ratio and standard errors are discussed in Ref. 1, Section V.

3. CONCLUSIONS

The examples of Section 2 demonstrate that covariance methods can be applied to a wide range of nuclear data analysis applications. Furthermore, if these methods were more widely used by experimentalists, the long-term effect would be a simplification of the evaluation process (or at least reduced arbitrariness) and steady improvement in the data base for nuclear technology.

Experimenters should realize that application of covariance methods will, in some cases actually reduce the extent of the labor required to analyze their experimental results. The numerical examples presented in this report are diverse, but they were all analyzed using the few computer subroutines presented in the Appendix. Had this not been possible, the work presented in this report would have been much more time consuming and most likely would not have been undertaken by the author.

Application of covariance methods in routine data analysis does impose demands upon the experimenter which have traditionally been overlooked, namely the examination of correlations between significant errors in the parameters. This can be a somewhat frustrating job, but reasonable estimates followed by proper error propagation analysis will surely lead to an improved understanding of the experiment. There are instances where the raw data are relatively free of correlations, but strong correlations in the errors for derived results are introduced by the data analysis procedures (e.g., curve fitting). The use of covariance methods then leads to the generation of more detailed information about the analyzed results than would evolve otherwise, at little cost of additional effort. Several of the examples discussed in Section 2 demonstrate this point.

Concern has been expressed that widespread consideration of covariances might lead to an information explosion which would strain existing data compilation institutions beyond their capacity. This is a serious question which falls out of the scope of the present report. The content of useful information in most covariance matrices generally falls short of the indicated size of the matrix. Procedures for collapsing matrices to manageable size are under consideration within the nuclear data community. Therefore, there is hope that this problem can be dealt with in a practical way.

ACKNOWLEDGMENTS

Some of the data used in the examples presented in Section 2 were provided by J. W. Meadows, J. F. Whalen and P. T. Guenther from Argonne National Laboratory. This work was supported by the U.S. Department of Energy.

REFERENCES

1. Donald L. Smith, "Covariance Matrices and Applications to the Field of Nuclear Data," ANL/NDM-62, Argonne National Laboratory, Argonne, Illinois, 60439, U.S.A. (1981).
2. W. Mannhart, "A Small Guide to Generating Covariances of Experimental Data," PTB-FMRB-84, Physikalisch - Technische Bundesanstalt, Braunschweig, Federal Republic of Germany (1981).
3. R. Peele, "Uncertainty in the Nuclear Data used for Reactor Calculations," to be published in Sensitivity and Uncertainty Analysis of Reactor Performance Parameters, ed. C. Weisbin. This monograph will be part of the series entitled "Advances in Nuclear Science and Technology" published by Pergamon Press, Oxford, U.K. The author can be contacted at: Engineering Physics Division, Oak Ridge National Laboratory, P.O. Box X, Oak Ridge, Tennessee, 37830, U.S.A.
4. F. Schmittroth, "Generalized Least-Squares for Data Analysis," HEDL-TME 77-51, UC-79d, Hanford Engineering Development Laboratory, Richland, Washington (1978).
5. W. P. Poenitz, J. F. Whalen and A. B. Smith, "Total Neutron Cross Sections of Heavy Nuclei," Nucl. Sci. Eng. 78, 333 (1981).
6. D. L. Smith, "A Spectrometer for the Investigation of Gamma Radiation Produced by Neutron-Induced Reactions," ANL/NDM-12, Argonne National Laboratory, Argonne, Illinois (1975).
7. D. L. Smith and J. W. Meadows, "Fast-Neutron Activation of 48.6-Min Cd-111m for Elemental Cadmium," to be published in Nuclear Science and Engineering.
8. J. W. Meadows, "Determination of the Energy Scale for Neutron Cross Section Measurements Employing a Monoenergetic Accelerator," ANL/NDM-25, Argonne National Laboratory, Argonne, Illinois (1976).
9. J. B. Marion, Rev. Mod. Phys. 38, 660 (1966).
10. E. H. Beckner, R. L. Bramblett and G. C. Phillips, Phys. Rev. 123, 2100 (1961).
11. J. G. Owen, D. R. Weaver and J. Walker, Nucl. Instr. Meth. 188, 579 (1981).
12. W. P. Poenitz, "Data Interpretation, Objective Evaluation Procedures and Mathematical Techniques for the Evaluation of Energy-Dependent Ratio, Shape and Cross Section Data," Proceedings of the Conference on Nuclear Data Evaluation Methods and Procedures, September 22-25, 1980 at Brookhaven National Laboratory, edited by B. A. Magurno and S. Pearlstein, Report Nos. BNL-NCS-51363 or NEANDC(U.S.)-209, Vol. I, p. 249 (March 1981).

13. A. B. Smith, P. Guenther and R. Sjoblom, "Note on the Experimental Determination of the Relative Fast-Neutron Sensitivity of a Hydrogenous Scintillator," ANL/NDM-21, Argonne National Laboratory, Argonne, Illinois (1976).
14. A. B. Smith, P. Guenther, R. Larsen, C. Nelson, P. Walker and J. F. Whalen, Nucl. Instr. Meth. 50, 277 (1967).
15. Donald L. Smith, "Some Comments on Resolution and the Analysis and Interpretation of Experimental Results from Differential Neutron Measurements," ANL/NDM-49, Argonne National Laboratory, Argonne, Illinois (1979).

APPENDIX

This Appendix describes the FORTRAN-IV subroutines LLSF and NLSF which are convenient for linear and non-linear least-squares analyses, respectively.

Linear Least-Squares Analysis (LLSF)

As indicated in Section VII of Ref. 1, most linear least-squares problems can be reduced to finding a solution vector \vec{p} , for the approximate equation

$$\vec{y} \approx \bar{A} \bullet \vec{p}, \tag{A.1}$$

which minimizes chi-square given by

$$\chi^2 = (\vec{y} - \bar{A} \bullet \vec{p})^T \bar{V}_y^{-1} \bullet (\vec{y} - \bar{A} \bullet \vec{p}), \tag{A.2}$$

where \bar{V}_y is the covariance matrix for the input values \vec{y} . The solution to this problem is given by

$$\bar{V}_p = (\bar{A}^T \bullet \bar{V}_y^{-1} \bullet \bar{A})^{-1}, \tag{A.3}$$

$$\vec{p} = \bar{V}_p \bullet \bar{A}^T \bullet \bar{V}_y^{-1} \bullet \vec{y}, \tag{A.4}$$

where \bar{V}_y^{-1} is the inverse of \bar{V}_y and \bar{V}_p is the covariance matrix for the solution vector \vec{p} .

A FORTRAN-IV subroutine named LLSF has been developed to solve this general problem. LLSF calls two additional subroutines entitled MATINV and JORDAN. These three subroutines must appear in the following order in the program:

```
Main Program
      :
      LLSF
      MATINV
      JORDAN
      :
```

MATINV inverts nonsingular matrices and JORDAN solves systems of linear equations by the Gauss-Jordan reduction method.

LLSF and its associated subroutines perform all aspects of the least squares analysis problem. The procedure for using subroutine LLSF is:

```
DIMENSION Y(N1), EY(N1), CY(N1,N1), VY(N1,N1), VYI(N1,N1), A(N1,M1),
          P(M1), EP(M1), CP(M1,M1), VP(M1,M1), VPI(M1,M1), QN(N1),
          WN(N1,N2), QM(M1), WM(M1,M2)
          :
```

CALL LLSF (IY, Y, EY, CY, VY, VYI, A, N, N1, N2, M, M1, M2, P, EP, CP, VP, VPI,
CHI2, CHI2NM, QN, WN, QM, WM)

⋮

There are two options for using LLSF, identified by the index IY. This index controls which variables are considered input and which are considered output. IY can be either 1 or 2; these two modes are defined in Table A.1.

The interpretation of the variables in LLSF is as follows:

- Y: Vector \vec{y} from Eq. (A.1).
- EY: Error vector $\vec{\hat{E}}_y$ for \vec{y} .
- CY: Correlation matrix \bar{C}_y for errors $\vec{\hat{E}}_y$.
- VY: Covariance matrix \bar{V}_y related to $\vec{\hat{E}}_y$ and \bar{C}_y as indicated by Eqs. (34) and (35) of Ref. 1.
- VYI: Inverse matrix \bar{V}_y^{-1} from Eq. (A.2)
- A: Matrix \bar{A} from Eq. (A.1) with dimension $N \times M$.
- N: Dimension parameter for Y, EY(N) and CY, VY, VYI($N \times N$).
- N1: Maximum size for N allowed in program.
- N2: Always $N1 + 1$.
- M: Dimension parameter for P, EP(M) and CP, VP, VPI($M \times M$). $M < N$ is required.
- M1: Maximum size for M allowed in program.
- M2: Always $M1 + 1$.
- P: Solution vector \vec{p} .
- EP: Error vector $\vec{\hat{E}}_p$ for solution vector \vec{p} .
- CP: Correlation matrix \bar{C}_p for errors $\vec{\hat{E}}_p$.
- VP: Covariance matrix \bar{V}_p for solution \vec{p} related to $\vec{\hat{E}}_p$ and \bar{C}_p as indicated by Eqs. (34) and (35) of Ref. 1.
- VPI: Inverse matrix \bar{V}_p^{-1} .
- CHI2: χ^2 from Eq. (A.2).
- CHI2NM: Normalized χ^2 computed by dividing χ^2 by $(N - M)$.

Subroutine LLSF is protected against nonsingular matrices. If a matrix which is being inverted is singular, subroutine LLSF directs the message "NO INV" to be printed on Unit 1 and halts execution by means of the FORTRAN statements

```

      :
      WRITE(1,8)
      8 FORMAT(6HNO INV)
      PAUSE
      :
  
```

Non-Linear Least-Squares Analysis (NLSF)

There is no unique way to approach the problem of non-linear least-squares fitting. Also, given a set of initial conditions, there is no guarantee that a particular algorithm will converge toward a solution. The FORTRAN-IV subroutine NLSF is based on an algorithm which involves linearization of the fitting problem followed by iterative application of the linear least-squares formalism embodied in subroutine LLSF discussed above. The approach is discussed in the example appearing on p. 54 of Ref. 1. This algorithm does not allow for constraints among the parameters, and no random steps are taken during the search procedure. The user should begin with an initial set of parameters which do not differ seriously from the anticipated solution. The formalism is as follows:

Data points \vec{y} , with errors \vec{E}_y and correlations \vec{C}_y (alternatively, covariance matrix \vec{V}_y), are approximated by a function $F(x, \vec{p})$. For \vec{y} , there is a vector \vec{x} so

$$y_i \approx F(x_i, \vec{p}) \quad (i = 1, n) \quad (\text{A.5})$$

and

$$F(x_i, \vec{p}) \approx F(x_i, \vec{p}_0) + \sum_{j=1}^m \frac{\partial F}{\partial p_j} (x_i, \vec{p}_0) (p_j - p_{0j}) \quad (i = 1, n), \quad (\text{A.6})$$

by Taylor's series expansion of F. Define

$$\vec{s} = \vec{p} - \vec{p}_0, \quad (\text{A.7})$$

$$z_i = y_i - F(x_i, \vec{p}_0) \quad (i = 1, n), \quad (\text{A.8})$$

then

$$\vec{z} \approx \vec{A} \bullet \vec{s}, \quad (\text{A.9})$$

where

$$A_{ij} = \frac{\partial F}{\partial p_j} (x_i, \vec{p}_0) \quad (i = 1, n; j = 1, m). \quad (\text{A.10})$$

As discussed in Ref. 1, the covariance matrix for \vec{z} is also \vec{V}_y . The solution for \vec{s} proceeds in the usual way with

$$\bar{V}_p = (\bar{A}^T \bullet \bar{V}_y^{-1} \bullet \bar{A})^{-1}, \quad (A.11)$$

$$\vec{s} = \bar{V}_p \bullet \bar{A}^T \bullet \bar{V}_y^{-1} \bullet \vec{z}, \quad (A.12)$$

$$\vec{p} = \vec{p}_0 + \vec{s}, \quad (A.13)$$

$$(\chi^2)_{p_0}^+ = \vec{z}^T \bullet \bar{V}_y^{-1} \bullet \vec{z}, \quad (A.14)$$

$$(\chi^2)_p^+ = (\vec{z} - \bar{A} \bullet \vec{s})^T \bullet \bar{V}_y^{-1} \bullet (\vec{z} - \bar{A} \bullet \vec{s}). \quad (A.15)$$

The fractional change, δ , in χ^2 obtained by deriving a correction \vec{s} to \vec{p}_0 to yield a new parameter set \vec{p} is given by

$$\delta = \left[(\chi^2)_p^+ - (\chi^2)_{p_0}^+ \right] / (\chi^2)_{p_0}^+. \quad (A.16)$$

Iteration is continued until χ^2 appears to converge (small δ). NLSF offers two options:

- 1) Check χ^2 after each iteration and stop search algorithm manually.
- ii) Iterate automatically until the fractional change in $\chi^2(\delta)$ drops below a preset level, or for a preset number of iterations (whichever comes first).

Subroutine NLSF calls subroutine LLSF. The proper order for the subroutines in the program is as follows:

```

Main Program
  :
  NLSF
  LLSF
  MATINV
  JORDAN
  FCN
  :
  :
  
```

The purpose of subroutine FCN will be clarified below. The procedure for using subroutine NLSF is:

```

DIMENSION X(N1), Y(N1), EY(N1), CY(N1,N1), VY(N1,N1), VYI(N1,N1), A(N1,M1),
          Pphi(M1), PI(M1), P(M1), EP(M1), CP(M1,M1), VP(M1,M1), VPI(M1,M1),
          QN(N1), WN(N1,N2), QM(M1), WM(M1,M2), Z(N1), S(N1)
  
```

EXTERNAL FNC

```

  :
  :
CALL NLSF(IY, X, Y, EY, CY, VY, VYI, A, N, N1, N2, M, M1, M2, IA, K, KMAX,
          DELTA, Pphi, PI, P, EP, CP, VP, VPI, CHI2phi, CHI2, CHI2NM, QN, WN,
          WM, Z, S, FCN)
  :
  :
  
```

The index IY plays the same role in NLSF as it did in LLSF. The index IA determines whether the iterative search proceeds in manual or automatic mode. Thus:

IA = 1:

Subroutine prints results of each iteration on Unit 1 and asks user if he wishes to continue or to terminate at the current iteration (selection based on index IC).

IA = 2:

Subroutine continues automatically for a preset number of iterations KMAX or until the fractional change in χ^2 (CHI2) drops below a preset level δ (DELTA), whichever occurs first.

The parameter IC allows for decision making in the manual search mode. So,

IC = $\begin{cases} 1 & \text{continue iteration,} \\ 2 & \text{terminate iteration and proceed toward end of subroutine NLSF.} \end{cases}$

Index IC is read from Unit 1 in I1 format. The variables in the call statement for NLSF are identified according to whether they represent input or output in Table A.2.

The interpretation of the variables in NLSF is as follows: Y, EY, CY, VY, VYI, A, P, EP, CP, VP, VPI, N, N1, N2, M, M1, M2, CHI2 and CHI2NM play the same roles as they do in subroutine LLSF, as described above.

X: This is the array of values \vec{x} for calculation of the functional values for F and its partial derivatives as indicated above.

K: Number of completed iterations at termination of the least-squares process.

KMAX: Limiting number of iterations to be performed during execution of least-squares process (provides a cutoff criterion for iterations).

DELTA: Value δ which represents a convergence criterion for χ^2 in least-squares process.

P ϕ : Initial guess parameter array \vec{p}_0 provided by user as the starting point for the search.

CHI2 ϕ : χ^2 value corresponding to initial parameter set \vec{p}_0 .

FCN: Function F used in least-squares process. This function must be defined in an EXTERNAL statement. FCN is the name of the external subroutine used to calculate both F and its partial derivatives. The form of the call statement in NLSF is:

CALL FCN(INDEX, J, X(I), PI, M, M1, FVALUE).

INDEX: INDEX = $\begin{cases} 1 & \text{calculate functional value for } F, \\ 2 & \text{calculate partial derivative of } F. \end{cases}$

J: If INDEX = 2, calculate J-th partial derivative ($\partial F / \partial p_j$).

X(I): Value x_i from array \bar{x} .

PI: Parameter array \bar{p} at current iteration of least-squares process.

FVALUE: Returned value from subroutine FCN.

M and M1 are defined above.

Since NLSF calls LLSF, the behavior is identical to LLSF when singular matrices are encountered.

Source listings for NLSF, LLSF, MATINV and JORDAN are presented at the end of the Appendix.

Table A.1
Input/Output Variable List for LLSF

IY	1	2
Y	I	I
EY	I	O
CY	I	O
VY	O	I
VYI	O	O
A	I	I
N	I	I
N1	I	I
N2	I	I
M	I	I
M1	I	I
M2	I	I
EP	O	O
CP	O	O
VP	O	O
VPI	O	O
CHI2	O	O
CHI2NM	O	O
QN WN QM WM	These are working arrays for LLSF which the user can ignore.	

I = Input O = Output

Table A.2
Input/Output Variable List for NLSF

IY	1	2
X	I	I
Y	I	I
EY	I	O
CY	I	O
VY	O	I
VYI	O	O
A	I	I
N	I	I
N1	I	I
N2	I	I
M	I	I
M1	I	I
M2	I	I
IA	I	I
K	O	O
KMAX ^a	I	I
DELTA ^a	I	I
PØ	I	I
P	O	O
EP	O	O
CP	O	O
VP	O	O
VPI	O	O
CHI2Ø	O	O
CHI2	O	O
CHI2NM	O	O
PI		
QN		
WN		
QM		
WM		
Z		
S		
FCN		Name of function defined in external subroutine

I = Input O = Output

^aThese are dummy variables if IA = 1.

SUBROUTINE NLSFC(Y,X,Y,EY,CY,VY,VYI,A,N,N1,N2,M,M1,M2,IA,K,KMAX,DE	0001
1LTA,PS,PI,P,EP,CP,VP,VPI,CHI20,CHI2,CHI2NM,QN,WN,OM,W1,Z,S,FCN)	0002
DIMENSION X(N1),Y(N1),EY(N1),CY(N1,N1),VY(N1,N1),VYI(N1,N1),A(N1,M	0003
11),PE(P1),PI(M1),P(M1),EP(M1),CP(M1,M1),VP(M1,M1),VPI(M1,M1),QN(N1	0004
2),WN(1,N2),GH(N1),W1(M1,N2),Z(N1),S(M1)	0005
G0 T0(1,3),IY	0006
1 D0 2 I=1,N	0007
D0 2 J=1,M	0008
2 VY(I,J)=CY(I,J)*EY(I)*EY(J)	0009
G0 T0 0	0010
3 D0 4 I=1,N	0011
4 EY(I)=SQRT(VY(I,I))	0012
D0 5 I=1,N	0013
D0 5 J=1,M	0014
5 CY(I,J)=VY(I,J)/EY(I)/EY(J)	0015
6 CALL RATINV(QN,VY,VYI,WN,NTEST,N,N1,N2)	0016
IF(NTEST.EQ.1) G0 T0 9	0017
7 WRITE(1,8)	0018
8 F0RMA(6HND INV)	0019
PAUSE	0020
9 K=0	0021
D0 10 J=1,M	0022
10 PI(J)=P0(J)	0023
11 D0 12 I=1,N	0024
CALL FCN(1,0,X(I),PI,M,M1,F)	0025
Z(I)=Y(I)-F	0026
D0 12 J=1,M	0027
CALL FCN(2,J,X(I),PI,M,M1,DF)	0028
12 A(I,J)=DF	0029
CHI2=0.0	0030
D0 13 K2=1,N	0031
D0 13 K1=1,N	0032
13 CHI2=CHI2+Z(K2)*VYI(K2,K1)*Z(K1)	0033
IF(K.GT.0) G0 T0 14	0034
CHI2J=CHI2	0035
CHI2S=CHI2	0036
14 DTEST=ABS(CHI2-CHI2S)/CHI2S	0037
CHI2S=CHI2	0038
G0 T0(15,20),IA	0039
15 WRITE(1,16) K,CHI2,DTEST	0040
16 F0RMA(/10HITERATION ,I2/7HCHI2 = ,E10.4,2X,8HDTEST = ,E10.4)	0041
WRITE(1,160)	0042
17 F0RMA(1nP)	0043
WRITE(1,17) (PI(J),J=1,M)	0044
17 F0RMA(6E10.4)	0045
IF(K.EQ.0) G0 T0 21	0046
WRITE(1,13)	0047
18 F0RMA(2HIC)	0048
READ(1,19) IC	0049
19 F0RMA(I1)	0050
G0 T0(21,20),IC	0051
20 IF(K.GT.0.AND.DTEST.LT.DELTA) G0 T0 26	0052
21 K=K+1	0053
IF(IA.EQ.2.AND.K.GT.KMAX) G0 T0 25	0054
D0 22 I=1,N	0055
D0 22 J=1,M	0056
VPI(I,J)=0.0	0057
D0 22 K2=1,N	0058
D0 22 K1=1,N	0059

22	VPI(I,J)=VPI(I,J)+A(K2,I)*VYI(K2,K1)*A(K1,J)	0060
	CALL MATINV(QM,VPI,VP,WH,NTEST,M,N1,N2)	0061
	IF(NTEST,EQ,0) GO TO 7	0062
	D0 23 J=1,M	0063
	S(J)=J,0	0064
	D0 23 K3=1,M	0065
	D0 23 K2=1,N	0066
	D0 23 K1=1,N	0067
23	S(J)=S(J)+VP(J,K3)*A(K2,K3)*VYI(K2,K1)*Z(K1)	0068
	D0 24 J=1,M	0069
	P(J)=PI(J)+S(J)	0070
24	PI(J)=P(J)	0071
	GO TO 11	0072
25	K=K-1	0073
26	D0 27 J=1,M	0074
27	EP(J)=SQRT(VP(J,J))	0075
	D0 25 I=1,M	0076
	D0 28 J=1,M	0077
28	CP(I,J)=VP(I,J)/EP(I)/EP(J)	0078
	CHI2NM=CHI2/FLLEAT(N=M)	0079
	RETURN	0080
	END	0081
		0082

SUBROUTINE LLSF(Y,Y,EY,CY,VY,VYI,A,N,N1,N2,M,M1,M2,P,EP,CP,VP,VPI	0001
1,CHI2,CHI2NM,QN,W,N,QM,WM)	0002
DIMENSION Y(N1),EY(N1),CY(N1,N1),VY(N1,N1),VYI(N1,N1),A(M	0003
1),EP(M1),CP(M1,M1),VP(M1,M1),VPI(M1,M1),QN(N1),WN(N1,N2),QM(M1),W	0004
2M(M1,2)	0005
GO TO(1,3),IY	0006
1 DO 2 I=1,N	0007
DO 2 J=1,N	0008
2 VY(I,J)=CY(I,J)*EY(I)*EY(J)	0009
GO TO 6	0010
3 DO 4 I=1,N	0011
4 EY(I)=SQRT(VY(I,I))	0012
DO 5 I=1,N	0013
DO 5 J=1,N	0014
5 CY(I,J)=VY(I,J)/EY(I)/EY(J)	0015
6 CALL MATINV(QN,VY,VYI,W,N,NTEST,N,N1,N2)	0016
IF(NTEST.EQ.1) GO TO 9	0017
7 WRITE(1,8)	0018
8 FORMAT(6HNO INV)	0019
PAUSE	0020
9 DO 10 I=1,M	0021
DO 10 J=1,M	0022
VPI(I,J)=0,0	0023
DO 10 K2=1,N	0024
DO 10 K1=1,N	0025
10 VPI(I,J)=VPI(I,J)+A(K2,I)*VYI(K2,K1)*A(K1,J)	0026
CALL MATINV(QM,VPI,VP,W,M,NTEST,M,M1,M2)	0027
IF(NTEST.EQ.0) GO TO 7	0028
DO 11 I=1,M	0029
P(I)=0,0	0030
DO 11 K3=1,M	0031
DO 11 K2=1,N	0032
DO 11 K1=1,N	0033
11 P(I)=P(I)+VP(I,K3)*A(K2,K3)*VYI(K2,K1)*Y(K1)	0034
DO 12 I=1,M	0035
12 EP(I)=SQRT(VP(I,I))	0036
DO 13 I=1,M	0037
DO 13 J=1,M	0038
13 CP(I,J)=VP(I,J)/EP(I)/EP(J)	0039
DO 14 I=1,N	0040
QN(I)=Y(I)	0041
DO 14 K1=1,M	0042
14 QN(I)=QN(I)-A(I,K1)*P(K1)	0043
CHI2=0,0	0044
DO 15 K2=1,N	0045
DO 15 K1=1,N	0046
15 CHI2=CHI2+QN(K2)*VYI(K2,K1)*QN(K1)	0047
CHI2NY=CHI2/FLDAT(N-M)	0048
RETURN	0049
END	0050
	0051

SUBROUTINE MATINV(B,D,Q,E,NTEST,NS,NARA,NMAX)	0001
DIMENSION B(NARA),D(NARA,NARA),Q(NARA,NARA),E(NARA,NMAX)	0002
IP = NS + 1	0003
BIG = 0.0	0004
DO 555 I=1,NS	0005
DO 555 J=1,NS	0006
ABD = ABS(D(I,J))	0007
IF(ABD-BIG) 555,555,554	0008
554 BIG = ABD	0009
555 CONTINUE	0010
FACT = SQRT(BIG)	0011
I = 1	0012
1 IF(I=NS) 2,2,20	0013
2 J = 1	0014
3 IF(J=NS) 4,4,6	0015
4 K = 1	0016
5 IF(K=NS) 6,6,7	0017
6 E(J,K) = D(K,J)/FACT	0018
K = K+1	0019
GO TO 5	0020
7 J = J+1	0021
GO TO 3	0022
8 L = 1	0023
9 IF(L=NS) 10,10,14	0024
10 IF(L=I) 11,13,11	0025
11 E(L,IP) = 0.0	0026
12 L = L+1	0027
GO TO 9	0028
13 E(L,IP) = 1.0	0029
GO TO 12	0030
14 CALL JORDAN(B,E,NTEST,NS,NARA,NMAX)	0031
IF(NTEST) 15,15,16	0032
15 RETURN	0033
16 M = 1	0034
17 IF(M=NS) 18,18,19	0035
18 Q(I,M) = E(M,IP)/FACT	0036
M = M+1	0037
GO TO 17	0038
19 I = I+1	0039
GO TO 1	0040
20 RETURN	0041
END	0042
	0043

SUBROUTINE JORDAN(B,C,INDEX,N,NARA,NMAX)	0001
DIMENSION B(NARA),C(NARA,NMAX)	0002
K=1	0003
1 IF(K=N) 2,2,22	0004
2 IF(C(K,K)) 10,3,10	0005
3 L=K+1	0006
4 IF(L=N) 5,5,21	0007
5 IF(C(L,K)) 7,6,7	0008
6 L=L+1	0009
GO TO 4	0010
7 M=1	0011
8 IF(M=N+1) 9,9,2	0012
9 B(M)=C(K,M)	0013
C(K,M)=C(L,M)	0014
C(L,M)=B(M)	0015
M=M+1	0016
GO TO 8	0017
10 J=N+1	0018
11 IF(J=N) 13,12,12	0019
12 C(K,J)=C(K,J)/C(K,K)	0020
J=J-1	0021
GO TO 11	0022
13 I=1	0023
14 IF(I=N) 16,16,15	0024
15 K=K+1	0025
GO TO 1	0026
16 IF(I=K) 18,17,18	0027
17 I=I+1	0028
GO TO 14	0029
18 II=N+1	0030
19 IF(II=K) 17,20,20	0031
20 C(I,II)=C(I,II)-C(I,K)*C(K,II)	0032
II=II-1	0033
GO TO 19	0034
21 INDEX=0	0035
GO TO 23	0036
22 INDEX=1	0037
23 RETURN	0038
END	0039